12-2013

THE EFFECT OF SKEW ANGLE ON AVERAGE QUEUE DELAY AT TEE-INTERSECTIONS: A SIMULATION STUDY USING THE TEXAS MODEL

Manogna Kaluva
University of Nebraska-Lincoln, manognakaluva@gmail.com

THE EFFECT OF SKEW ANGLE ON AVERAGE QUEUE DELAY AT TEE-INTERSECTIONS: A SIMULATION STUDY USING THE TEXAS MODEL

By

MANOGNA KALUVA

A THESIS

Presented to the Faculty of the Graduate College at the University of Nebraska

In Partial Fulfillment of Requirements

For the Degree of Master of Science

Major: Civil Engineering

Under the Supervision of Professor: Elizabeth G. Jones

Lincoln, Nebraska

December 2013

THE EFFECT OF SKEW ANGLE ON AVERAGE QUEUE DELAY AT TEE-INTERSECTIONS: A SIMULATION STUDY USING THE TEXAS MODEL

Manogna Kaluva, M.S.

University of Nebraska, 2013

Advisor: Elizabeth G. Jones

This thesis explores the effect of intersection skew angle on average queue delay through simulation. The simulation model used is the TEXAS (Traffic Experimental and Analytical Simulation) model. This microscopic simulation model uses a general non-linear car-following model. It simulates individual intersections and was designed to capture the interaction of traffic operations and intersection geometry.

Simulation models were developed for three stop-controlled, tee-intersections in Lincoln, Nebraska. Field data to develop and calibrate the simulation models were collected. All simulation models were calibrated by adjusting the car following parameters. An experimental design was developed to test the effect of skew angle on average queue delay. Skew angles from 1 degree to 30 degrees were evaluated. The average queue delay reported for each skew angle is based on 30 runs of the simulation model. The results indicate that skew angle does affect average queue delay. The results also suggest that the TEXAS model can capture the effect of skew on average queue delay for small skew angles of 1 degree from the base conditions.

ACKNOWLEDGEMENTS

The first person I am deeply grateful to is my advisor, Dr. Elizabeth Jones. Her constant guidance and support were a huge motivation and comfort throughout the completion of the project. Regular interaction and discussions were very helpful to clearly understand the objectives and methodologies to achieve them. I am truly thankful for her willingness to share her ideas and suggestions on a regular basis. I am very thankful for all of her valuable advice and guidance throughout this project completion.

I am sincerely thankful to my committee member, NTC director Dr. Laurence Rilett, for his continuous support and motivation both financially and academically. I would like to thank Karen Schurr for her help with the previous study from which some of the data was borrowed for this project. I truly appreciate Dr. Anuj Sharma for being on my committee.

Dr. Thomas Rioux, the developer of the TEXAS simulation model, was very helpful in familiarizing me with the model in the initial stage of this project. His continuous advice and regular clarification of my doubts were an important source toward understanding and operating the simulation model efficiently. I do not have words to express his kind and humble attitude in helping me through this entire journey. Without his involvement, the TEXAS model would not have been as comfortable to deal with. I am forever in debt to him.

Several student members were very kind to help me during the data collection process. Sincere thanks to Diego Franca, Bhaven Naik, Justice Appiah, Tim Foss, Kiran Kothamachu, Teja Phanidar Kunju, Ved Vyas Kamarajugadda, Greg McKnight and Brian Gardner for all the hard work. I am also deeply grateful to Valerie Lefler, Emilea

D. Brook, Jordan Muller and Jordan Pokorny for all their help at the Nebraska Transportation Center.

Finally I am grateful to God for blessing me with family members who always supported and stood behind me every day through this challenging phase of my life. I am very happy to have my sister Manasa Kaluva, who as a friend and guide always understood my pain and hard work and held my hand throughout this time.

TABLE OF CONTENTS

LIST OF FIGURES

LIST OF TABLES

CHAPTER 1 INTRODUCTION

1.1. Background

According to the Green Book, "an intersection is defined as the general area where two or more highways join or cross" (*Green Book, 2004*). The most common type of intersection is an at-grade intersection where two highways intersect (*Green Book, 2004*). The intersection of two highways can have three or four legs with the three-legged intersection commonly called a "tee-intersection." Typically the two intersecting highways carry different amounts of traffic. The highway with the higher traffic volumes is called the major road and the other highway is called the minor road.

The angle between the two highways is measured in a clockwise direction between the centerlines of the highways and is given a notation of φ as shown in Figure 1.

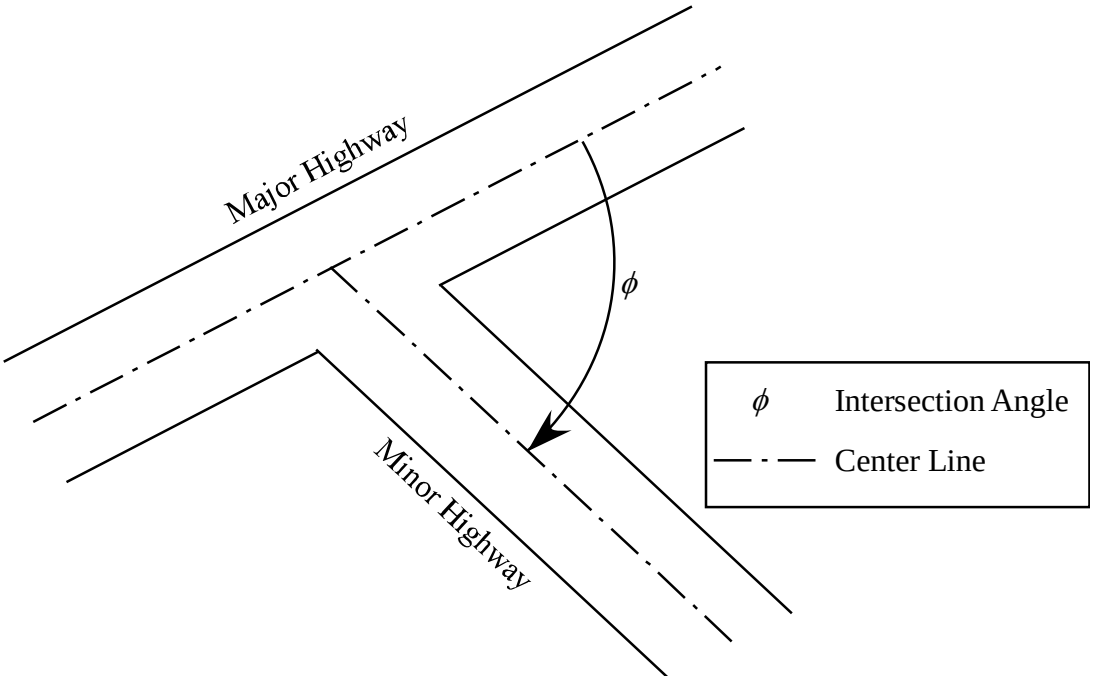

FIGURE 1 Sketch of a tee-intersection showing the intersection angle between the major and minor highways

If the intersecting highways are not exactly perpendicular then the intersection is said to be skewed. The amount of angular deviation from perpendicular in a clockwise direction is defined as the skew angle, θ, as shown in Figure 2.

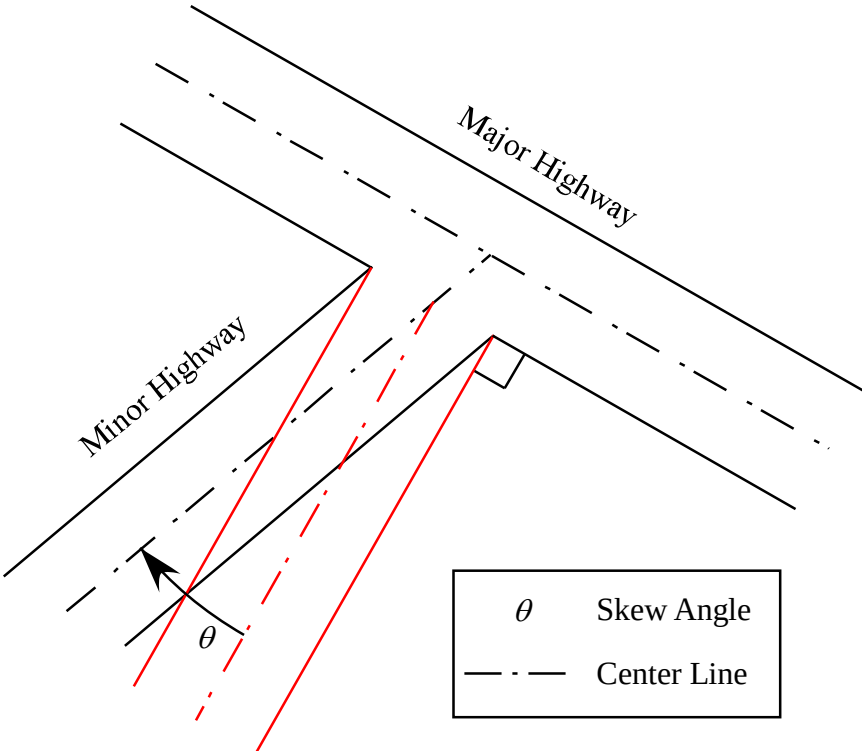

FIGURE 2 Skewed intersections

Skewed intersections can be left- or right-skewed. If the intersection angle is greater than 90 degrees then it is said to be left-skewed as shown in Figure 3. Left skew is considered to be a positive skew angle.

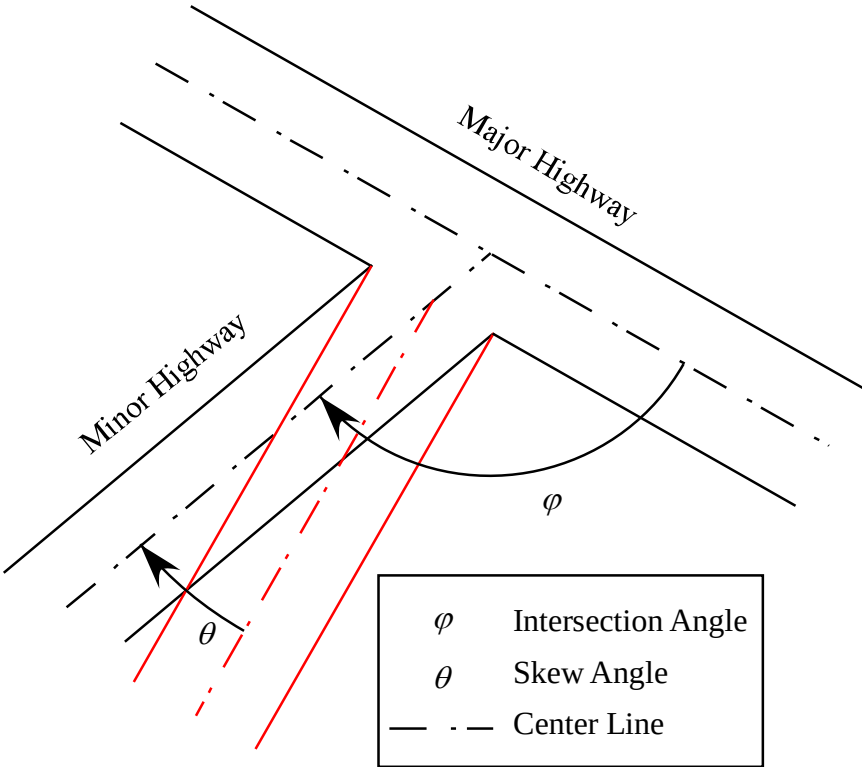

FIGURE 3 Left-skewed intersection with a positive skew angle

Figure 4 shows a minor approach, again with an intersection angle of φ that is less than 90°. This is defined as a right-skewed intersection (*Gattis, Low, 1997)*. The measurement of the skew angle is the same but in a counterclockwise direction. Since this intersection angle is less than 90°, the skew angle is negative.

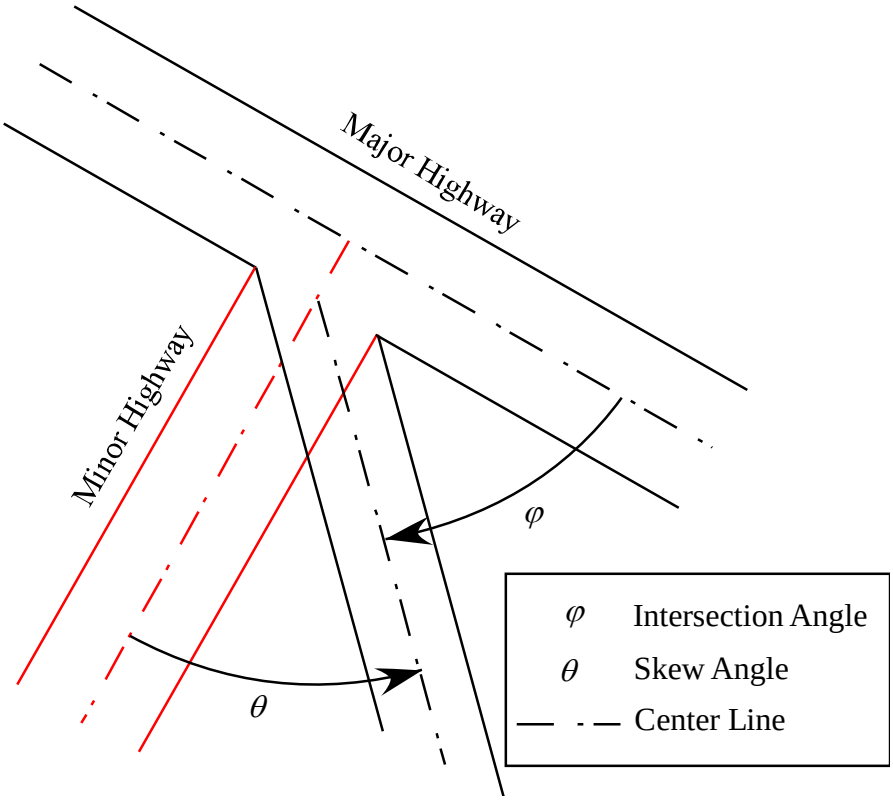

FIGURE 4 Right-skewed intersection with negative skew angle

The intersection shown in Figure 5 is an intersection with no skew. The minor highway is located at exactly 90° from the major highway. Hence, the intersection angle φ is 90°. As mentioned above, skew is the deviation from the perpendicular angle. But as there is no deviation in this instance, the skew angle, θ, is 0°.

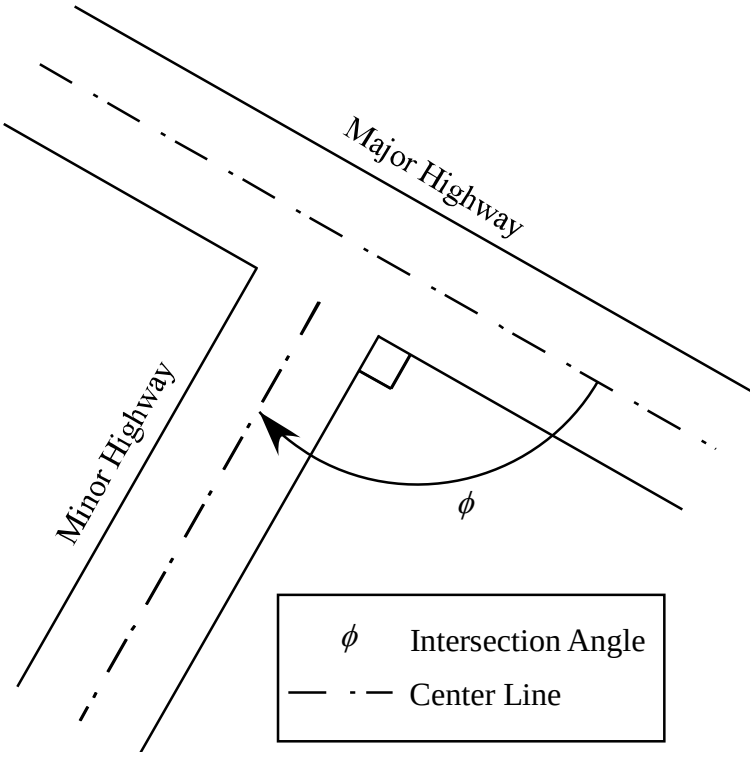

FIGURE 5 Intersection with no skew, $\theta = 0°$

1.2. Skewed Intersection Issues

Skewed intersections have several issues associated with them that make them awkward. These issues can be grouped as geometric design, traffic operations and safety issues (*Walker, 1981).* Each is discussed below.

1.2.1 Geometric Design

The physical intersection can be defined by the curb lines as shown in Figure 6. Skewed intersections in comparison to intersections with no skew have longer curb lines and a larger intersection area (*TFHRC, 2004*). These two aspects are demonstrated by comparing the calculations both at no skew and skew conditions.

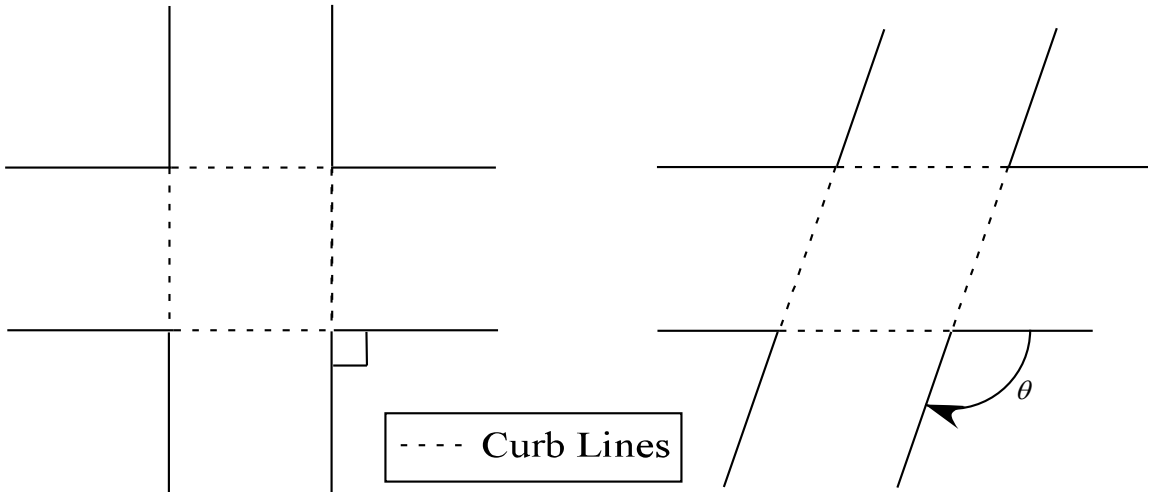

FIGURE 6 Physical intersection defined by curb lines (a) Intersection with no skew (b) Skewed intersection with skew angle θ

Let w_1 and w_2 be the width of intersecting highways. Let d_1 and d_2 be the length of curb lines, and A and A' as the areas of the non-skewed and skewed intersections as shown in Figure 7.

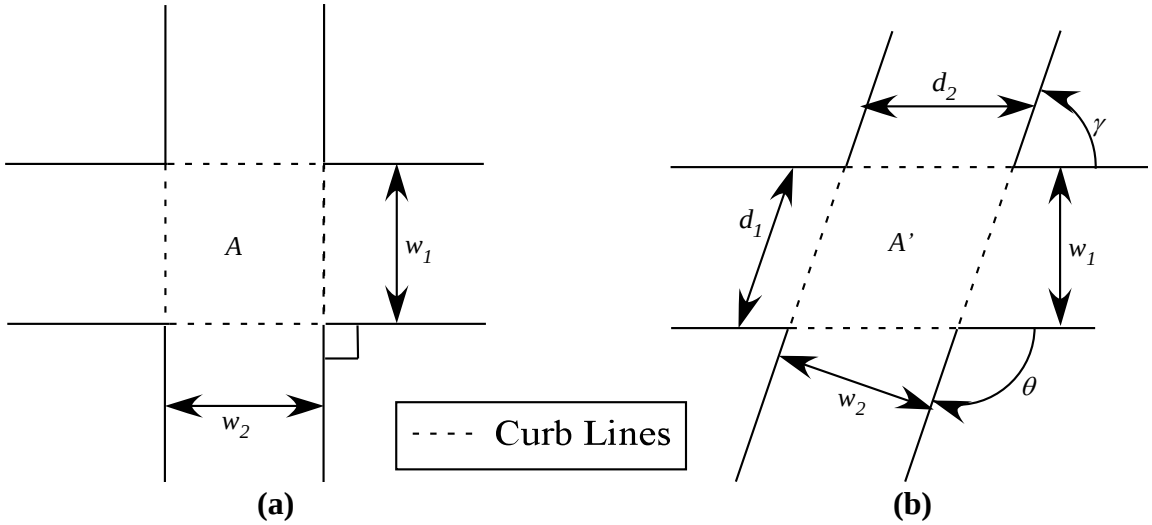

FIGURE 7 Physical intersection with dimensions and area shown (a) Intersection with no skew. (b) Skewed intersection with skew angle θ.

1.2.1.1 Curb Line Length

The curb line lengths for an intersection with no skew are the same as the width of the highways forming the intersection. This can be stated mathematically as:

$$d_1 = w_1 \tag{1}$$

$$d_2 = w_2 \tag{2}$$

For skewed intersections, the curb line length is a function of the skew angle and the widths of the intersecting highways as shown in Equations 4 and 5.

$$\gamma = 180 - \theta \tag{3}$$

$$d_1 = \frac{w_1}{\sin\gamma} = \frac{w_1}{\sin\theta} \tag{4}$$

$$d_2 = \frac{w_2}{\sin\gamma} = \frac{w_2}{\sin\theta} \tag{5}$$

Note that $\sin(180 - \theta) = \sin\theta$. $\sin\theta$ has a maximum value of 1 at 90° and a minimum value of 0 at 0°. Since the skew angle is an angle other than 90°, d_1 and d_2 will both be larger than w_1 and w_2. Hence, curb lines are longer at skewed intersections than at non-skewed intersections.

1.2.1.2 Intersection Area

The area of an intersection with no skew is rectangular. Equation 6 expresses A in terms of the widths of the intersecting highways.

$$A = w_1 w_2 \tag{6}$$

The area of a skewed intersection is a function of the skew angle and the widths of the intersecting highways. This area is trapezoidal in shape. Equation 7 is a mathematical expression of A'.

$$A' = w_1 d_2 \tag{7}$$

Using the expression for d_2 found in Equation 5 and $\sin(180 - \theta) = \sin\theta$,

$$A' = \frac{w_1 w_2}{\sin\gamma} = \frac{w_1 w_2}{\sin\theta} \quad (8)$$

Therefore, the area of a skewed intersection is larger than the area of an intersection with no skew.

1.2.2 Traffic Operations

Traffic flow is adversely affected by skew angle in terms of distance and sharpness of turns (*Walker, 1981*). Because of the increased intersection area, drivers travel longer distances through the intersection and experience longer travel times to cover the longer distance (*Gattis, Low, 1997; Neuman, 1985; Walker, 1981*).

For intersections with no skew, the right turn is sharp and the left turn is wide as shown in Figure 8a. Furthermore, the right turn has smaller radius and is sharper in comparison to the left turn. The left turn has larger radius and is wider in comparison to the right turn. Hence the drivers making left turns are able to travel at higher speeds than those making right turns.

The scenario changes at the skewed intersections as shown in Figure 8b. For the movements from the lower right and from the upper left approaches the following situation is observed. The right turn is less sharp than at an intersection with no skew and thus drivers making right turns may be able to make them at higher speeds than at non-skewed intersections. For drivers making left turns, the left turn is less wide than at intersections with no skew and hence the left turns may be slower than at non-skewed intersections. The scenario for the movements on the other two approaches is opposite to those just discussed. The right turn is sharper and may be slower than at a non-skewed

intersection. Finally the left turn is wider and may be faster than at a non-skewed intersection.

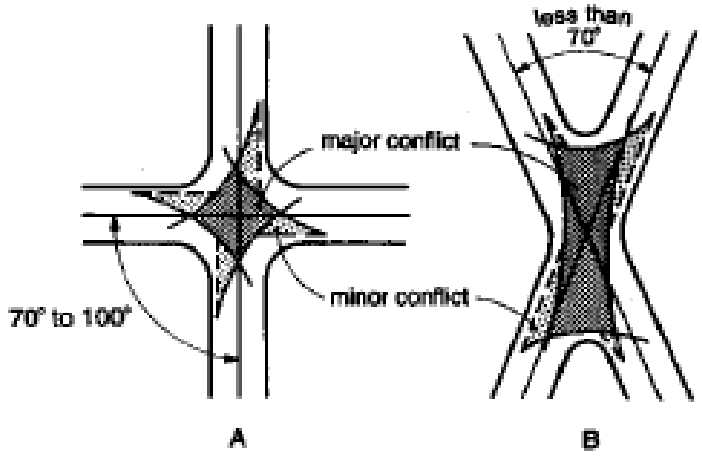

FIGURE 8 Conflict area at (a) a perpendicular intersection (b) a skewed intersection (*Walker, 1981*)

1.2.3 Safety

Skewed intersections are considered to have two main safety issues. The first is a large conflict area. As was discussed in Section 1.2.1.2, a skewed intersection has a larger area. A large intersection area increases the conflict area at skewed intersections as shown in Figure 8. As a result vehicles are exposed to conflicting traffic for a longer time (*Neuman, 1985; Gattis, Low, 1997; Walker, 1981*).

The second safety concern is related to sight distance. At skewed intersections drivers' sight distances may be reduced in some directions due to difficulty in a driver's ability to turn his or her head to completely view a conflicting approach. This becomes more critical for drivers with physical limitations and also for older drivers. As mentioned previously some right turns become sharper and some left turns wider at skewed intersections. So, at right-skewed intersections, drivers making sharp right turns

might intrude into the oncoming lane of traffic in an effort to see conflicting traffic. Whereas at left-skewed intersections, drivers making left turns may speed up and use unsafe gaps in making a turn (*Gattis, Low, 1997).*

1.3. Problem Statement

The purpose of this research is to evaluate the effect of skew angle on traffic operations at three-legged stop-controlled intersections. The operational effect will be measured by using average queue delay. Average queue delay is used by the Highway Capacity Manual to determine level of service (LOS) at stop-controlled intersections (*Highway Capacity Manual, 2000*). The first hypothesis of this research is that the average queue delay increases with skew angle and the lowest average queue delay will be experienced when no skew exists. The expected results in terms of skew angle versus average queue delay are expected to have a trend similar to that shown in Figure 9 (*Bonneson, 1993*).

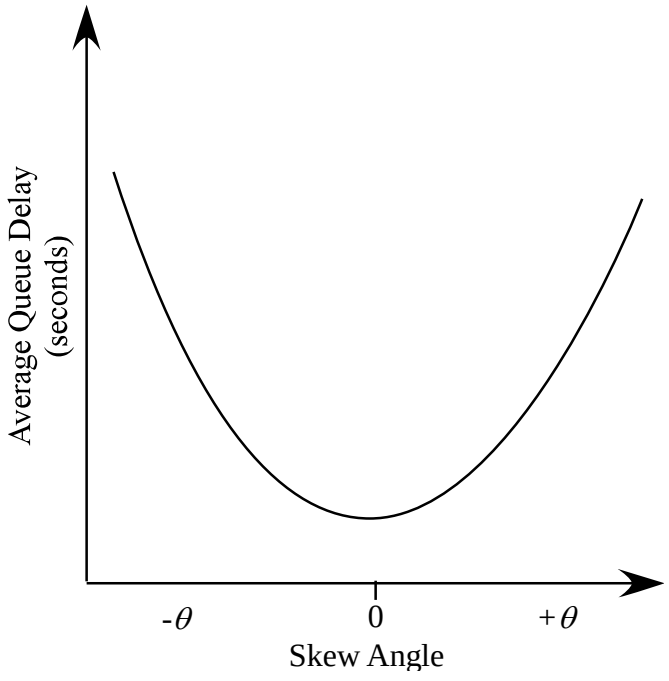

FIGURE 9 Effect of skew angle on average queue delay

The TEXAS (Traffic Experimental and Analytical Simulation) model is a micro-simulation model designed to capture both the effects of geometry and traffic conditions on traffic operations and traffic safety for individual intersections. This model will be used to study the relationship between skew angle and average queue delay. The second hypothesis to be tested is that TEXAS is capable of evaluating the effect of geometric changes on traffic operations.

1.4. Methodology

The primary goal of this study is to analyze the effect of skew angle on average queue delay with the help of a simulation tool called TEXAS. In order to accomplish this goal there are several tasks that need to be performed. The first and foremost challenge was to make sure that all the data required as input into the simulation model for each study site is available. For this project the data came from two sources: a previous study and by collecting data in the field. The three locations chosen for this project were taken from the previous study. The data that was borrowed are: minor street vehicle arrival and departure time at the stop sign, spot speeds, vehicle types, and highway measurements. Video was recorded of all these study sites either during morning or evening peak times. The video camera was positioned on the shoulder of the major street and perpendicular to the major street traffic direction. The data was collected for this project with an intention to determine the effect of sight distance obstruction on queue delay of minor street vehicles. All the three intersections had separate turning lanes on the minor street. If both the left- and right-turning vehicles arrived at the stop sign at the same time, the sight distance of the vehicles was obstructed by the adjacent vehicle. As a result it is suspected

that vehicles will experience more delay. But apart from the above data, more data was required as input into the simulation model. This missing data was either collected from the field, such as spot speeds, or was calculated from previous data, such as average queue delay, traffic counts and vehicle classes.

Once all the required data is gathered, the simulation model is developed for each study site. Before actually running the simulation model in order to check the two hypotheses of this research, first it is verified to see whether the input and output results exactly match. Then the model is calibrated using the car following parameters if there is a difference between field average queue delay and simulated average queue delay. Then an experimental design is conducted in order to analyze the kind of relationship between skew angle and average queue delay.

1.5. Research Objectives

To test the two hypotheses, several research objectives must be met. A literature review is done to place the research presented here in the broader context of similar research found in the literature. This is done in Chapter 2. The next objective, summarized in Chapter 3, is to collect the field data required as input into the TEXAS simulation model and for calibration of the simulation model. Data from a previous research effort related to tee-intersections will be used in addition to data collected specifically for this research. The third objective is to build a simulation model for each of the four tee-intersections used in a previous study using the field data from this previous study as well as the data collected for this research (Chapter 4). The next objective is to calibrate the simulation models to field data. This is covered in Chapter 5. Chapter 6 presents an experimental

design developed to help guide the analysis as well as the analysis and the results needed to test the research hypotheses. The thesis closes with conclusions and recommendations for future research in Chapter 7.

CHAPTER 2 LITERATURE REVIEW

2.1. Introduction

The main objective of this chapter is to review the past work done in two areas relevant to this project. These areas are the effect of skew and a review of the use of the TEXAS model.

2.2. Effect of Skew

The angle of an intersection influences traffic movements, safety and driver behavior. It can lead to several problems as was discussed in the previous chapter. This section discusses relevant literature not previously covered with an emphasis on safety issues.

The skew of an intersection has an influence on the ease with which drivers move through an intersection. Skewed intersections can confuse drivers as they may not easily navigate through an intersection (*Woodson, Barry, 1992*). A non-skewed intersection provides the best operating conditions as drivers can easily sense the direction in which they are travelling, estimate the speeds of the opposing traffic and smoothly complete a maneuver in shorter time. Any deviation from a 90° intersection angle causes a shift from the above scenario making the intersection less safe. The maximum allowed skew used by the state of Nebraska is 30° (*NDOR Roadway Design Manual, 2006*). Visibility is better at right-angle intersections than at skewed intersections. At skewed intersections, the ability of drivers to recognize any conflicting vehicles diminishes in comparison to right-angle intersections. Additionally, because of the increase in pavement area, longer travel times can be expected. At left-skewed intersections, the

bodies of vehicles obstruct line of sight to the right. In this case, a maximum allowable skew angle should be 20° (*Garica, Esplugues, 2007*).

The intersection sight distance is also affected by skew angle. If the intersection angle is less than 60° and realignment is not preferable, then intersection sight distance should be adjusted for skew. As shown in Figure 10, the sight triangles' legs are parallel to the approach. Also, sight triangles at skewed intersections are different than at normal perpendicular intersections. The travel path length increases at obtuse angle intersections. The angle between AB and the vehicle path either on minor approach or major approach is small. Hence, the drivers will not have much difficulty viewing the oncoming traffic and small head movements are usually sufficient to clearly see the oncoming traffic. On the contrary, at acute angle intersections the angle between BC and vehicle paths is large. Sight distance is obstructed at these intersections and drivers cannot easily view the conflicting traffic. Because of this, skewed intersections with no control should not be used. A sight distance at least equal to that of intersections with stop control on minor approach or intersections with yield control on minor approach, whichever is greater, should be provided (*AASHTO, 2004*).

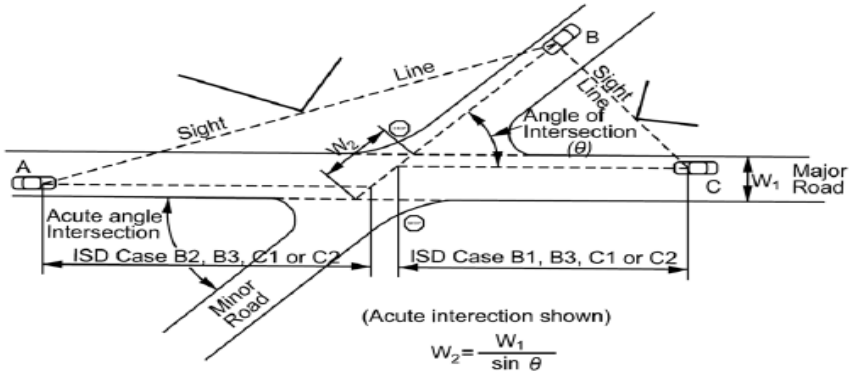

FIGURE 10 Effect of skew on sight distance (*Green Book, 2004*)

Limited sight distance at skewed intersections leads to safety issues. Intersection angle is one of the geometric factors that affects the sight distance available to drivers at stop-controlled minor approaches. At skewed intersections drivers need more time to cross an intersection. This results in an increased exposure time to conflicting traffic and also intersection sight distance. Longer exposure results in the drivers' presence in a danger zone for longer times, thus resulting in accidents. Findings from research by Son, Kim and Lee found that for large vehicles or semi-trailers a skew of more than 20° is not recommended (*Son, Kim and Lee, 2002*). Unsignalized skewed intersections are less safe than normal 90° intersections because of the obstructed sight distance at skewed intersections. A Poisson regression analysis was conducted on the accidents at 29 two-way stop-controlled intersections in Nebraska. Skew angle at these intersections varied from 10° to 45°. The results showed that the accidents increase annually with skew angle and traffic volume (*Tripi, 1994*). A study conducted to examine the effect of skew angle on safety of expressways found that skewed intersections had higher crashes and fatality rates than normal intersections (*Burchett and Maze, 2006*). The impact of skew angle on safety is less severe at three-legged stop-controlled multilane intersections in comparison to four-legged and signalized intersections. This is because at four-legged intersections the traffic pattern is more complex than at three-legged intersections. At signalized intersections, skew has less effect on safety. A threat to safety is posed at skewed intersections because of sight distance obstruction; drivers will find it difficult to make a turning movement and contradictory driver behavior can be observed at these types of intersections (*Oh, Washington and Choi, 2004*).

A study that examined the effect on safety due to the presence of skew at three-legged and four-legged stop-controlled intersections found that the occurrence of crashes at intersections with skew angles of 10° and 45° is higher than at non-skewed intersections (*Hardwood, Council, Hauer, Hughes and Vogt, 2000*). A study conducted on the relationship between design and safety in China found that the crash rate is two to three times higher at skewed intersections than perpendicular intersections. Primary reasons for this were found to be inadequate sight distance and right-turning vehicles at acute angle intersections entering into opposing lanes. Safety can be improved by realignment to 90° or lesser skew. (*Zhong, Wang, Zhong, Zhu, Jia, Zhao, Ma and Liu, 2007*). The visibility problem at skewed intersections results in higher crash rates, particularly at left-skewed intersections (*Savolainen and Tarko, 2004*). Peak hour delays and severe traffic congestion were primary concerns along a 10-mile-long segment along MD 210 (Indiana Head Highway) from I-95/495 to MD 228. It was found that the skewed side approaches resulted in capacity being reduced when compared to a regular perpendicular intersection (*Grayson, 1976*). At the intersection of John Young Parkway and Pleasant Hill Road in Orlando, 36 accidents were reported in a five-year span from 1999 to 2003. Pleasant Hill Road is located at approximately 115° to John Young Parkway. The skew was believed to be the primary reason behind the crashes from field review (*Harwood, et al., 2000*). Large vehicles can obstruct the sight distance to the right at 60-degree left-skewed intersections. Limiting intersection angles to no less than 70° or 75° will improve the sight distance (*Gattis, Low, 1997*).

In the above discussion, some of the studies recommended the maximum skew that should be allowed. Several states within the U.S. have maximum allowable limits

for skew. These values are recorded in Table 1 (*Neuman, 1985*). As the table indicates, 30° seems to be the accepted skew angle by most of the states.

TABLE 1 Maximum allowed skew angles (*Neuman, 1985*)

State	Maximum Allowed Skew Angle
Nebraska	30°
Alaska	30°
Illinois	30°
Wisconsin	30°
Colorado	30°
Minnesota	20° (with consideration for realignment)
Ohio	30° satisfactory 20° recommended 40° only for salvage projects
Idaho	20° minimum 15° desirable

Apart from safety, presence of a skew causes inconvenience to drivers, especially elderly drivers. A study in Arlington, Virginia, on a four-legged 65-degree signalized skewed intersection found that the drivers had to rotate their heads through angles larger than normal in search for safe gaps to merge into the intersection. Skewed intersections are unfavorable in comparison to non-skewed intersections because at skewed intersections drivers made the least attempts to make a right turn on red (*Tarawneh and McCoy, 1996*). In 1971, a study to determine the effect of vehicle position on lag acceptance time concluded that the stopped vehicles located at angles 90, 135 and 180 degrees with respect to the major traffic stream had no effect on the lag time (*Gatling and Whyte, 1971*). The extensive head movement required at skewed intersections, especially at acute angled intersections, could be challenging for older drivers and also affect their safety. Notably, this issue was not taken into consideration in the AASHTO's intersection design policies (*Hauer, 1988*). A similar observation was made by Hunter-

Zaworski. She found that at skewed intersections, older drivers had problems turning their heads in order to judge the safe gap length and approaching vehicle's speed. Since the vehicle waiting to enter the intersection is stopped on the minor approach, a larger gap will be required to accelerate into the main stream of traffic. Coupled with poor sight distance problems at these kinds of intersections, driving becomes much more challenging for older drivers (*Hunter-Zaworski, 1988*).

2.3. TEXAS Simulation Model

The TEXAS simulation model was developed to simulate a single isolated intersection and to be an evaluation tool that can be used to analyze several different geometric and traffic scenarios. Since its development, the model has been used in different ways: mostly it is used to understand the effect of few parameters on traffic operations and intersection geometry. One of the hypotheses of this study is that the TEXAS model is capable of evaluating the effect of geometric changes on traffic operations. Hence, it becomes necessary to see if the past users found it to be a credible tool or not. The following is a discussion of past work completed using the TEXAS model.

The TEXAS model was validated using field data in Texas by Naguib (*Naguib, 1989*). Five sets of variables were adjusted from their default values to test their effect on queue delay. The first two sets of variables are 1) the percentage of vehicles in each lane and 2) the car following parameters of lambda and alpha and the headway distribution. The results showed that car following parameters do have an effect on the average stopped delay especially in case of left turns (*Naguib, 1989*). To test the efficiency of TEXAS as an evaluation tool, simulations of four intersections in Dallas were created.

To this end, traffic volumes and stopped delays at these intersections were compared with simulated values for this purpose. After a comparison it was found that for moderate to low traffic volumes, field and simulated values are in agreement with each other. But at heavy traffic flow conditions, there are differences between the two data sets. In order to resolve this, the vehicle and driver mix were changed from default and a few changes to the code resulted in excellent agreement. Field and simulated results varied within 10 percent for almost two thirds of simulation conditions. It was concluded from the study that the TEXAS model can be used to simulate this unique type of phase (*Machemehl and Acampora, 1991*).

To analyze the traffic operations at a diamond interchange, the TEXAS model was used to simulate the actuated traffic signal control and traffic behavior. The model was validated using two diamond interchanges located in San Antonio. The TEXAS model was found to be a powerful evaluation tool for determining optimal signal setting for certain conditions. It is recommended to use this model for comparing the alternatives before implementing the design in reality (*Lum and Lee, 1992*).

Five simulation models were selected to simulate a single point diamond interchange (SPDI) and a conventional diamond interchange located in Phoenix. One of the five models was the TEXAS model. The availability of various traffic signal options, different headway distributions for each approach and animation display were found to be better than the NETSIM model, which was also chosen for the study. Comparison of stopped delay between field and simulation results showed that the TEXAS model results are in agreement for three out of the four approaches. This research indicated that the TEXAS model has the ability to simulate SPDI operations. Since the TEXAS model can

only simulate isolated single intersections this model could not be used in the case of conventional diamond interchanges (*Radwan and Hatton, 1990*).

Several methods to evaluate the operations at left turn lane analyses at signalized intersections were reviewed. Out of the methods used, it was found that using a micro-simulation model such as the TEXAS model avoided the complexity of mathematical models. Also people who used the TEXAS model found that the effort required to develop a new procedure was far easier than the prevailing manual methodology (*Machemehl, 1986).*

In a study to investigate whether or not signals should be installed at marginally warranted locations, a simulation model was used to simulate the relevant types of intersections in Texas. The TEXAS model was used as the simulation tool. Due to a lack of field data for various geometric conditions and volumes in the field, TEXAS was chosen as it allows a user to select from various traffic control options and a broad range of approach flow rates. These intersections were evaluated for a variety of traffic volumes and three types of traffic control: two way, stop controlled, and actuated signal. Signalization will increase delay and the number of stops at marginally warranted intersections. Safety was found to be enhanced only at low-speed rural areas. These simulation results were in accordance with the expectation of the authors (*Williams and Ardekani, 1996*).

To determine the capacity of level of service at single unsignalized intersections, the TEXAS model was employed. It was selected as the appropriate tool for this study because of its diverse features such as its microscopic nature, large vehicle class types, and ability to input detailed geometry parameters and to display output results for any

selected simulation time. The attributes of an intersection are geometry, traffic control, volumes and the level of service it provides. If one of the above four data is missing, then the unknown can be calculated using the TEXAS model (*Lee and. Savur, 1979*).

At 53 signalized intersections in Richardson, Texas, it was found that left turn phasing was not needed because of the low peak traffic left turns observed. This resulted in unnecessary delay to opposing through traffic. Then a signalized intersection similar to the above mentioned intersections was simulated. The model was run for five phase signalization and then for a two phase, and it was found that the two phase signal is efficient. The TEXAS model helped strengthen the advice of traffic managers. It is recommended that more traffic agencies should use this tool because of the readily available information on speeds and delay in comparison to the difficulty in obtaining these values from the field (*Grayson, 1981*).

The TEXAS model was used in developing new warrants and investigating the efficiency of existing warrants. The TEXAS simulation model was used to develop warrants for installing a left turn lane or separate signal phase. The level of detail in output was the main reason for choosing this model over NETSIM. Though the model can deal with only a single intersection and not the whole network, in comparison to other macroscopic models the TEXAS model was believed to be the best choice to study left turn operations (*Lin, Machemehl, Lee and Herman, 1984*).

Grayson used the TEXAS model to evaluate the adequacy of existing and proposed signal warrants by MUTCD. To efficiently evaluate the warrants, the wide variety of intersection layouts and traffic scenarios that exist in the field must be considered. As the TEXAS model input can handle this issue, a broad range of volumes

above and below the warrants and five types of traffic control plans were used for intersections with control from a two-way stop-control to actuated traffic signal control. The results were then used to justify a type of traffic control based on cost estimates. The model was found to be a useful tool because of its ability to allow the user to input a wide range of traffic volumes and different types of traffic control (*Grayson, 1976*).

To develop guidelines for typical phase sequence patterns, the TEXAS model was used to study the effects of left turn signal phase patterns on traffic operations. This model was selected as each and every vehicle is scanned on a second-to-second basis and dynamically interacts with traffic control, other vehicles and intersection geometry (*Machemehl and Mechler, 1983*).

The TEXAS model was used to analyze the traffic signal warrants recommended by MUTCD on the basis of cost effectiveness. The volume and delay data from the simulation model are analyzed and several conclusions are drawn as to which type of traffic control device is cost effective in comparison to others (*Lee, Savur and Grayson, 1978*).

The TEXAS model has the ability to model emissions and fuel consumption. This is done via what is called the EMPRO processor. The EMPRO processor was used to determine the mobile source emissions and fuel consumption. The original processor was developed using the old 1975 emission rates. In order to reflect the new rates, a modified EMPRO was used for the study. The revised EMPRO processor yielded reasonable vehicle emission and fuel consumption results (*Liao and Machemehl, 1995*).

A study was performed to compare the fuel savings from a free U-turn lane with U-turns at two closely spaced intersections at a diamond interchange. The results from

the TEXAS model concluded that a free U-turn lane is a better choice in this context. The TEXAS model is a powerful tool to evaluate alternative design scenarios in terms of traffic volumes, fuel consumption and vehicle emissions (*Rodriguez, Lee, and Machemehl, 1997*).

A new fuel consumption model was developed as a technique to optimize the operations at a signalized intersection. The results from the model are compared with TEXAS model results to gain confidence in the model. To obtain an optimal signal cycle length for minimization of fuel consumption, results were compared over various ranges of traffic volumes and cycle lengths. Fuel consumption model results and simulation model results were in agreement. However, the suggested optimal cycle lengths for different flow rates were different. Contrary to expectations, the TEXAS model suggested lower cycle lengths for higher flow rates. Random traffic characteristics of the model were identified as the reason for deviation (*Liao and Machemehl, 1995*).

On high-speed signalized intersections drivers face the dilemma of whether to stop or to proceed during the signal change from green to yellow hence resulting in rear end collisions. Also due to high traffic volumes in urban areas, large delays may be faced by the drivers in comparison with rural areas. Hence, if detectors are used to reduce delay and provide dilemma zone protection the same setup cannot be used in both scenarios. This calls for deciding the optimal location for placing the detectors. In this context, the TEXAS model was recognized as the appropriate tool as it can simulate both isolated and diamond intersections. Also, a wide variety of traffic control options from uncontrolled to full actuated signal control are available. The original study was revised to overcome the limitation of the detector option in the TEXAS model. Based on the

findings of the research further enhancements in detector options of the model are proposed for a better representation of reality (*Woods and Koniki, 1994*).

To minimize the interchange delay, efficient location for installing loop detectors was determined. The TEXAS simulation model was used to analyze the performance of detectors for two types of signal phases. Though the model was identified to have limitations in terms of simulating the number of detectors in comparison to the TRAF-NETSIM model, its ability to simulate the Texas Diamond controller made it a good choice for this study. Certain problems, such as inability to access detector code and errors for zero second red clearance intervals, required work-around solutions. After finding the optimal location for detectors in this study, certain deficiencies such as provision for multiple loop detectors and good documentation on special intervals are suggested for future development of the model (*Prabhakar, 1994*).

In certain cases the TEXAS model was not found to be helpful as illustrated through the cases mentioned previously. At two-way stop-controlled intersections the effect of a right turn on vehicular delay was investigated. A microscopic model that could simulate single intersections was needed for this study. The TEXAS model was recognized as an appropriate tool for this purpose. Furthermore, it was selected since the default values can be changed in the model to better reflect the current study traffic scenario. The model was used to evaluate the alternative designs across various geometric and traffic volume conditions. The results showed that rather than right turns, major and minor street volumes influence the delay on the minor approach. The simulation method was not found to be useful (*Radwan and Eure, 1991*).

To enable the traffic engineers to choose the type of left turn phasing for a particular kind of intersection, left turn signal phasing warrants were developed. A part of this study was to find a procedure to evaluate intersection operations. Several approaches were considered for this purpose and one of them was to use a simulation model. In order to analyze the differences in traffic operations under five different types of signal phases, the TEXAS model was believed to be the right tool. The results from the model were inconsistent, however. Though the model properly estimated the through delay, it ended up overestimating the left turn delay for three types of phasing. It was concluded that the TEXAS model could not replicate the real behavior of drivers making left turns at signalized intersections. Hence, it cannot be used to evaluate any differences in operations due to different left turning phases (*Upchurch, Radwan and Dean, 1991*).

The TEXAS model was initially considered for simulating traffic operations at all-way stop-controlled intersections. But later this model was rejected because it was found to overestimate delay for volumes higher than 280 vph and underestimate delay for lower volumes about 100 vph and below; simultaneously, a maximum simulation time of only one hour is allowed without any volume changes (*Kyte, Kittelson, Zhong, Robinson and Vandehey, 1996*).

NETSIM and the TEXAS model were evaluated using field data with approach delay as a measure of effectiveness. The results showed that both simulation results are not in agreement with each other or with the field results. It was believed that the TEXAS model is incapable of simulating the left turning behavior accurately. Several problems arose while using the TEXAS model in this study. Plots were required to debug the geometrical input errors. Extreme care needs to be exercised while preparing

the input data for the model in comparison to NETSIM. Other problems such as higher delays, incorrect travel times, excess CPU time, initialization time, and others must be handled using work-around techniques (*Torres, Banks, Halati and M. Danesh, 1980*).

This section shows that the TEXAS model was used as an evaluation tool to analyze the traffic operations and different types of signalized intersections or interchanges. Sometimes it was used to investigate warrants or to help new ones, to understand the amount of fuel consumed by stopped vehicles as an attempt to reduce the consumption, and to locate detector placement for optimal operations. It was also found to have mixed results – some studies found it useful and others found it to produce inconsistent results.

2.4. Chapter Summary

In this chapter reviewed literature associated with the effects of skew on intersection safety and operation as well as the use of the TEXAS model as a simulation tool to better understand how traffic operations and intersection geometry interact. This information serves as a background for the research described in the following chapters.

CHAPTER 3 DATA COLLECTION

There are two data sets involved in this research project. The first data set was available from a previous study. This data includes geometric measurements, minor street vehicle arrival and departure time at the stop sign, vehicle types and spot speeds. Additional data was collected that was missing and was needed as input for the TEXAS model. This chapter discusses in detail about how this additional data was collected and analyzed.

3.1. Locations

Data collection was carried out at three study sites, which were chosen from a previous research project. All the three study sites are stop-controlled tee-intersections. These study sites are located in Lincoln, NE at:

(1) N 24th and Superior Street

(2) S 56th and Saltillo Road and

(3) S 90th and O Street

An aerial view of each of these intersections is shown in Figures 12-15. Also, all these intersections had no skew and this is clarified in the following figures.

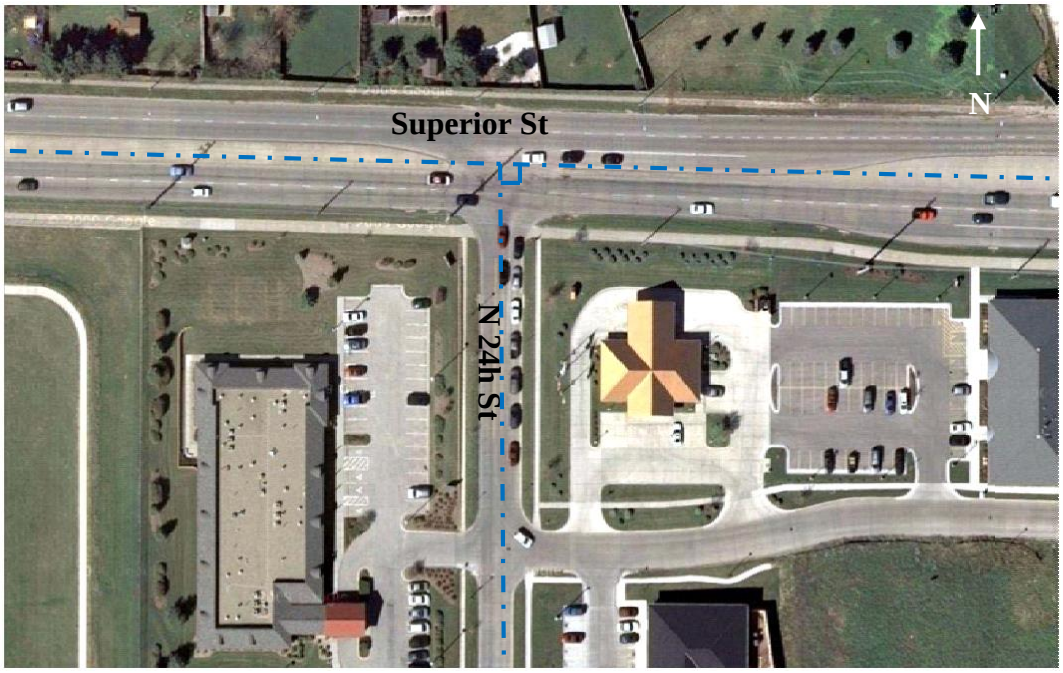

FIGURE 11 N 24th and Superior Street

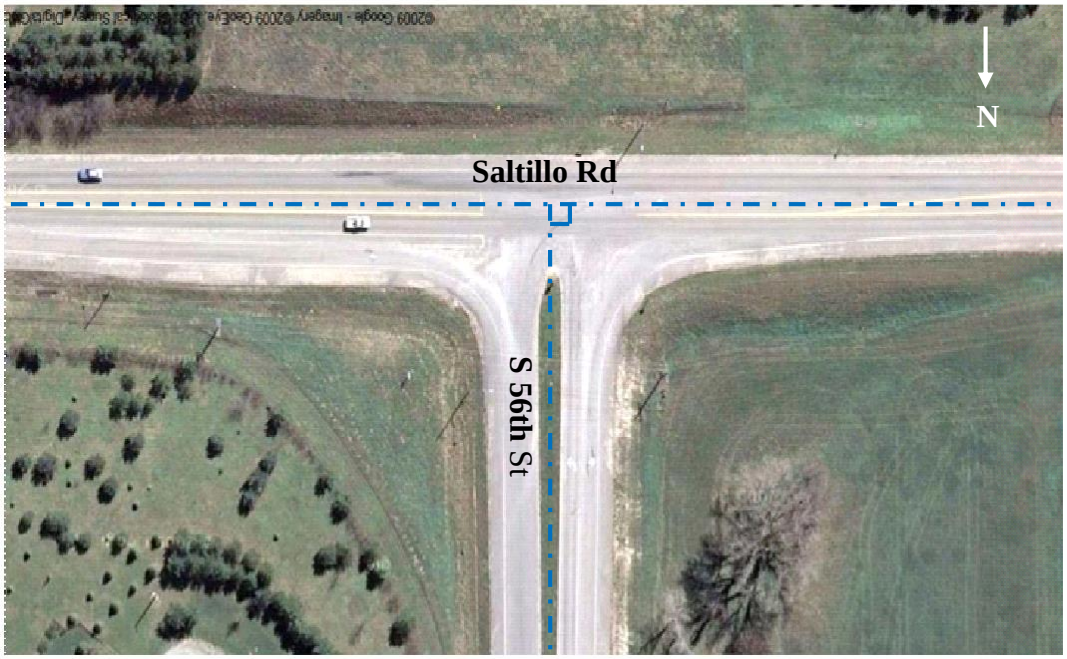

FIGURE 12 S 56th Street and Saltillo Road

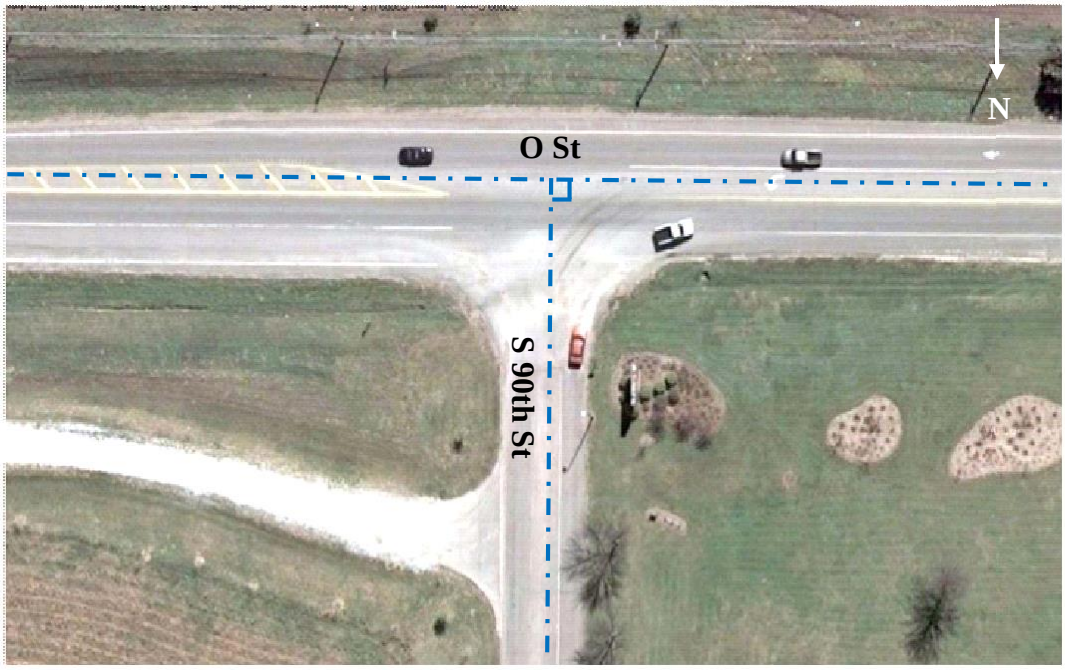

FIGURE 13 S 90th Street and O Street

3.2. Speeds

The TEXAS simulation model requires mean speed and 85th percentile speed information for each leg of the intersection as input data. From earlier study, spot speeds information was not available for all the streets of a study site. Hence, for the missing streets, speeds were collected in the field using radar guns. These missing streets include: the northbound approach of N 24th and Superior Street, all approaches of S 56th and Saltillo Road and the entire S 90th and O street intersection.

Firstly, to determine the number of speed observations that needed to be collected Equation 1 was used (*Currin, 2001*):

$$\text{Number of observations} = \left[\frac{Z_{\propto} S}{e}\right]^2 \quad (9)$$

Where,

$Z_{\propto}$ = Normal statistic for a confidence level of $\alpha = 1.96$ for a 95% confidence level

S = Expected standard deviation and

e = Amount of error allowed = 1.0.

Using a previous speed study at these sites as a reference, standard deviation was determined at each of these sites and is shown in Table 2.

TABLE 2 Expected standard deviation at study sites

Intersection	Approach	Standard Deviation
N 24th and Superior Street	EB	4.38
	WB	3.85
	Average	4.12
S 56th and Saltillo Road	EB	5.33
	WB	5.33
S 90th and O Street	EB	5.78
	WB	7.76
	Average	6.77

Using above values for S, 1.96 for $Z_{\propto}$ and 1 for e, and with the help of Equation 9, the number of observations were calculated, as shown in the first column of Table 3. To help ensure that enough data were collected, it was decided to take the number of observations computed and then round them up to the nearest 50 or 25 to ensure that enough data were collected. The primary concern was to collect at least 100 observations.

TABLE 3 Number of speed observations

Intersection	Calculated No. of Observations	Used No. of Observations
N 24th Street and Superior Street	66	100
S 56th Street and Saltillo Road	110	125
S 90th Street and O Street	177	200

For example, in the case of the N 24th and Superior Street intersection using Equation 9 the minimum number of observations is calculated as shown below:

$$\text{Number of observations} = \left\lfloor \frac{1.96 * 4.12}{1.0} \right\rfloor^2 = 66$$

Similarly for the rest of the intersections these calculations are included in Appendix A.

3.3. Speed Traps

Once the number of speed observations to be collected was determined, the next task was to decide where on the approach the speeds should be collected. The idea was to collect speeds at a distance greater than the stopping sight distance. In order to obtain this distance, Equation 10 (*Green Book, 2004*) was used.

$$d = 1.47 * V * t + \left\lfloor \frac{1.07V^2}{a} \right\rfloor \quad (10)$$

Where,

d = Braking distance

V= Speed in mph

t = reaction time = 2.5s and

a = Threshold acceleration = 11.2ft/s^2.

By using the posted limit on the major approach at each of these sites and the above value for reaction time and acceleration, this distance was calculated at each site and is summarized in Table 3.

For example, consider the northbound approach of N 24th Street and Superior Street. Using Equation 10,

$$d = 1.47*25*2.5 + \left\lfloor \frac{1.07*25^2}{11.2} \right\rfloor$$

$$= 151.7\text{ft}$$

Minor streets have low volumes and low speeds, hence twice the distance was used for them as can be seen in Table 4. In the field, based on convenience, at a certain distance beyond stopping sight distance, speeds are collected using a radar gun. This spot is named a speed trap for convenience. These speed trap distances from stopping sight distance are mentioned in Table 4. Further, in Figure 14 the line marked on the northbound approach of N 24th and Superior Street corresponds to the location of the speed trap in the field. In this particular case, the speed trap is at a distance of 187.3ft from the stopping sight distance and the radar gun was held at 15.4ft from the shoulder. Appendix A includes these calculations and speed trap figures for rest of the intersections.

FIGURE 14 Speed trap on northbound approach of N 24th and Superior Street. Speed trap is shown with a black line on the northbound approach.

TABLE 4 Speed trap distances on the approaches of study sites

Intersection	Speed Limit (mph)	Approach	Stopping Sight Distance (SSD) (ft)	Distance of Speed Trap from SSD (ft)
N 24th and Superior Street	40	EB	NA	NA
	40	WB	NA	NA
	25	NB	303.5	187.3
S 56th and Saltillo Road	55	EB	492.2	15.0
	50	WB	423.5	22.0
	55	SB	984.4	6.0
S 90th and O Street	65	EB	644.1	16.5
	60	WB	565.7	30.0
	20	SB	223.6	82.0

NA = Not Applicable (speed values were taken from previous study)

3.4. Spot Speeds Analysis

Spot speeds collected in the field have to be analyzed in order to obtain the required mean speed and 85th percentile speed. Using field spot speeds, frequency tables are created and

from it mean speed can be calculated. Whereas, 85th percentile speeds can be obtained from cumulative frequency plots (*Currin, 2001*). Table 5 is the speed frequency table of the northbound approach of the N 24th and Superior Street intersection. For the rest of the intersections, this information is included in Appendix A.

TABLE 5 Intersection information and frequency table of spot speeds on northbound approach of N. 24th Superior Street

N 24th and Superior Street

Intersection: N 24th and Superior Street
Approach: Superior Street
Direction of Travel: NB
Distance of speed trap from intersection: 303.5ft
Speed limit: 25 mph
Observers: Manogna, Diego
Date: 1/22/2008
Time of study: 11:40 am – 3:40 pm
Weather: 20˚ F
Observations: 100
Distance of radar gun from speed trap: 15.4ft from shoulder, 187.3ft from speed trap

Speed Group	Number Observed f_i	Class Mid Value u_i	f_i/u_i	Frequency (%)	Cumulative Frequency (%)	Observed Speed (mph)
12	1	12.5	0.0800	1	1	13
13	0	13.5	0.0000	0	1	14
14	0	14.5	0.0000	0	1	15
15	2	15.5	0.1290	2	3	16
16	4	16.5	0.2424	4	7	17
17	3	17.5	0.1714	3	10	18
18	4	18.5	0.2162	4	14	19
19	6	19.5	0.3077	6	20	20
20	5	20.5	0.2439	5	25	21
21	6	21.5	0.2791	6	31	22
22	9	22.5	0.4000	9	40	23
23	3	23.5	0.1277	3	43	24
24	9	24.5	0.3673	9	52	25
25	6	25.5	0.2353	6	58	26
26	9	26.5	0.3396	9	67	27
27	10	27.5	0.3636	10	77	28
28	7	28.5	0.2456	7	84	29
29	6	29.5	0.2034	6	90	30
30	5	30.5	0.1639	5	95	31
31	2	31.5	0.0635	2	97	32
32	1	32.5	0.0308	1	98	33
33	1	33.5	0.0299	1	99	34
34	1	34.5	0.0290	1	100	35
	100		4.2694	100		

Now, the mean speed (harmonic mean) is calculated using Equation 11 as (*Roess, Prassas and McShane, 2004*):

$$u = \left\lfloor \frac{1}{\frac{1}{N}\left\lceil \left(\sum_{i=1}^{G} \frac{f_i}{u_i} \right) \right\rceil} \right\rfloor \quad (11)$$

Where,

G = Number of groups

f_i = Frequency of group i

u_i = mid-point of group i and

N = Number of observations = $\sum_{i=1}^{G} f_i$.

Using Equation 11 and Table 5,

Mean speed, u = 100/4.2694 = 23.4 mph

Next, in order to calculate 85th percentile speed, a plot is created with cumulative frequency on the Y axis and observed speeds on the X axis. Using Table 5, the cumulative frequency plot is drawn as shown in Figure 15. The corresponding speed value on the X axis for a cumulative frequency of 85% on the Y axis is the required 85th percentile speed. Hence, from Figure 15, the 85th percentile speed for the northbound approach of N 24th and Superior Street is 29.2 mph.

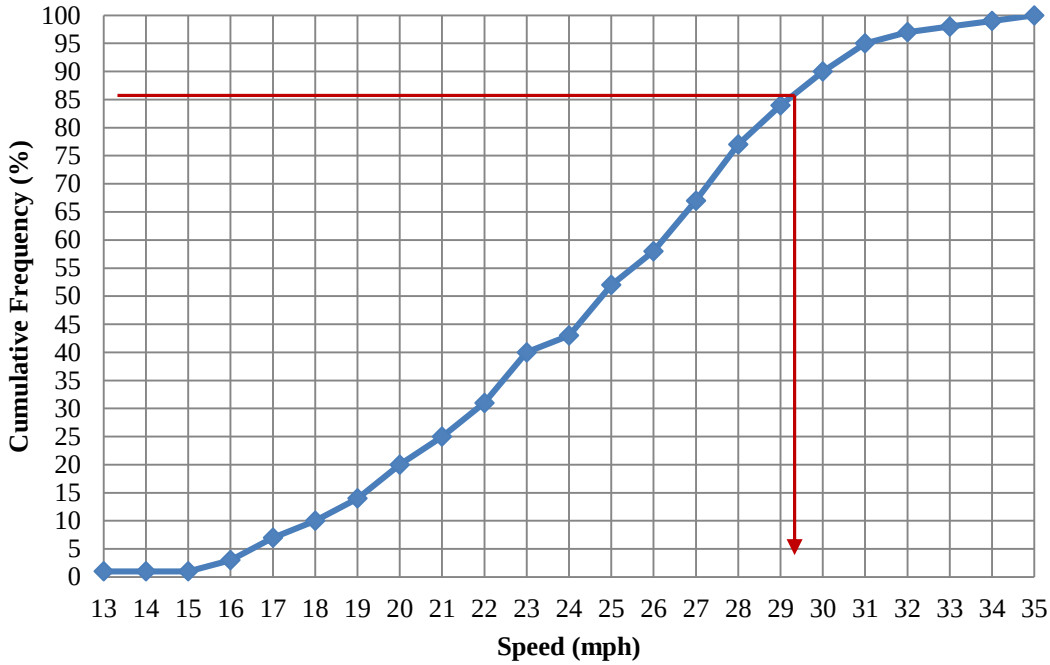

FIGURE 15 Cumulative frequency plot of spot speeds on northbound approach of N 24th and Superior Street

From the above graph, 85% speed = 29.2 mph. Using the harmonic speed formula from Equation 11 and cumulative frequency plots in a similar fashion for the remaining intersections, the values obtained are mentioned and are summarized in Table 6. Relevant calculations for other sites can be found in Appendix A.

TABLE 6 Mean and 85th percentile speeds

Intersection	Approach	Mean Speed (mph)	85% Speed (mph)
N 24th and Superior Street	NB	23.4	29.2
	EB	41.0	45.0
	WB	39.1	45.0
S 56th and Saltillo Road	EB	44.8	52.3
	WB	51.2	56.8
	SB	49.8	55.3
S 90th and O Street	EB	49.8	56.2
	WB	45.5	51.3
	SB	23.2	27.9

3.5. Approach Volumes

Inbound approach volume is one of the important input parameters required to develop the simulation model. So, in order obtain this information, intersection videos from the previous study were watched and results are summarized in Table 7.

TABLE 7 Field approach volumes

Intersection	Approach	Volume (vph)
N 24th and Superior Street	WB Thru 1	398
	WB Thru 2	372
	WB Left	56
	NB Left	31
	NB Right	69
	EB Thru and Right	489
	EB Thru and Right	313
S 56th and Saltillo Road	EB Thru	157
	EB Left	66
	SB Left	96
	SB Right	94
	WB Thru	145
	WB Right	65
S 90th and O Street	EB Thru	192
	EB Left	129
	SB Left	9
	SB Right	173
	WB Thru	188
	WB Right	8

3.6. Vehicle Classes

The traffic volume while watching videos was observed to be composed of different types of vehicles. There are 12 vehicle classes defined by the TEXAS simulation model. The data obtained from previous study did contain information on type of vehicles, which included: car, SUV, minivan, light truck, light truck with trailer, heavy truck, bus, semi-trailer and bus. Each of these vehicles is grouped into appropriate vehicle class as shown

in Table 8. The composition of vehicles before grouping into classes is included in Appendix A. Bikes are not included.

TABLE 8 Composition of vehicle classes

Intersection	Approach	Class 3	Class 4	Class 6	Class 7	Class 12	Total
N 24th and Superior Street	WB	52.5%	44.6%	1.3%	0.2%	1.3%	100%
	NB	51.0%	47.0%	0.0%	0.0%	2.0%	100%
	EB	56.2%	41.5%	1.2%	0.5%	0.5%	100%
S 56th and Saltillo Road	EB	48.4%	50.5%	0.7%	0.0%	0.5%	100%
	SB	52.9%	45.2%	1.3%	0.3%	0.3%	100%
	WB	50.8%	44.6%	2.6%	0.0%	1.9%	100%
S 90th and O Street	EB	60.4%	30.1%	3.0%	1.1%	5.5%	100%
	SB	79.3%	19.6%	0.6%	0.0%	0.6%	100%
	WB	49.7%	36.7%	2.6%	0.8%	10.2%	100%

Class 3 = Car and Minivan, Class 4 = SUV + Lt truck + Lt truck with trailer + Large van, Class 6 = Heavy truck, class 7 = Bus and Truck, Class 12 = Semi-trailer

3.7. Average Queue Delay

Field average queue delay was calculated using data from the previous study. It was measured as the time between when the minor approach vehicle stops to when it starts entering into the intersection (*Lee, Rioux, and Copeland,* 1977).

The average value of all the individual vehicle queue delay is the average queue delay value reported in last column of Table 9 for left turn and right turns. The total corresponds to the average queue delay of the minor approach as a whole. This value is obtained by dividing the total delay from both the turning lanes by the total number of vehicles on the approach during the study period. Previous study contained data regarding vehicle arrival and stop time only for minor streets and not for major streets. Hence, the average queue delay value was calculated only for minor streets of all the three study intersections. As an example, the individual queue delay values for each turning lane along with their average values for N 24th and Superior Street is included in Appendix A.

TABLE 9 Field average queue delay

Intersection	Minor Street	Average Queue Delay (s)
N 24th and Superior Street	Left Turn	20.7
	Right Turn	9.2
	Total	12.8
S 56th and Saltillo Road	Left Turn	9.9
	Right Turn	2.2
	Total	6.1
S 90th and O Street	Left Turn	15.6
	Right Turn	4.6
	Total	5.2

3.8. Chapter Summary

This chapter describes how the additional data was collected in the field and was analyzed. The additional data found to be required were spot speeds, volumes, vehicle classification and field average queue delay. At this point since all the data is available both from the previous study and also from the field, the next task was to develop a simulation model for each one of the study sites. This entire process is demonstrated in Chapter 4.

CHAPTER 4 TEXAS SIMULATION MODEL DEVELOPMENT

4.1. TEXAS Simulation Model

The TEXAS (Traffic Experimental and Analytical Simulation) model is a microscopic simulation model developed to evaluate the traffic performance at a single isolated intersection or interchange for a variety of traffic control, geometry and driver options. This model can be applied to study the effect on traffic operations due to modifications in roadway, driver, vehicle, traffic control, lane control and signal plans. This model requires mainly two types of data: GDVDATA, geometry and driver-vehicle information, and SIMDATA, or simulation data (*Lee, Rioux and Copeland, 1977*; *Lee, Grayson, Copeland, Miller, Rioux and Savur, 1977*). The basic look of this model with these two types of data is shown in Figure 16:

FIGURE 16 TEXAS simulation model interface

Each type of data provided as input by the user into the simulation model is stored in one of the three processors: GEOPRO, DVPRO and SIMPRO. GEOPRO is a geometric processor that stores all the information relevant to the intersection geometry and driver-vehicle characteristics for an intersection. Geometry information includes the number of lanes, curb radius, lane length and width, number of approaches, and other variables. This processor calculates the geometric paths that will be travelled by the drivers, points of conflict and the minimum sight distance available to the drivers as they approach the intersection. This information is then made available to the simulation processor, SIMPRO (*Lee, Rioux and Copeland, 1977*).

DVPRO, or the driver and vehicle processor, is in charge of generating individual vehicles on the paths created by GEOPRO. The type of vehicle and driver class can be included in the input. Depending on the headway distribution mentioned by the driver for each approach, traffic will be generated. This information is passed on to the SIMPRO. In the simulation model, the above two processors are combined into one processor, known as GDVDATA, which merges geometry, driver and vehicle data (*Lee, Rioux and Copeland, 1977*). Figures 17 and 18 show the GDVDATA interface.

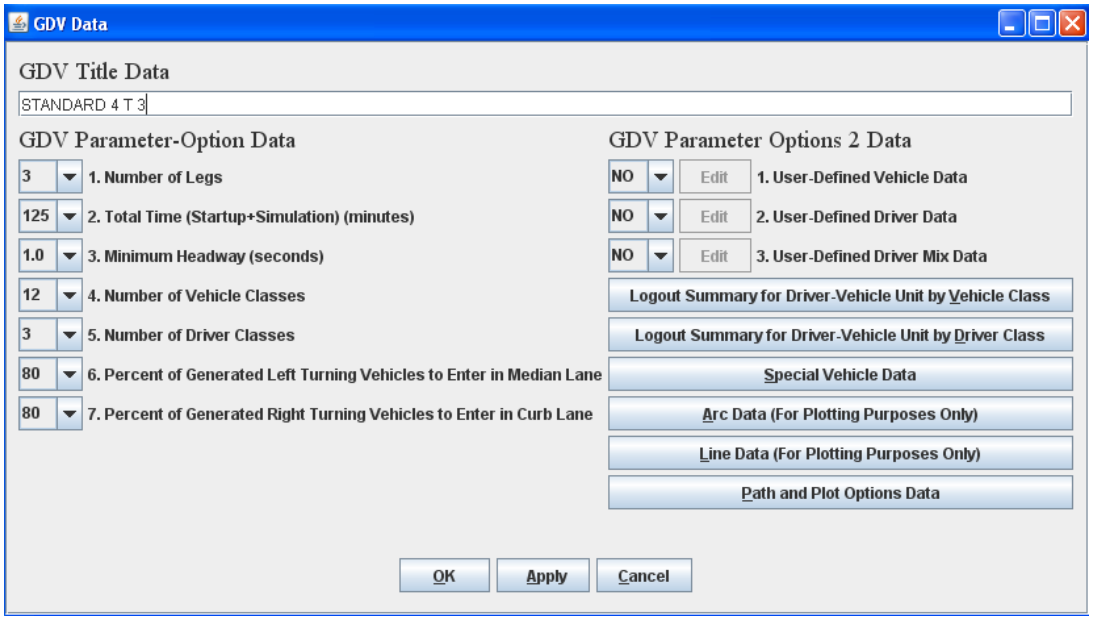

FIGURE 17 Geometry and driver vehicle data (GDVDATA) interface

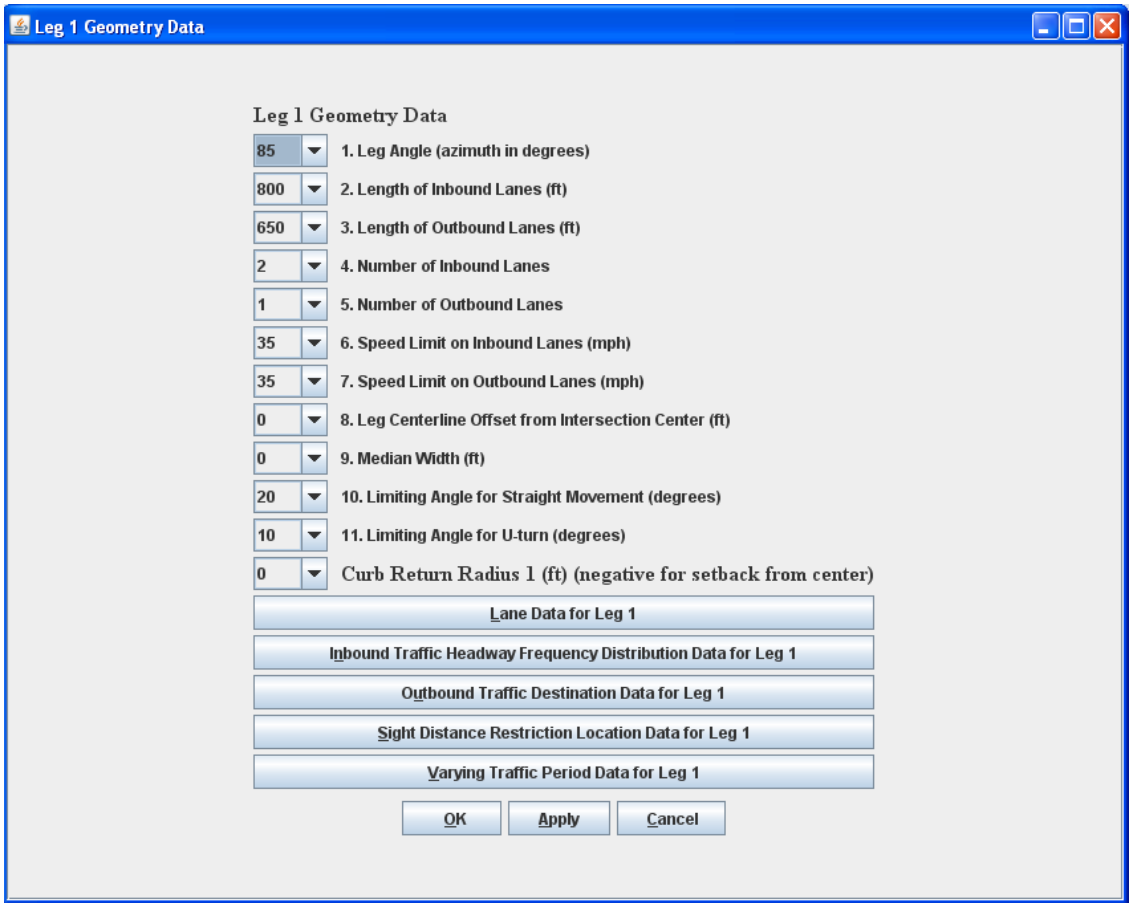

FIGURE 18 Leg wise geometry data interface

Finally, SIMPRO, the simulation processor, takes all the information provided by GEOPRO and DVPRO and some additional information in order to simulate the vehicles. The additional information required by this processor includes the amount of time the simulation model should run, startup time, length of queue, car following parameters, type of intersection control, lag and lead time zones, etc. Figure 19 shows an image of the SIMDATA interface.

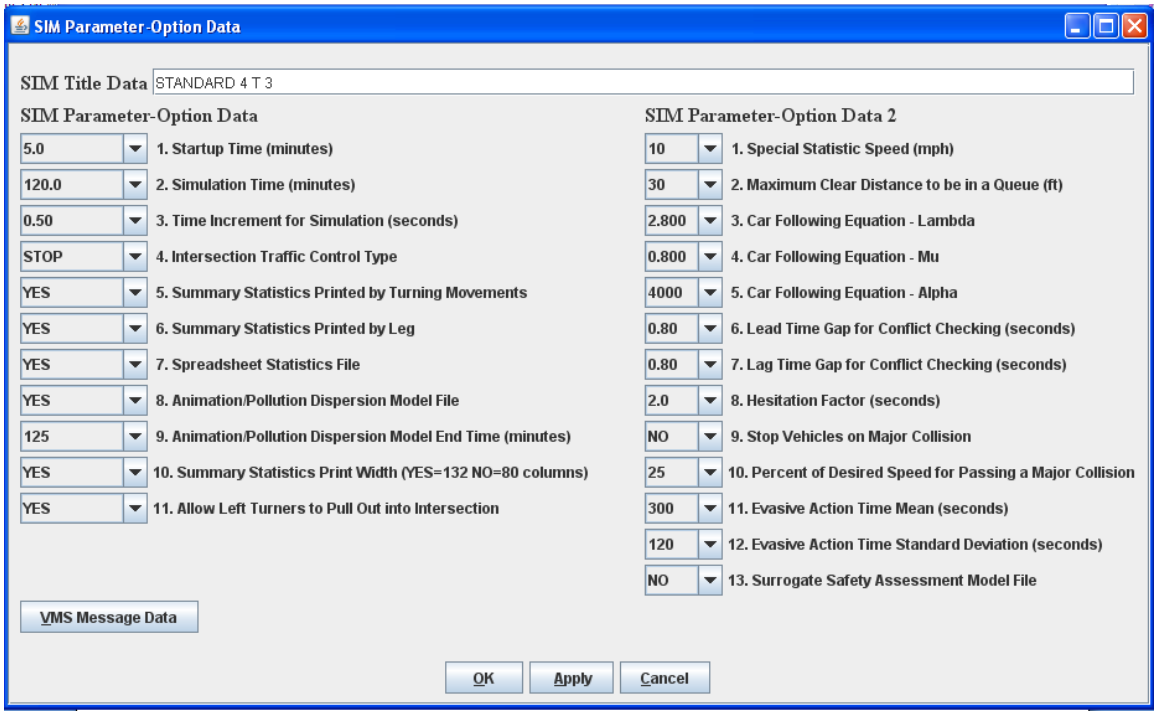

FIGURE 19 Simulation data (SIMDATA) interface

4.2. Simulation Model Development for Study Intersections

The data collected either in the field or from the previous study were inputted into the TEXAS simulation model as the first step toward building the model for each one of the three study sites. All the input data of N 24th and Superior Street is shown in Table 10. Red values correspond to input whereas black figures are the default values. The simulation model is run at a tolerance level of 10%.

TABLE 10 Input data for N 24th and Superior Street

GDV Data	Input
Number of legs	3
Total time (min)	15
Minimum headway (s)	1
Number of vehicle classes	12
Number of driver classes	3
Percent of generated left turning vehicles to enter in median lane	80
Percent of generated right turning vehicles to enter in curb lane	80
User defined vehicle data	NO
User defined driver data	NO
User defined driver mix data	NO
Leg 1 , Leg 2, Leg 3	
Leg angle (azimuth in degree)	90,180,270
Length of inbound lanes	800, 800, 800
Length of outbound lanes	422, 250, 550
Number of inbound lanes	3, 2, 2
Number of outbound lanes	2, 1, 2
Speed limit on inbound lanes	40, 25, 40
Speed limit on outbound lanes	40, 40, 40
Leg centerline offset from intersection center (ft)	-5, 0, 0
Median width (ft)	4, 0, 15
Limiting angle of straight movement (deg)	20, 20, 20
Limiting angle of u turn (deg)	10, 10, 10
Curb return radius 1-3 (ft)	0, 30, 30
Lane data for leg 1-3	
Inbound	
Lane width (ft)	11/13/13, 10/10, 13/13
Movement code	L/S/S, L/R, S/SR
Length of usable lane near intersection center (ft)	152/0/0, 50/0, 0/0
Length of usable lane from outer end (ft)	0, 0, 0
Offset of inbound stop line or outbound entry line (ft)	-58/-58/-58 ,0/0, 12/12
Percent of generated inbound traffic to enter an inbound lane leg wise	0/50/50, 0/100, 50/50
Outbound	
Lane width (ft)	13/13, 13, 13/13
Movement code	S/SR, LR, LS/LS
Length of usable lane near intersection center (ft)	0, 0, 0
Length of usable lane from outer end (ft)	0, 0, 0
Offset of inbound stop line or outbound entry line (ft)	-11/-11, 0, -100/-100
Inbound traffic headway frequency distribution for leg 1-3	
Name of inbound traffic headway distribution	SNEXP, SNEXP, SNEXP
Total hourly volume on leg (vph)	826, 100, 802
Minimum headway (s)	1, 1, 1
Mean speed of entering vehicles (mph)	39.1, 23.4, 41.0
85% speed pf entering vehicles (mph)	43.0, 29.2, 45.0
User defined traffic mix data	YES, YES, YES
Random seed number	95767, 62377, 36486
Outbound traffic destination data for leg 1-3	
Percent of inbound traffic with destination to leg 1-3	0/7/93, 69/0/31, 98/2/0

TABLE 10 Input data for N 24th and Superior Street (continued)

GDV Data	Input
Sight distance restriction location data for leg 1-3	
Sight distance restriction data for leg 1-3	0, 0, 0
Varying traffic period data for leg 1-3	0
Simulation Data	
Start up time (min)	5
Simulation time (min)	60
Time increment for simulation (s)	0.5
Intersection traffic control type	STOP
Summary statistics printed by turning movements	YES
Summary statistics printed by leg	YES
Spreadsheet statistics files	YES
Animation/ pollution dispersion model file	YES
Animation/ pollution dispersion model end time (min)	65
Summary statistics print width	YES
Allow left turners to pull out into intersection	YES
Special statistic speed(mph)	10
Maximum clear distance to be in a queue (ft)	30
Car following equation-lambda	2.8
Car following equation-mu	0.8
Car following equation-alpha	4000
Lead time gap for conflict checking (s)	0.8
Lag time gap for conflict checking (s)	0.8
Hesitation factor (s)	2
Stop vehicles on major collision	NO
Percent of desired speed for passing a major collision (mph)	25
Evasive action time mean (s)	300
Evasive action time standard deviation (s)	120
Surrogate safety assessment model	NO
Lane control	
Leg 1	UN, UN, UN
Leg 2	ST, ST
Leg 3	UN,UN

*Input, Default

4.3. Verification

Once the simulation model is built, the first step in simulation modeling is to verify the model. It is a process of determining if the simulation model operates as intended. This process was conducted by comparing the output results with the field values. If a close match was found between two sets of data then the conclusion was that the developed simulation model actually reflected the conceptual model. Field and simulated flow rates were compared in this context. It was found that both sets of data were equal and hence it was considered to be verified. Table 11 compares field and

simulated flow rates for each study site along with the difference between both data sets. Figure 20 shows that both sets of data are a close match because they lie close to the 45° line. Therefore, the model is built correctly.

TABLE 11 Comparison of field and simulated flow rates

Intersection	Environment	Leg 1 (vph)			Leg 2 (vph)			Leg 3 (vph)			Total
		Thru	Left	Sum	Left	Right	Sum	Thru	Right	Sum	
N 24th and Superior Street	Simulation	766.3	56.5	822.8	30.5	70.2	100.7	787	15.7	802.7	1726.2
	Field	770	56	826	31	69	100	782	20	803.3	1729
	Absolute Diff	3.7	0.5	3.2	0.5	1.2	0.7	5	4.3	0.6	3.1
	% Difference	0.48%	0.89%	0.39%	1.61%	1.74%	0.70%	0.64%	21.50%	0.07%	0.18%
N 90th and O Street	Simulation	191	128.9	319.9	9.4	173.1	182.5	188.8	7.6	196.4	698.8
	Field	192	129	321	9	173	182	188	8	196	699
	Absolute Diff	1	0.1	1.1	0.4	0.6	1	0.8	0.4	0.4	0.3
	% Difference	0.52%	0.08%	0.34%	4.44%	0.35%	0.55%	0.43%	5.00%	0.20%	0.04%
S 56th and Saltillo Road	Simulation	154	67	221	97	91.3	188.3	147.2	65.5	212.7	622
	Field	157	66	222	96	94	190	145	65	210	621
	Absolute Diff	2.5	1.5	1	1	2.2	1.2	2.7	0.5	3.2	1
	% Difference	1.60%	2.29%	0.45%	1.04%	2.35%	0.63%	1.87%	0.77%	1.53%	0.16%

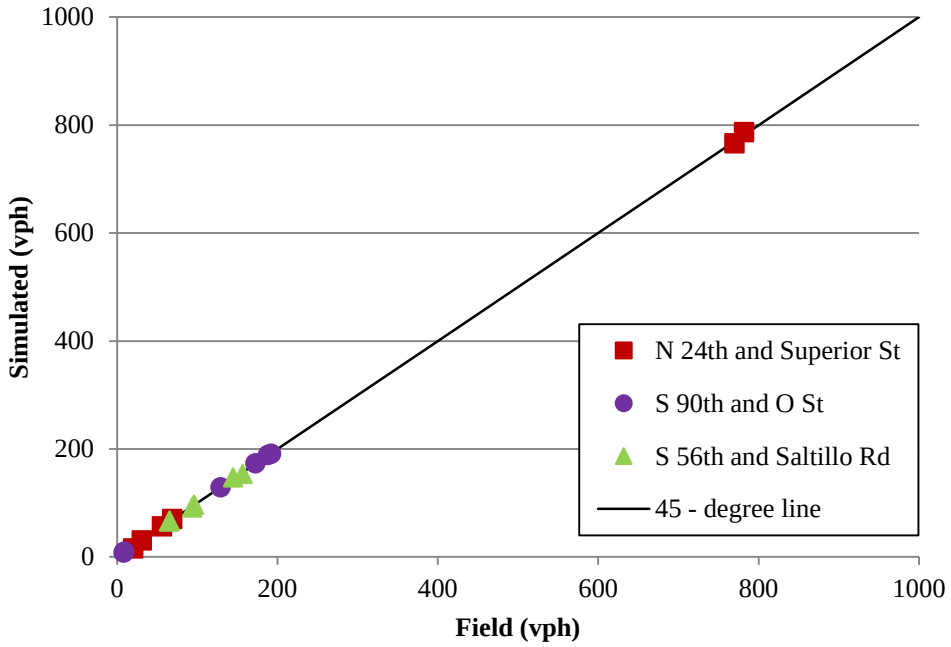

FIGURE 20 Comparison of field and simulated flow rates

4.4. Chapter Summary

In this particular chapter, firstly, introduction to the TEXAS simulation model is provided. The various processors and the three different types of data required as input into the simulation model are mentioned. Then, with N 24th and Superior Street as an example, the entire input data that was used to build the simulation model for this intersection is presented. Next, using flow rates, the simulation model developed was verified. The next stage in the simulation process is calibration, which is described in Chapter 5.

CHAPTER 5 CALIBRATION

5.1. Purpose

The second stage in the simulation process is calibration. It is defined as the process where default simulation parameters are adjusted so as to replicate the field traffic behavior as accurately as possible (*Park and Qi, 2005*). From Table 12, it can be observed that there is a large percentage difference between field and simulated average queue delay values. So, in order to minimize this difference, the default parameters need to be adjusted. For this study, the default parameter chosen for calibration are the three car following parameters: Lambda (λ), Mu (μ) and Alpha (α). The details regarding these parameters and the theory behind their development is discussed in detail in the next section.

TABLE 12 Field and simulated average queue delay

Intersection	Minor Street	Field Average Queue Delay (s)	Sim Average Queue Delay (s)	Difference (s)	Percentage Difference (%)
S 90th and O Street	Left Turn	15.57	4.80	10.77	69.17%
	Right Turn	4.64	8.90	4.26	91.81%
	Total	5.18	8.70	3.52	**67.94%**
N 24th and Superior Street	Left Turn	20.67	10.40	10.27	49.69%
	Right Turn	9.23	6.90	2.33	25.24%
	Total	12.78	8.00	4.78	**37.40%**
S 56th and Saltillo Road	Left Turn	9.86	6.00	3.86	39.15%
	Right Turn	2.16	5.20	3.04	140.74%
	Total	6.05	5.60	0.45	**7.45%**

5.2. Car Following Parameters

A nonlinear generalized car following model was developed by General Motors (GM) Corporation in 1961. This model is used by the TEXAS model in order to simulate car

following behavior. Car following theory is based on the concept that a car following another car in dense traffic is based on a stimulus-response differential law. This theory assumes that a driver reacts in a specific way to the stimulus from the cars behind or ahead of the subject car, and this hypothesis is based on single-lane traffic with no passing. This law is only applicable to high volumes of traffic and should not be interpolated for low volumes (*Gazis, Herman and Rothery, 1961; Jones, Chandler, Herman and Montroll, 1958; Gazis, Herman and Potts, 1959; Herman and Potts, 1961; Eddie, 1961*).

This law can be stated as: Response = Sensitivity * Stimulus

The response of the driver is taken as acceleration since it can be measured easily. The stimulus is chosen as the relative speed of the car and the one ahead. The first model of car following behavior assumes that sensitivity is constant. If (n+1) car is following an nth car, then the equation is stated as:

$$\ddot{X}n+1\,(t+T) = \alpha\,[\dot{X}n\,(t) - \dot{X}n+1\,(t)] \qquad (12)$$

Where,

α = sensitivity

t = time,

T = lag time,

X_n = position of nth car,

X_{n+1} = position of (n+1) car,

$\dot{X}n$ = speed of nth car,

$\dot{X}n+1$ = speed of (n+1) car and

$\ddot{\dot{X}}n+1$ = acceleration of (n+1) car.

First, two cars were driven on General Motors' Test Track assuming that they compose homogenous traffic. The results of this test are shown in Table 13.

TABLE 13 First car following model experiment results

Measure Value	Reaction Time, Δt (s)	Sensitivity, α (s^{-1})
Minimum	1.00	0.17
Average	1.55	0.37
Maximum	2.20	0.74

Next, a step function was created for sensitivity as it was found that it is not a constant value. The second model can be stated as:

$$\ddot{X}n + 1\,(t + T) = \frac{a}{b}\,[\dot{X}n\,(t) - \dot{X}n + 1\,(t)] \qquad (13)$$

However, the above results also suggested that there might actually be a relation between sensitivity, λ, and relative spacing, s. Gazis, Herman and Potts plotted sensitivity, λ, against the inverse of spacing, 1/s. From the graph it can be noticed that λ increases with average spacing. But as it could not be measured directly in the field, a third model with new sensitivity function was developed. In the third model, sensitivity was found to be related to the average spacing, s, between two cars. The below plot shows that, as expected, sensitivity actually decreases with increased spacing.

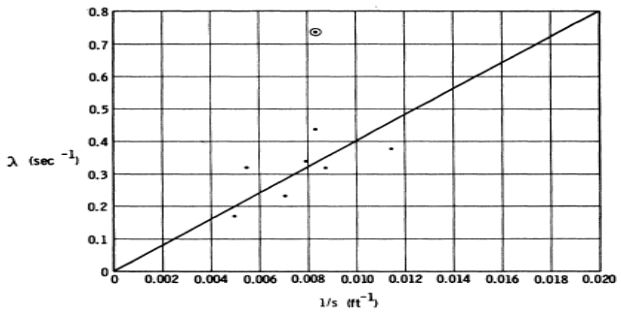

Fig. 6. Sensitivity, λ(sec⁻¹), versus the reciprocal of the car spacing, 1/s(ft⁻¹). The least-squares straight line is represented by λ = (40.2/s)sec⁻¹. The data were obtained from reference 3. The encircled point was not included in the fit.

FIGURE 21 A plot of sensitivity against average spacing

The third car following model is expressed as:

$$\ddot{X}_{n+1}\,(t+T) = \frac{\alpha}{[X_n\,(t) - X_{n+1}\,(t)]}\,[\dot{X}_n\,(t) - \dot{X}_{n+1}\,(t)] \qquad (14)$$

The results obtained by using the above third model are shown in Table 14.

TABLE 14 Third car following model experiment results

Location	Reaction Time, Δt (s)	Sensitivity, α_0 (s^{-1})
GM Test Track	1.5	40.3
Holland Tunnel	1.4	26.8
Lincoln Tunnel	1.2	29.8

Then, in 1961, Eddie assumed sensitivity as shown below:

$$\lambda = \frac{\alpha\,[\dot{X}_{n+1}\,(t+T)]}{[X_n\,(t) - X_{n+1}\,(t)]^2} \qquad (15)$$

Whereas Greenshields, in 1935, in the equation for steady state traffic flow, described the sensitivity function as:

$$\lambda = \frac{\alpha}{[X_n\,(t) - X_{n+1}\,(t)]^2} \qquad (16)$$

Based on the above two equations, the car following model can be generalized as:

$$\ddot{X}_{n+1}\,(t+T) = \frac{\alpha\,[\dot{X}_{n+1}\,(t+T)]^m}{[X_n\,(t) - X_{n+1}\,(t)]^l}\,[\dot{X}_n\,(t) - \dot{X}_{n+1}\,(t)] \qquad (17)$$

By substituting the following values shown in Table 15 for m and l in the above equation, all the four car following models can be obtained from the generalized model.

TABLE 15 Values for m and l for first to fourth model

m	l	Model
0	0	First, Second
0	1	Third
1	1	Fourth

In the TEXAS simulation model, notations of μ and λ are used for the m and l parameters, respectively. The lowest value for parameter lambda, a value of 1, is used during the calibration process as opposed to the lowest value of 2.3 available in the simulation model. From Table 16, the lowest value for lambda was found to be 1, hence this value is used. This value is named GM4, meaning General Motors fourth model value. This is because by substituting a lambda value of 1 in the generalized car following model, the fourth model is obtained.

5.3. Warm-Up Time

Warm-up time is the amount of time required by the simulation model to reach a steady state. If the model is run without reaching a steady state, then the results are unreliable. Hence, warm-up time for each study site was determined.

In order to determine the warm-up period, the following procedure is adopted. For a constant warm-up time of 0 minutes and simulation times varying from 0 to 60 minutes the average queue delay values are plotted. For the first 15 minutes of simulation time 1 minute increments are used. After 15 minutes and until 60 minutes, 5-minute intervals are plotted as shown in Figures 22-24 below. For N 24th and Superior Street the corresponding average queue delay values are shown in Table 16.

From the charts, it was found that each intersection had a different warm-up time. For instance, for N 24th and Superior Street it is 15 minutes, for S 56th and Saltillo Road it is 5 minutes and for S 90th and O Street it is 15 minutes. But in order to be consistent for all the study sites, the maximum warm-up time of 15 minutes was chosen for the study.

TABLE 16 Average queue delay for each run of warm-up time determination of N 24th and Superior Street

Warm-Up Time (minutes)	Length of Simulation (minutes)	Left Turn Lane Avg Queue Delay (s)	Right Turn Lane Avg Queue Delay (s)	Minor Street Avg Queue Delay (s)
0	0	0.0	0.0	0.0
0	1	0.0	2.5	2.5
0	2	5.5	4.3	4.6
0	3	6.6	6.2	6.4
0	4	6.1	6.2	6.2
0	5	6.7	5.4	6.1
0	6	6.4	5.4	6.0
0	7	5.7	5.4	5.6
0	8	5.7	5.3	5.5
0	9	5.8	5.3	5.6
0	10	6.3	4.9	5.6
0	11	5.5	5.9	5.7
0	12	6.3	5.3	5.9
0	13	4.7	5.0	4.8
0	14	4.6	5.4	5.0
0	15	5.1	5.6	5.3
0	20	4.7	5.4	5.1
0	25	7.0	5.6	6.3
0	30	5.8	5.8	5.8
0	35	6.4	4.7	5.6
0	40	5.8	6.2	6.0
0	45	5.7	5.4	5.6
0	50	5.6	5.4	5.5
0	55	6.3	5.9	6.1
0	60	6.0	5.6	5.8

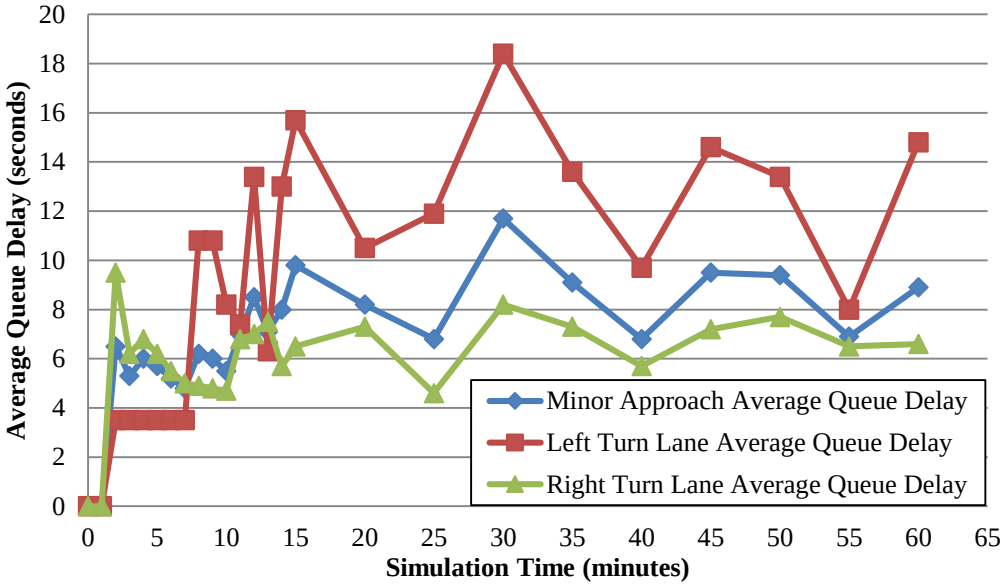

(a)

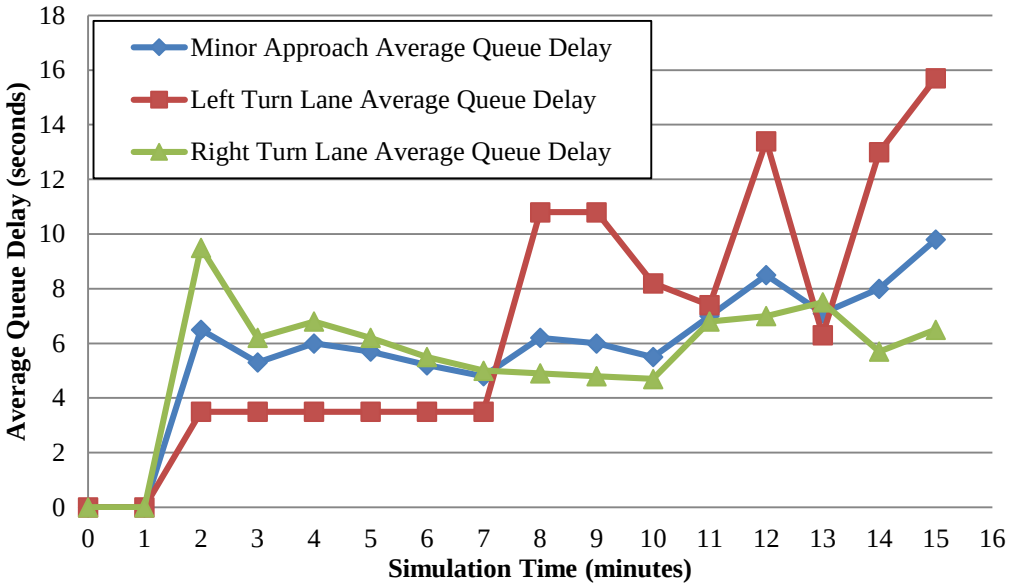

(b)

FIGURE 22 A plot for determination of warm-up time for N 24th and Superior Street (a) In 5-minute increments for 1 hour duration of simulation time (b) In 1-minute increments for first 15 minutes of simulation time

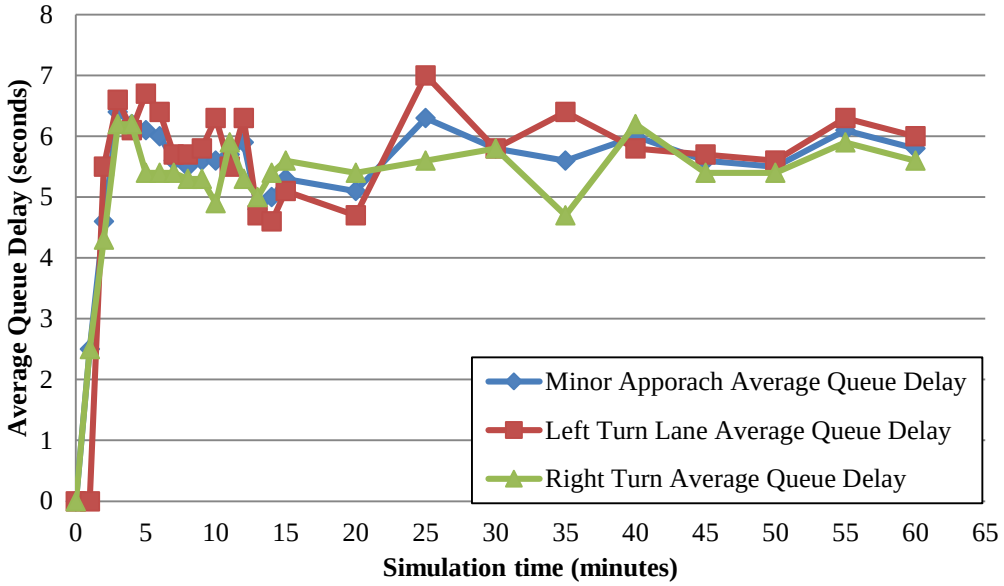

(a)

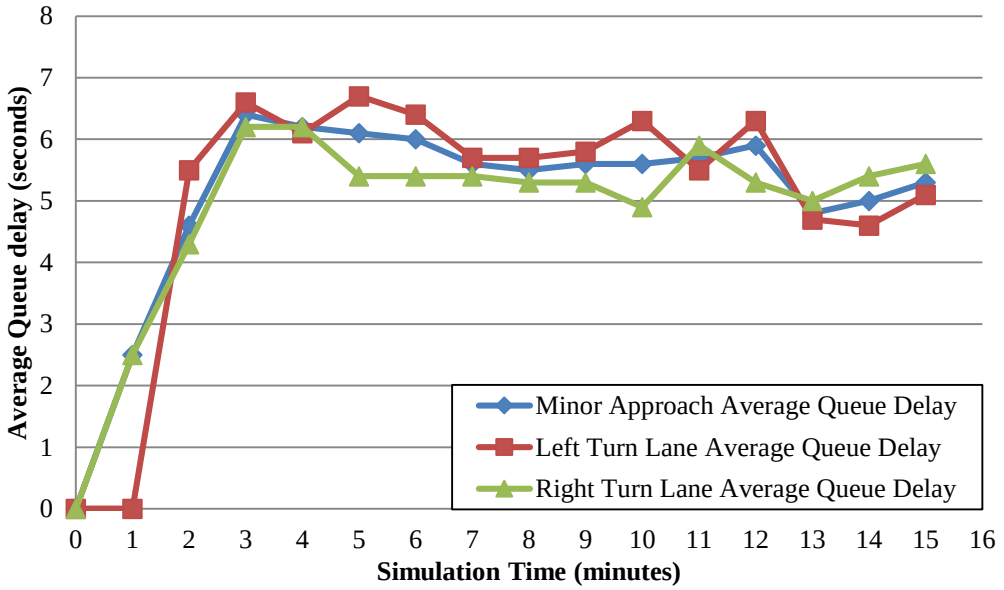

(b)

FIGURE 23 A plot for determination of warm-up time for S 56th and Saltillo Road (a) In 5-minute increments for 1 hour duration of simulation time (b) In 1-minute increments for first 15 minutes of simulation time

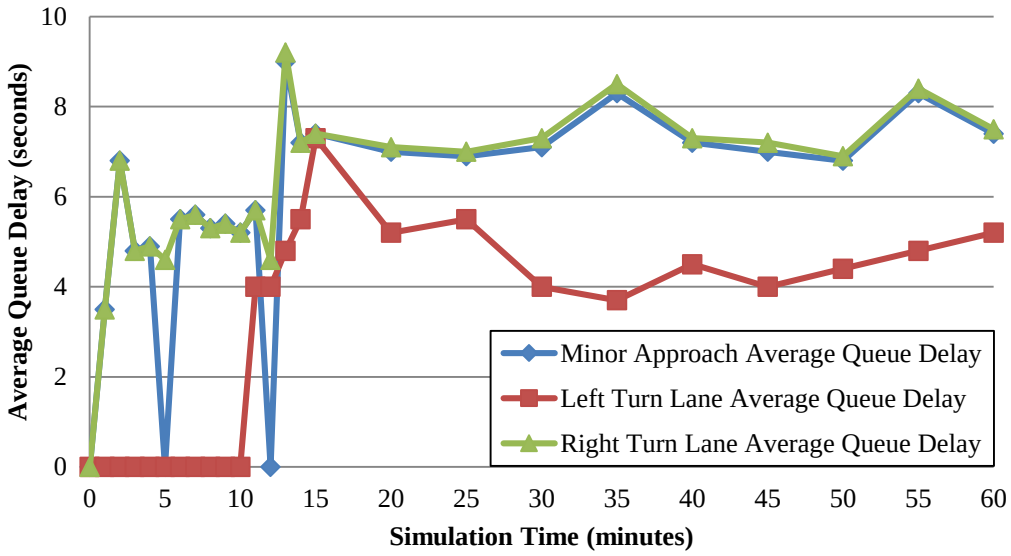

(a)

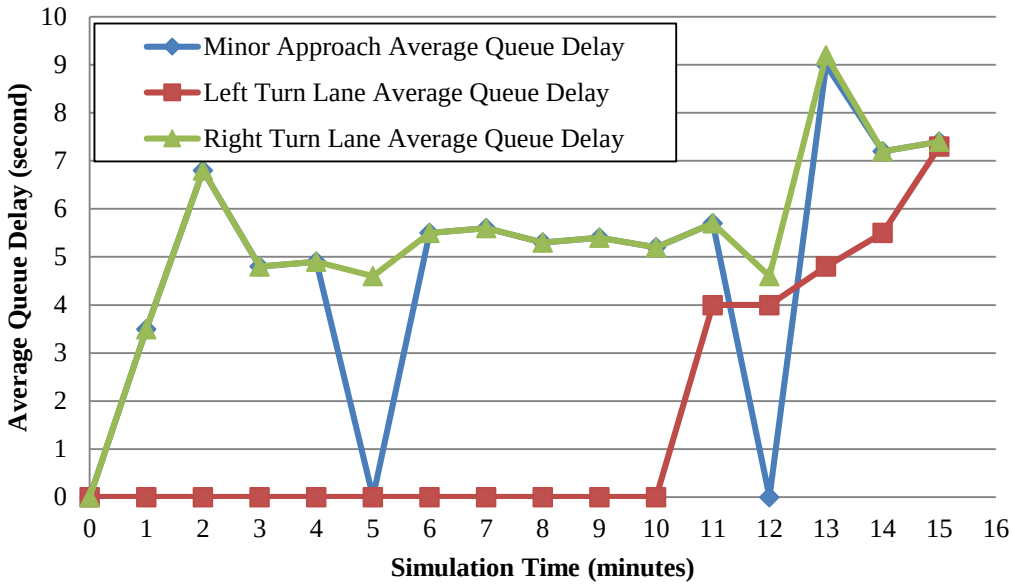

(b)

FIGURE 24 A plot for determination of warm-up time for S 90th and O Street (a) In 5-minute increments for 1 hour duration of simulation time and (b) In 1-minute increments for first 15 minutes of simulation time

5.4. Procedure

A trial-and-error method of calibration is used in this study. Through manual adjustments and common sense, the three car following parameters were adjusted from their default values until a close match between simulation and field average queue delay was obtained. Using the N 24th and Superior Street intersection results, this calibration procedure will be demonstrated. The simulation model was run at a 10% tolerance level.

The first step was to understand in which direction the calibration procedure should be continued. So at first the model was run at default values of car following parameters. Then, the model was run at the lowest value and finally at the highest value available in the simulation model. For example, in the case of lambda, first the model was run at the default value (d) of 2.8, then at the lowest value of 1 (GM4) and finally at the highest value (h) of 4. When lambda is varied, the remaining parameters mu and alpha are kept constant. A similar procedure is carried out for the remaining two car following parameters mu and alpha. The corresponding results are shown in Table 17 and Figures 25-27.

From Figure 25, it is evident that the optimum value for lambda is its General Motors value (which is lower than the lowest value available in the model) as it lies closer to the unity slope line. Therefore, the calibration process for lambda is started from its low value and is increased in small increments until the field and simulated average queue delay have a minimal difference between them. For the rest of the intersections, these directional charts and corresponding data are included in Appendix B.

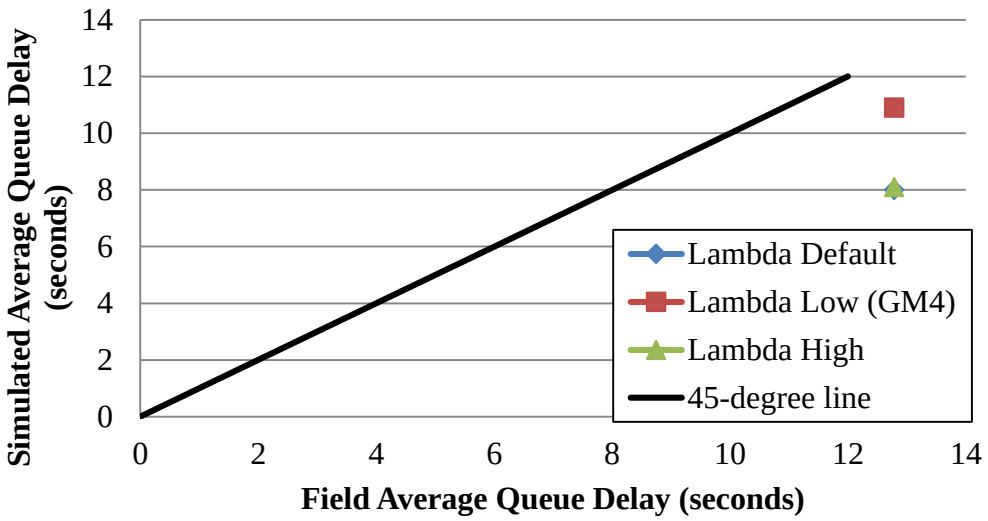

FIGURE 25 Lambda calibration direction for N 24th and Superior Street

The mu value is almost the same at all the three levels of variation. But from Table 18, it can be seen that the mu high value is slightly closer to the unit slope line, thereby the calibration was started for mu from its highest value and then gradually decreased.

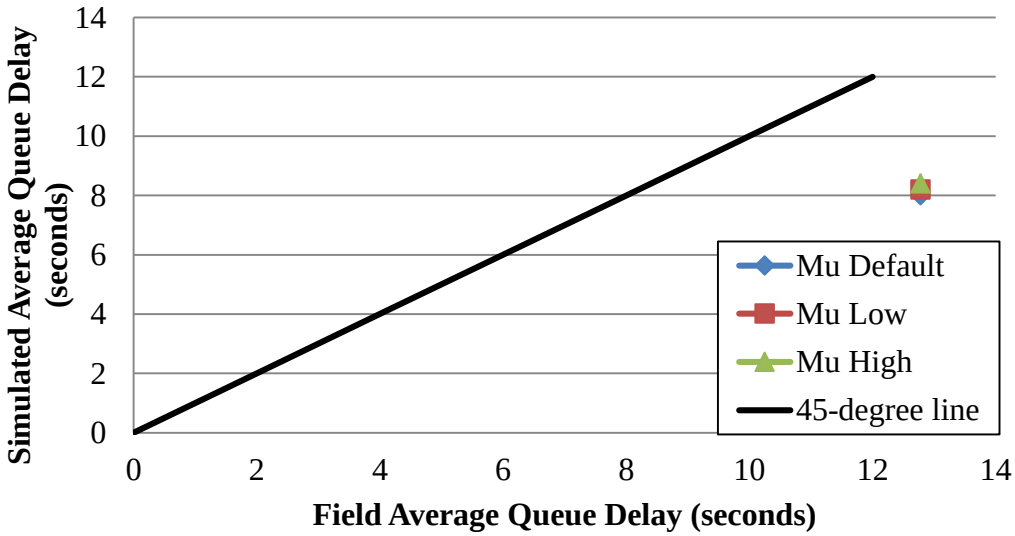

FIGURE 26 Mu calibration direction for N 24th and Superior Street

From Figure 27, it can be concluded that the alpha value at its high level is close to the unity slope line. So, the calibration for alpha will be started from its highest value and will be decreased in small increments.

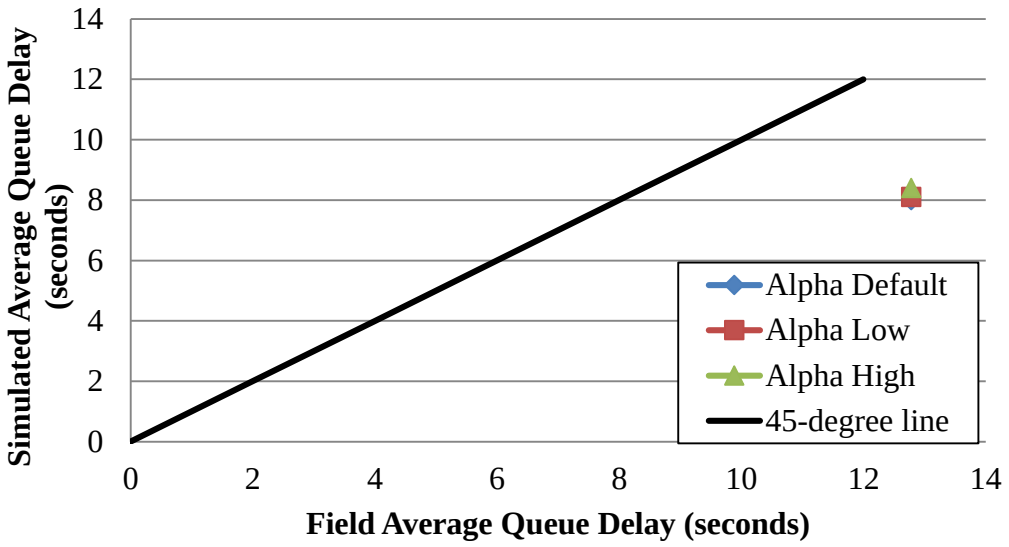

FIGURE 27 Alpha calibration direction for N 24th and Superior Street

TABLE 17 First stage calibration results of N 24th and Superior Street

Minor Street	Car Following Parameters	Field Average Queue Delay (s)	Sim Average Queue Delay (s)	Absolute Difference (s)	% Difference
LT Turn	Lambda = 2.8 (d)	20.67	10.4	10.27	49.69%
RT Turn	Mu = 0.8 (d)	9.23	6.9	2.33	25.24%
Total	Alpha = 4000 (d)	12.78	8	4.78	37.40%
LT Turn	Lambda = 1 (GM4)	20.67	12.9	7.77	37.59%
RT Turn	Mu = 0.8 (d)	9.23	7.5	1.73	18.74%
Total	Alpha = 4000 (d)	12.78	9.1	3.68	28.79%
LT Turn	Lambda = 4 (h)	20.67	11.8	8.87	42.91%
RT Turn	Mu = 0.8 (d)	9.23	6.5	2.73	29.58%
Total	Alpha = 4000 (d)	12.78	8.1	4.68	36.62%
LT Turn	Lambda = 2.8 (d)	20.67	12.3	8.37	40.49%
RT Turn	Mu = 0.6 (l)	9.23	6.5	2.73	29.58%
Total	Alpha = 4000 (d)	12.78	8.2	4.58	35.84%
LT Turn	Lambda = 2.8 (d)	20.67	13	7.67	37.11%

RT Turn	Mu = 1 (h)	9.23	6.4	2.83	30.66%
Total	Alpha = 4000 (d)	12.78	8.4	4.38	34.27%

TABLE 17 First stage calibration results of N 24th and Superior Street (continued)

Minor Street	Car Following Parameters	Field Average Queue Delay (s)	Sim Average Queue Delay (s)	Absolute Difference (s)	% Difference
LT Turn	Lambda = 2.8 (d)	20.67	12	8.67	41.94%
RT Turn	Mu = 0.8 (d)	9.23	6.4	2.83	30.66%
Total	Alpha = 1 (l)	12.78	8.1	4.68	36.62%
LT Turn	Lambda = 2.8 (d)	20.67	13.3	7.37	35.66%
RT Turn	Mu = 0.8 (d)	9.23	6.3	2.93	31.74%
Total	Alpha = 9999 (h)	12.78	8.4	4.38	34.27%

d = default, GM4 = General Motors fourth model, h = high, l = low

So, in summary, the lowest value for lambda and the highest values for mu and alpha are the optimum set at this initial stage. Next, by manual adjustment these parameters will be increased from their lowest value or decreased from their highest value until a close match between field average queue delay and simulated average queue delay is achieved. Table 19 shows the results of this fine tuning where the first process is started with the initial optimum set and finally ends when the lowest percentage difference between field and simulation average queue delay for the total minor street is obtained.

TABLE 18 Second stage calibration results of N 24th and Superior Street

Minor Street	Car Following Parameters	Field Avg Queue Delay (s)	Sim Avg Queue Delay (s)	Absolute Difference	% Difference
LT Turn	Lambda = 1	20.67	12.9	7.77	37.59%
RT Turn	Mu = 1 (h)	9.23	7.5	1.73	18.74%
Total	Alpha =9999	12.78	9.1	3.68	28.79%
LT Turn	Lambda = 1 (GM4)	20.67	12.9	7.77	37.59%
RT Turn	Mu = 0.8 (d)	9.23	7.5	1.73	18.74%
Total	Alpha = 6000	12.78	9.1	3.68	28.79%
LT Turn	Lambda = 1 (GM4)	20.67	12.9	7.77	37.59%
RT Turn	Mu = 0.8 (d)	9.23	7.5	1.73	18.74%
Total	Alpha = 8000	12.78	9.1	3.68	28.79%
LT Turn	Lambda = 1 (GM4)	20.67	12.9	7.77	37.59%
RT Turn	Mu = 0.8 (d)	9.23	7.5	1.73	18.74%
Total	Alpha = 2000	12.78	9.2	3.58	**28.01%**

For the rest of the intersections, these calibration results are included in Appendix B. In summary, the optimum set of car following parameters for each intersection is shown in Table 19.

TABLE 19 Calibration results

Intersection	Minor Street	Car Following Parameters	Field Average Queue Delay (s)	Sim Average Queue Delay (s)	Difference (s)	Percentage Difference (%)
S 90th and O Street	Left Turn	Lambda = 2.8 (d)	15.57	5.00	10.57	67.89%
	Right Turn	Mu = 0.8 (d)	4.64	5.10	0.46	9.91%
	Total	Alpha = 6000	5.18	5.10	0.08	**1.55%**
N 24th and Superior Street	Left Turn	Lambda = 1 (GM4)	20.67	12.90	7.77	37.59%
	Right Turn	Mu = 0.8 (d)	9.23	7.50	1.73	18.74%
	Total	Alpha = 2000	12.78	9.20	3.58	**28.01%**
S 56th and Saltillo Road	Left Turn	Lambda = 1 (GM4)	9.86	6.30	3.56	36.11%
	Right Turn	Mu = 0.8 (d)	2.16	5.90	3.74	173.15%
	Total	Alpha = 4000 (d)	6.05	6.10	0.05	**0.82%**

While running the model there were a few errors such as clear zone intrusion, vehicles using a different approach and vehicles eliminated. These errors do not affect the output results and hence were ignored.

5.5. Chapter Summary

The theory behind the development of the car following model is discussed. Warm-up time is determined for each study site, and in order to be consistent a maximum value of 15 minutes is used for all sites. Large differences between the field and simulated average queue delay values dictated the need to calibrate the simulation model. Calibration was done using the three car following parameters. The trial and error

method of calibration was utilized. Car following parameters were adjusted based on the direction in which the percentage difference between field and simulated average queue delay was decreasing. The calibrated model is ready to be used as an evaluation tool. Therefore, Chapter 6 describes the procedure regarding how the effect of skew angle on average queue delay is evaluated using the TEXAS simulation model.

CHAPTER 6 ANALYSIS AND RESULTS

6.1. Introduction

The main objective of this research is to evaluate the effect of skew angle on average queue delay with the help of the TEXAS simulation model. The Green Book (*AASHTO, 2011*) suggests that the legs of an intersection should be perpendicular with each other. In other words, the skew angle between them should be 0°. But in reality, if this cannot be achieved, then the skew angle of an intersection should not exceed 30°. Hence, with 30° as the maximum skew angle value, the analysis was performed. In order to understand the effect of skew angle on average queue delay, the simulation model was run at various skew angle increments. The skew angle is varied or deviated from the base skew angle observed in field. For all the three study site intersections, skew angle is 0°. Then the corresponding average queue delay value for each skew angle increment is plotted to see if the plot follows the expected pattern of a "U" shape.

6.2. Running the Model

Initially, the model was run for skew angle increments of: ±30°, ±15°, ±10° and ±5°. Right skew is considered to be negative skew angle and left skew is positive skew angle. For each one of the above skew angle increments, the model was run for 30 runs. From one run to another run, only skew angle and random numbers are varied; remaining parameters are kept constant. The average queue delay value reported for each skew angle increment is the average value of 30 runs.

By following the above procedure for each study site, the average queue delay values were recorded for each skew angle increment. These results are shown in Tables 20-22,

and plots showing the trend of this effect are included in Figures 28-30. The average queue delay for each skew angle increment is also expressed in terms of the percentage of base skew angle (0°).

TABLE 20 Average queue delay for skew angle increments for N 24th and Superior Street

Skew Angle Deviation from Base Skew (degrees)	Left Turns		Right Turns		Minor Street Total	
	Delay (s)	Delay as % of Base Delay (%)	Delay (s)	Delay as % of Base Delay (%)	Delay (s)	Delay as % of Base Delay (%)
-30	9.9	77%	6.7	90%	7.7	83%
-15	13.9	108%	8.2	109%	9.9	107%
-10	12.1	94%	7.0	94%	8.5	93%
-5	12.8	100%	6.8	90%	8.6	93%
0	12.9	100%	7.5	100%	9.2	100%
5	13.5	105%	7.1	94%	9.0	98%
10	13.6	105%	7.7	103%	9.5	103%
15	14.3	111%	7.6	102%	9.7	105%
30	19.3	150%	8.3	110%	11.5	125%

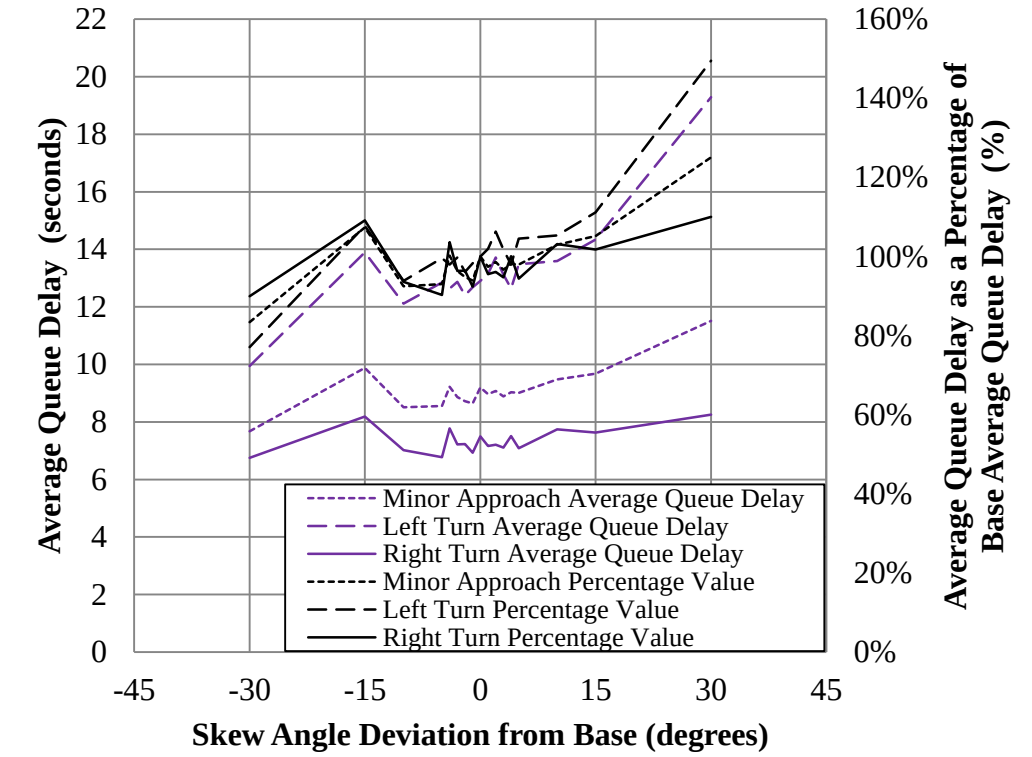

FIGURE 28 Plot showing the effect of skew angle increments on average queue delay for N 24th and Superior Street

From Figure 28, it was observed that for the N 24th and Superior Street intersection, for skew angle increments of up to ±15° from the base case of 0° skew, the expected U shape pattern was seen. But beyond ±15° this trend did not continue.

TABLE 21 Average queue delay for skew angle increments for S 56th and Saltillo Road

Skew Angle Deviation from Base Skew (degrees)	Left Turns		Right Turns		Minor Street Total	
	Delay (s)	Delay as % of Base Delay (%)	Delay (s)	Delay as % of Base Delay (%)	Delay (s)	Delay as % of Base Delay (%)
-30	4.8	76%	5.0	85%	4.9	80%
-15	5.3	85%	5.4	92%	5.4	88%
-10	6.0	96%	6.0	102%	6.0	99%
-5	6.4	101%	6.1	103%	6.2	102%
0	6.3	100%	5.9	100%	6.1	100%
5	7.0	112%	6.6	113%	6.8	112%
10	7.0	110%	6.6	112%	6.8	111%
15	7.1	112%	6.4	109%	6.8	111%
30	7.5	119%	6.7	113%	7.1	116%

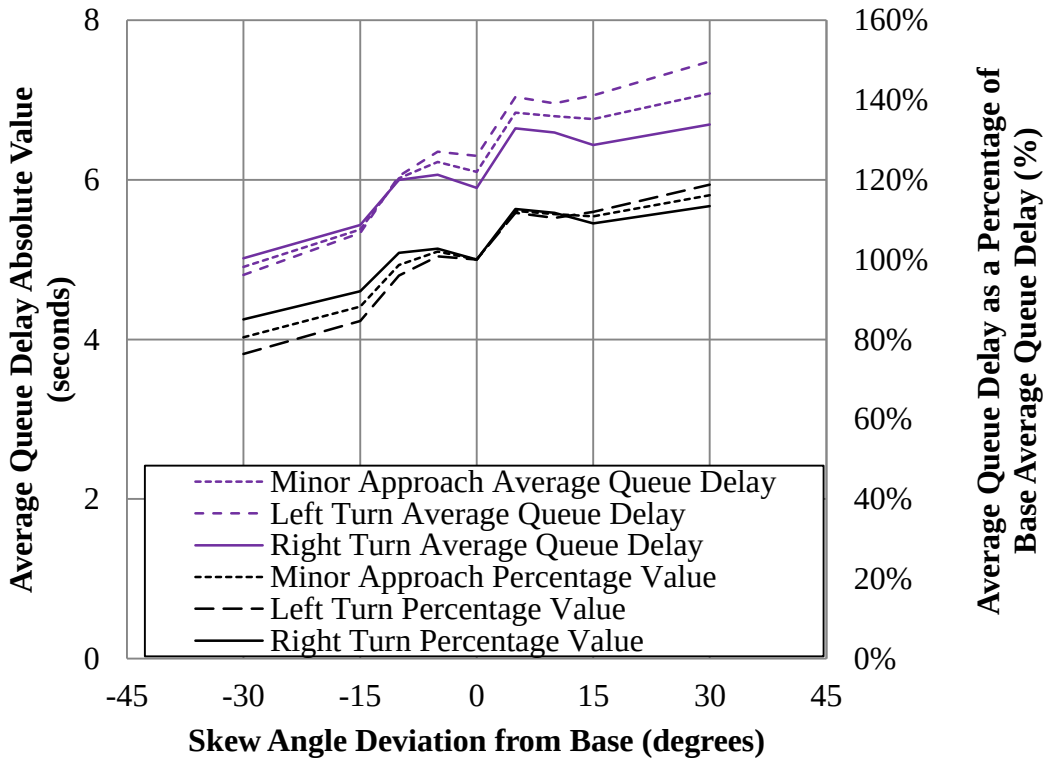

FIGURE 29 Plot showing the effect of skew angle increments on average queue delay for S 56th and Saltillo Road

The expected U shape pattern could be seen right at the center of Figure 29. This pattern ended beyond ±5° skew angle.

TABLE 22 Average queue delay for skew angle increments for S 90th and O Street

Skew Angle Deviation from Base Skew (degrees)	Left Turns		Right Turns		Minor Street Total	
	Delay (s)	Delay as % of Base Delay (%)	Delay (s)	Delay as % of Base Delay (%)	Delay (s)	Delay as % of Base Delay (%)
-30	4.1	84%	5.7	112%	5.6	110%
-15	4.3	88%	5.8	114%	5.7	113%
-10	4.3	89%	5.9	116%	5.8	114%
-5	4.3	88%	6.0	117%	5.9	115%
0	4.9	100%	5.1	100%	5.1	100%
5	4.8	98%	6.2	122%	6.2	121%
10	4.6	93%	6.3	123%	6.2	122%
15	4.8	99%	6.4	125%	6.3	123%
30	5.0	103%	7.3	143%	7.2	141%

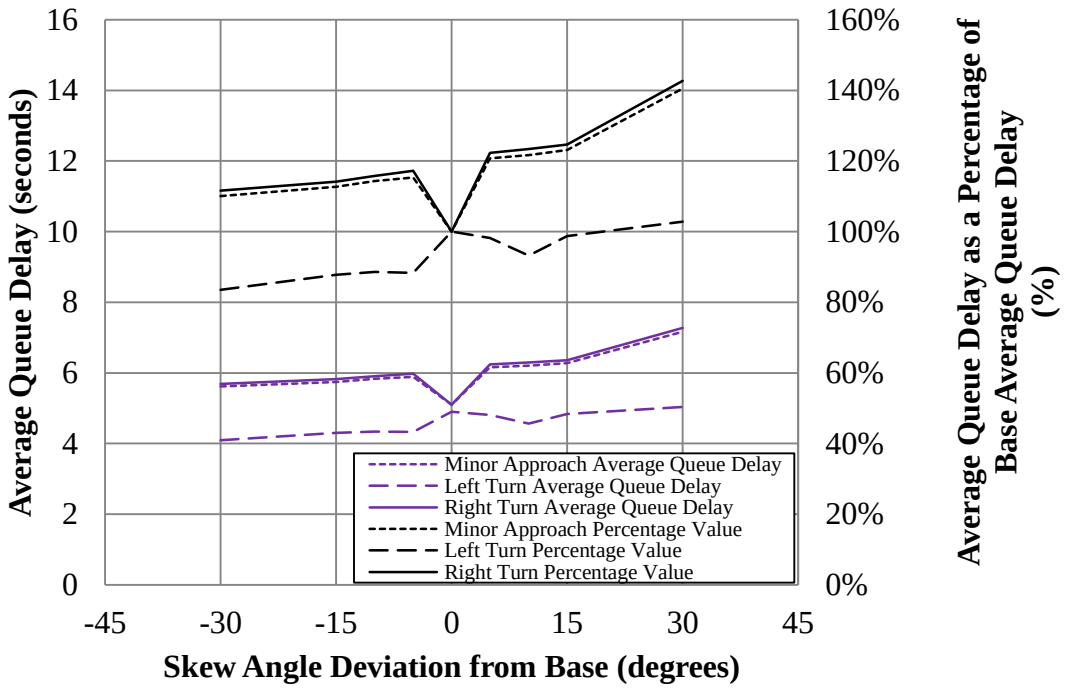

FIGURE 30 Plot showing the effect of skew angle increments on average queue delay for S 90th and O Street

Except for left turns, for skew angle of up to ±5° the expected U shape pattern could be noticed for the S 90th and O Street intersection.

For small skew angle increments of up to ±5°, the simulation results showed that average queue delay varies with skew angle as per the expectation. In order to further verify this aspect, additional runs were performed. Hence, the model was further run for 1° skew angle increments between 0° and ±5°. So, the additional skew angle increments analyzed are: ±1°, ±2°, ±3° and ±4°. These results are shown in Tables 23-25 and plots in Figures 31-33.

TABLE 23 Average queue delay for 1° skew angle increments for N 24th and Superior Street

Skew Angle Deviation from Base Skew (degrees)	Left Turns		Right Turns		Minor Street Total	
	Delay (s)	Delay as % of Base Delay (%)	Delay (s)	Delay as % of Base Delay (%)	Delay (s)	Delay as % of Base Delay (%)
-5	12.8	100%	6.8	90%	8.6	93%
-4	12.6	98%	7.8	104%	9.2	100%
-3	12.9	100%	7.2	96%	8.9	96%
-2	12.4	96%	7.2	96%	8.7	95%
-1	12.7	98	6.9	92	8.6	94%
0	12.9	100%	7.5	100%	9.2	100%
1	13.2	102	7.2	96	9.0	97%
2	13.7	106%	7.2	96%	9.1	99%
3	13.1	102%	7.1	95%	8.9	97%
4	12.6	98%	7.5	100%	9.0	98%
5	13.5	105%	7.1	94%	9.0	98%

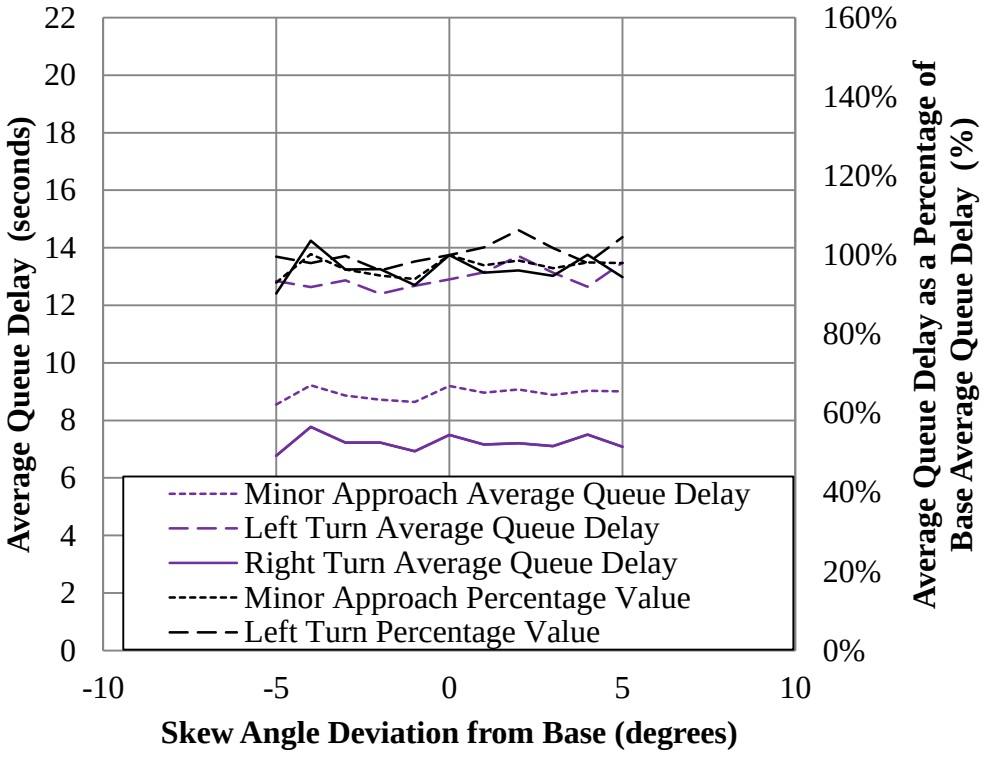

FIGURE 31 Plot showing the effect of 1° skew angle increments on average queue delay for N 24th and Superior Street

Figure 31 shows that the expected U shape pattern could be seen only until ±4°, instead of until ±5°, which was concluded earlier from Figure 28.

TABLE 24 Average queue delay for 1° skew angle increments for S 56th and Saltillo Road

Skew Angle Deviation from Base Skew (degrees)	Left Turns		Right Turns		Minor Street Total	
	Delay (s)	Delay as % of Base Delay (%)	Delay (s)	Delay as % of Base Delay (%)	Delay (s)	Delay as % of Base Delay (%)
-5	6.4	101%	6.1	103%	6.2	102%
-4	6.4	102%	6.4	109%	6.4	105%
-3	6.6	104%	6.4	108%	6.5	106%
-2	6.5	103%	6.6	112%	6.6	108%
-1	6.6	104%	6.2	106%	6.4	105%
0	6.3	100%	5.9	100%	6.1	100%
1	6.5	103%	6.5	109%	6.5	106%
2	6.9	109%	6.5	111%	6.7	110%
3	6.8	108%	6.6	112%	6.7	110%
4	6.8	108%	6.6	111%	6.7	109%
5	7.1	112%	6.6	111%	6.8	112%

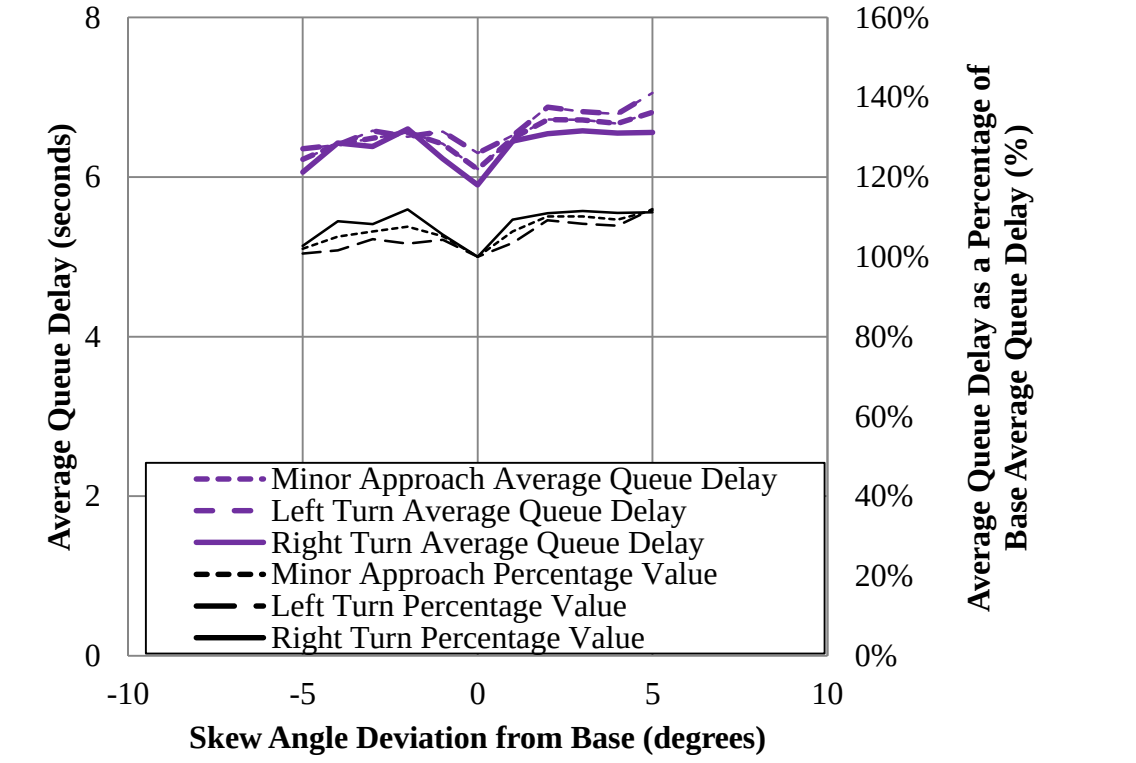

FIGURE 32 Plot showing the effect of 1° skew angle increments on average queue delay for S 56th and Saltillo Road

Beyond ±1° skew angle increment, average queue delay does not vary with skew angle in the assumed fashion for S 56th and Saltillo Road.

TABLE 25 Average queue delay for 1° skew angle increments for S 90th and O Street

Skew Angle Deviation from Base Skew (degrees)	Left Turns		Right Turns		Minor Street Total	
	Delay (s)	Delay as % of Base Delay (%)	Delay (s)	Delay as % of Base Delay (%)	Delay (s)	Delay as % of Base Delay (%)
-5	4.3	88%	6.0	117%	5.9	115%
-4	4.5	91%	5.9	116%	5.9	115%
-3	4.4	90%	5.9	116%	5.8	114%
-2	4.5	92%	6.0	117%	5.9	116%
-1	4.6	94%	6.0	117%	5.9	115%
0	4.9	100%	5.1	100%	5.1	100%
1	4.6	93%	6.1	121%	6.1	119%
2	5.4	110%	5.8	114%	5.8	114%
3	4.6	94%	6.0	118%	5.9	116%
4	4.7	96%	5.4	106%	5.4	106%
5	4.8	98%	6.2	122%	6.2	121%

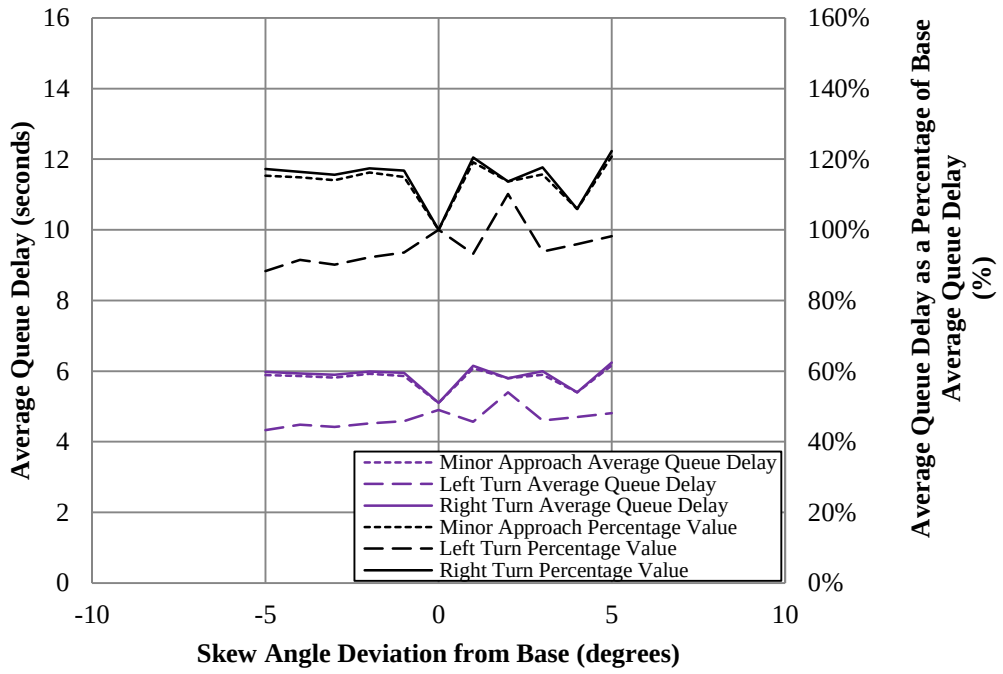

FIGURE 33 Plot showing the effect of 1° skew angle increments on average queue delay for S 90th and O Street

From Figure 30, it can be observed that until ±1° skew angle, the U shape pattern follows with an exception for left turns. Earlier, when plotted in ±5° skew angle increments, the desired effect was found until ±°5. Appendix C contains data regarding individual average queue delay values for 30 runs for each one of the above skew angle increments for N 24th and Superior Street as an example.

6.3. Chapter Summary

An experiment was designed to study the effect of skew angle on average queue delay. This experiment was composed of running the simulation model for each study site at skew angle increments of ±30°, ±15°, ±10°, ±5°, ±4°, ±3°, ±2° and ±1° from base skew angle in the field. Based on these results, conclusions are drawn and also future recommendations are made in the last chapter.

CHAPTER 7 CONCLUSION AND RECOMMENDATIONS

7.1. Conclusions

The two hypotheses of this research are firstly to evaluate the effect of skew angle on average queue delay and secondly to verify that the TEXAS model is capable of considering the effect of geometric changes on traffic operations. The second hypothesis will become true if the results follow the expected U shape trend. Based on the results presented in an earlier chapter, and in view of the above two hypotheses, the following conclusions can be drawn:

(1) If average queue delay is plotted in ±5° skew angle increments from base skew angle observed in the field, then for up to skew angle of ±5°, the desired U shape pattern was noticed. Further runs of ±1° skew angle increments showed that instead of ±5°, for ±1° skew angle increments, the expectations are met.

(2) The effect of skew angle on average queue delay is assumed to follow a trend similar to that of a U shape. This expected pattern could be seen for small skew angle increments of ±1°. For large skew angle increments, the simulation results did not follow this trend. Hence, TEXAS simulation results met the expectations only for small skew angle increments.

(3) The average queue delay value was found to be changing with varying skew angles. Hence, the TEXAS model seems to be considering the effect of changes in geometry on traffic behavior.

7.2. Future Recommendations

The three study sites of this project chosen from a previous study are all non-skewed intersections. If the average queue delay data for intersections that were earlier skewed and later were reconfigured to a reduced skew angle or no skew was available, then it can be helpful to speculate on the accuracy of simulation results. The calibration results were better when the fourth General Motors value is used as the lowest value for the car following parameter lambda instead of the original lowest value available in the simulation model. The lower boundary value for this parameter may need to be considered for revision. Sight distance has an effect on the queue delay experienced by the minor street drivers. The study sites have separate lanes for left turns and right turns on minor streets, instead of the typical single lane for both turns. As a result of this the sight distance of the vehicles is obstructed when two vehicles arrive at the stop sign at the same time. The TEXAS simulation model considers the sight distance obstruction caused only due to the presence of tall buildings and not vehicles. If the TEXAS model sight distance logic can include this effect too, then the simulation model will be better.

REFERENCES

1. http://www.sha.state.md.us/WebProjectLifeCycle/PG221_11/htdocs/Documents/EIS/04_purp_need.pdf. Accessed July 2010.
2. A Policy on Geometric Design of Highways and Streets. AASHTO, Washington, D.C., 2011.
3. Bonneson, J.A. Bridge Size and Clearance Time of Single-Point Urban Interchange. Journal of Transportation Engineering, Vol. 119, No.1, American Society of Civil Engineers, Washington, D.C., 1993.
4. Burchett, G.D. and T.H. Maze. Rural Expressway Intersection Characteristics as Factors in Reducing Safety Performance. In Transportation Research Record 1953, Transportation Research Board, National Research Council, Washington, D.C., 2006, pp.71-80.
5. Central Florida Geographic Information systems. 2005. http://www.cfgis.org/projectdiary/filestore/1208_20050324_project%20info.pdf. Accessed July 2010.
6. Chandler,. R.E., R. Herman, and E.W. Montroll. Traffic Dynamics: Studies in Car Following. Operations Research Vol. 6, 1958, pp. 165-184.
7. Currin, T.R. Introduction to Traffic Engineering. A manual for Data Collection and Analysis. Brooks/Cole, CA, 2001.
8. Eddie, L.C. Car-Following and Steady State Theory for Non Congested Traffic. Operations Research 9, 1961, pp. 66-76.

9. Garcia, A. and E.B. Esplugues. Lateral Vision Angles in Roadway Geometric Design. Journal of Transportation Engineering Vol. 133, No. 12, ASCE, 2007, pp. 654-662.

10. Gatling, F. and A. Whyte. The Effect of Vehicle Positioning on Lag Acceptance. Public Roads, Vol. 36, No. 9, August 1971, pp. 190-191.

11. Gattis, J.L. and S.T. Low. Intersection Angles and Driver's Field of View. Mack-Blackwell Transportation Center, University of Arkansas, Fayetteville, AR, 1997.

12. Gazis, D.C., R. Herman, and R.W. Rothery. Nonlinear Follow-the-Leader Models of Traffic Flow. Operations Research vol. 9, No. 4, pp. 545-567, 1961.

13. Gazis, D.C., R. Herman, and R.B. Potts. Car Following Theory of Steady-State Traffic Flow. Operations Research 7, 1959, pp. 499-505.

14. Grayson, G.E. Typical Application of the TEXAS model. Transportation Special Report 194, Transportation Research Board, Washington, D.C., 1981.

15. Grayson, G.E. Evaluation of Traffic Signal Warrants Using the Texas Simulation Model. Master's thesis, Department of Civil Engineering, University of Texas, Austin, 1976.

16. Harwood, D.W., F.M. Council, E. Hauer, W.E. Hughes, and A. Vogt. Prediction of the Expected Safety Performance of Rural Two-Lane Highways. Report No. FHWA-RD-99-207, Midwest Research Institute, Kansas City, Missouri, 2000.

17. Hauer, E. The Safety of Older Persons at Intersections. Transportation in an Aging Society. Special Report 218, Vol. 2. Transportation Research Board, National Research Council, Washington, D.C., 1988, pp. 194-254.

18. Herman, R. and R.B. Potts. Single Lane Traffic Theory and Experiment. Theory of Traffic Flow Proceedings, Research Laboratories, General Motors Corporation 1959, Elsevier Scientific Publishing Company 1961, pp. 120-146.

19. Highway Capacity Manual. Transportation Research Board, National Research Council, Washington, D.C., 2000.

20. Hunter-Zaworski, K.M. T Intersection Simulator Performance of Drivers with Physical Limitations. In Transportation Research Record 1281, Transportation Research Board, National Research Council, Washington, D.C., 1988, pp.11-15.

21. Jones, E. Density on Uninterrupted Flow Facilities. CIVE 864; lecture, Civil Engineering Department, University of Nebraska, Lincoln.

22. Kyte, M., W. Kittelson, T.Z. Zhong, B. Robinson, and M. Vandehey. Analysis of Traffic Operation at All-Way Stop-Controlled Intersections by Simulation. In Transportation Research Record 1555, Transportation Research Board, National Research Council, Washington, D.C., 1996, pp. 65-73.

23. Lee, C.E. and V.S. Savur. Analysis of Intersection Capacity and Level of Service by Simulation. In Transportation Research Record 699, Transportation Research Board, National Research Council, Washington, D.C., 1979, pp. 34-41.

24. Lee, C.E., V.S. Savur, and G.E. Grayson. Application of the Texas Model for Analysis of Intersection Capacity and Evaluation of Traffic Control Warrants.

Report No. FHWA-TX-79-184-4F, Center for Transportation Research, University of Texas at Austin, July 1978.

25. Lee, C.E., T.W. Rioux, and C.R. Copeland. The TEXAS Model for Intersection Traffic-Development. Research Report Number FHWATX-78-184-1, Center for Highway Research, University of Texas at Austin, TX, 1977.

26. Lee, C.E., G.E. Grayson, C.R. Copeland, J.W. Miller, T.W. Rioux, and V.S. Savur. The TEXAS Model for Intersection Traffic-User's Guide. Research Report Number FHWATX-78-184-3, Center for Highway Research, University of Texas at Austin, TX, 1977.

27. Liao, T.Y. and R.B. Machemehl. Prediction of Mobile Source Emissions and Fuel Consumption Using the Texas model. Report No. SWUTC/95/60032-1, Center for Transportation Research, University of Texas at Austin, 1995.

28. Liao, T.Y. and R.B. Machemehl. Energy Conservation through Enhanced Traffic Signal Responsiveness. Report No. SWUTC/95/60063-1, Center for Transportation Research, University of Texas at Austin, June 1995.

29. Lin, H.J., R.B. Machemehl, C.E. Lee, and R. Herman. Guidelines for Use of Left Turn Lanes and Signal Phases. Report No. FHWA/TX-84/07+258-1, Center for Transportation Research, University of Texas at Austin, 1984.

30. Lum, K.M. and C.E. Lee. Actuated Traffic Signal Control at Diamond Interchange. Journal of Transportation Engineering Vol. 118, No. 3, .ASCE, 1992, pp. 410-429.

31. Machemehl, R.B. and M. Acampora. Texas Model Validation for Left Turn Phasing Alternatives. Report No. TX-91+1906-1F, Center for Transportation Research, University of Texas at Austin, 1991.

32. Machemehl, R.B. An Evaluation of Left-Turn Analysis Procedures. ITE Journal, Institute Transportation Engineers, Nov. 1986, pp. 37-41.

33. Machemehl, R.B. and A.M. Mechler. Comparative Analysis of Left Turn Phase Sequencing. Report No. FHWA/TX-84/07+258-2, Center for Transportation Research, University of Texas at Austin, 1983.

34. McShane, W.R., P. Roess, and E.S. Prassas. Traffic Engineering, Third Edition, Prentice Hall, New Jersey, 2004, pp. 212.

35. Naguib, F. Validation of TEXAS Simulation Model using Field Data. M.S. thesis, Department of Civil Engineering, Arizona State University, Tempe, Aug 1989.

36. Neuman, T.R. Intersection Channelization and Design Guide. National Cooperative Highway Research Report 279, Transportation Research Board, National Research Council, Washington, D.C., 1985, pp. 40-46.

37. Oh., J., S. Washington, and K. Choi. Development of Accident Prediction Models for Rural Highway Intersections. In Transportation Research Record 1897, Transportation Research Board, National Research Council, Washington, D.C., 2004, pp. 18-27.

38. Park, B. and H Qi. Development and Evaluation of Simulation Model Calibration Procedure. In Transportation Research Record 1934, Transportation

Research Board, National Research Council, Washington, D.C.2005, pp. 208-217.

39. Prabhakar, D. Effective Placement of Detectors at Diamond Interchanges. Master's thesis, Department of Civil Engineering, Texas A&M University, College Station, Dec. 1994.

40. Radwan, A.E. and R.L. Hatton. Evaluation Tools of Urban Interchange Design and Operation. In Transportation Research Record 1280, Transportation Research Board, National Research Council, Washington, D.C., 1990, pp. 148-155.

41. Radwan, A.E. and E.T. Eure. Effect of Right Turning Vehicles on Traffic Signal Volume Warrants. Report No. FHWA-AZ-91-307, Center for Advanced Research in Transportation, Arizona State University, Tempe, AZ, March 1991.

42. Roadway Design Manual. Nebraska Department of Roads, 2006, p. 4-9. http://www.dor.state.ne.us/roadway-design/pdfs/rwydesignman.pdf. Accessed July 2010.

43. Rodriguez, L.L., C.E. Lee, and R.B. Machemehl. Fuel Savings from Free U-Turn Lanes at Diamond Interchanges. Report No. SWUTC/97/467301-1, Center for Transportation Research, University of Texas at Austin, 1997.

44. Savolainen, P., and A. P. Tarko. Safety of Intersections on High-Speed Road Segments with Superelevation. Report FHWA/IN/JTRP-2004/25, School of Civil Engineering, Purdue University, West Lafayette, IN, 2004. http://docs.lib.purdue.edu/cgi/viewcontent.cgi?article=1655&context=jtrp. Accessed July 2010.

45. Son, T., S.G. Kim, and J.K Lee. Methodology to Calculate Sight Distance Available to Drivers at Skewed Intersections. In Transportation Research Record 1796, Transportation Research Board, National Research Council, Washington, D.C., 2002, pp. 41-47.

46. Tarawneh, M.S. and P.T. McCoy. Effect of Intersection Channelization and Skew on Driver Performance. In Transportation Research Record 1523, Transportation Research Board, National Research Council, Washington, D.C., 1996, pp.73-82.

47. Torres, J.F., T. Banks, H, Halati, and M. Danesh. Evaluation of the TEXAS Intersection Simulation Model. Contract DOT-FH-11-9681, JFT Associates, Los Angeles, CA, 90045, Nov. 1980.

48. Tripi, E.J. Guidelines for Realignment of Skew Intersections. Master's thesis, Department of Civil Engineering, University of Nebraska, Lincoln, Nebraska, 1994.

49. Upchurch, J.E., A.E. Radwan, and A.G. Dean. Development Evaluation and Application of Left Turn Signal Warrants. Report No. FHWA-AZ-91-267, Center for Advanced Research in Transportation, Arizona State University, Tempe, AZ, August 1991.

50. U.S. Department of Transportation, Federal Highway Administration. Turner Fair Bank Highway Research Center. Signalized Intersections: Informational Guide. FHWA-HRT-04-091, August, 2004. http://www.tfhrc.gov/safety/pubs/04091/03.htm. Accessed July 2010.

51. Walker, R.J. Coordination of Basic Design Elements: Overview. In Transportation Research Record 1385, Transportation Research Board, National Research Council, Washington, D.C., 1981, pp. 51-59.

52. Williams, J.C. and S.A. Ardekani. Impact of Traffic Signal Installation at Marginally Warranted Intersections. Report No. FHWA/TX-94/1350-1F, Civil and Environmental Engineering Department, University of Texas at Arlington, 1996.

53. Woods, D.L. and L.M. Koniki. Optimizing Detector Placement for High Speed Isolated Signalized Intersections using Vehicular Delay as Criterion. Report No. FHWA/TX-94/1392-3, Texas Transportation Institute, College Station, Texas, 1994.

54. Woodson, W.E. and T. Barry. Human Factors Design Handbook. Information and Guidelines for Design of Systems, Facilities, Equipment and Products for Human Use. McGraw Hill, New York, 1992, pp. 93.

55. Zhong, X., Y. Wang, L. Zhong, X. Zhu, J. Jia, M. Zhao, J. Ma, and X. Liu. Study on the Relationship of Intersection Design and Safety of Urban Unsignalized Intersection in China. Third Urban Street Symposium, Transportation Research Board, Washington, D.C., 2007.

APPENDIX A FIELD MEASUREMENTS AND CALCULATIONS

Appendix A1 Number of Spot Speed Observations

From equation (9),

$$\text{No. of observations} = \left\lfloor \frac{Z_{\propto} S}{e} \right\rfloor^2$$

Where,

$Z_{\propto}$ = Normal statistic for a confidence level of $\alpha = 1.96$ for 95% confidence level

S = Expected standard deviation and

e = Amount of error allowed = 1.0

These calculations are illustrated for each of the remaining three intersections below:

S 56th and Saltillo Road:

No. of observations $\left\lfloor \frac{1.96*5.33}{1.0} \right\rfloor^2 = 110$

S 90th and O Street:

No. of observations $\left\lfloor \frac{1.96*6.77}{1.0} \right\rfloor^2 = 177$

Appendix A2 Braking Distances

From equation (10),

Braking Distance, d = 1.47*V*t + $\left\lfloor \frac{1.07V^2}{a} \right\rfloor$

Where,

d = Braking distance

V= Speed in mph

t = Reaction time = 2.5s and

a = Threshold acceleration = 11.2ft/s^2

The braking distance calculations for each approach of every site are shown below:

S 56th and Saltillo Road:

Eastbound:

Speed limit = 55 mph

Braking distance, d = 1.47*V*t + $\left\lfloor \frac{1.07V^2}{a} \right\rfloor$

$$= 1.47*55*2.5+\left\lfloor \frac{1.07*55^2}{11.2} \right\rfloor = 492.2\text{ft}$$

Westbound:

Speed limit = 50 mph

Braking distance, d = 1.47*V*t + $\left\lfloor \frac{1.07V^2}{a} \right\rfloor$

$$= 1.47*50*2.5+\left\lfloor \frac{1.07*50^2}{11.2} \right\rfloor = 423.5\text{ft}$$

Southbound:

Speed limit = 55 mph

Braking distance, d = 1.47*V*t + $\left\lfloor \frac{1.07V^2}{a} \right\rfloor$

$$= 1.47*55*2.5+\left\lfloor \frac{1.07*55^2}{11.2} \right\rfloor = 492.2\text{ft}$$

Hence, 2d = 2 *492.2 = 984.4ft

S 90th and O Street:

Eastbound:

Speed limit = 65 mph

Braking distance, d = 1.47*V*t + $\left\lfloor \frac{1.07V^2}{a} \right\rfloor$

$$= 1.47*65*2.5+\left\lfloor \frac{1.07*65^2}{11.2} \right\rfloor = 644.1\text{ft}$$

Westbound:

Speed limit = 60 mph

Braking distance, d = 1.47*V*t + $\left\lfloor \frac{1.07V^2}{a} \right\rfloor$

$$= 1.47*60*2.5+\left\lfloor \frac{1.07*60^2}{11.2} \right\rfloor = 565.7\text{ft}$$

Southbound:

Speed limit = 20 mph

Braking distance, d = 1.47*V*t + $\left\lfloor \frac{1.07V^2}{a} \right\rfloor$

$$= 1.47*20*2.5+\left\lfloor \frac{1.07*20^2}{11.2} \right\rfloor = 111.8\text{ft}$$

Hence, 2d = 2 *111.8 = 223.6ft

Appendix A3 Spot Speeds

Appendix A3.1 N 24th and Superior Street

TABLE 26 Intersection information and frequency table of spot speeds on eastbound approach of N 24th and Superior Street

N 24th and Superior Street

Intersection: N 24th and Superior Street
Approach: N 24th Street
Direction of Travel: EB
Speed limit: 40 mph
Observers: from previous study
Observations: 180

Speed Group	Number Observed f_i	Class Mid Value u_i	f_i/u_i	Frequency (%)	Cumulative Frequency (%)	Observed Speed (mph)
28	1	28.5	0.0351	0.56	1	29
29	0	29.5	0.0000	0.00	1	30
30	0	30.5	0.0000	0.00	1	31
31	0	31.5	0.0000	0.00	1	32
32	0	32.5	0.0000	0.00	1	33
33	2	33.5	0.0597	1.11	2	34
34	3	34.5	0.0870	1.67	3	35
35	5	35.5	0.1408	2.78	6	36
36	7	36.5	0.1918	3.89	10	37
37	8	37.5	0.2133	4.44	14	38
38	23	38.5	0.5974	12.78	27	39
39	17	39.5	0.4304	9.44	37	40
40	27	40.5	0.6667	15.00	52	41
41	15	41.5	0.3614	8.33	60	42
42	21	42.5	0.4941	11.67	72	43
43	14	43.5	0.3218	7.78	79	44
44	10	44.5	0.2247	5.56	85	45
45	10	45.5	0.2198	5.56	91	46
46	6	46.5	0.1290	3.33	94	47
47	3	47.5	0.0632	1.67	96	48
48	1	48.5	0.0206	0.56	96	49
49	3	49.5	0.0606	1.67	98	50
50	1	50.5	0.0198	0.56	98	51
51	0	51.5	0.0000	0.00	98	52
52	1	52.5	0.0190	0.56	99	53
53	0	53.5	0.0000	0.00	99	54
54	0	54.5	0.0000	0.00	99	55
55	0	55.5	0.0000	0.00	99	56
56	1	56.5	0.0177	0.56	99	57
57	0	57.5	0.0000	0.00	99	58

TABLE 26 Intersection information and frequency table of spot speeds on eastbound approach of N 24th and Superior Street (continued)

Speed Group	Number Observed f_i	Class Mid Value u_i	f_i/u_i	Frequency (%)	Cumulative Frequency (%)	Observed Speed (mph)
59	0	59.5	0.0000	0.00	99	60
60	0	60.5	0.0000	0.00	99	61
61	0	61.5	0.0000	0.00	99	62
62	0	62.5	0.0000	0.00	99	63
63	0	63.5	0.0000	0.00	99	64
64	0	64.5	0.0000	0.00	99	65
65	0	65.5	0.0000	0.00	99	66
66	1	66.5	0.0150	0.56	100	67
	180		4.3891	100		

Speed values from previous study

Mean speed = 180/4.3891 = 41.0 mph

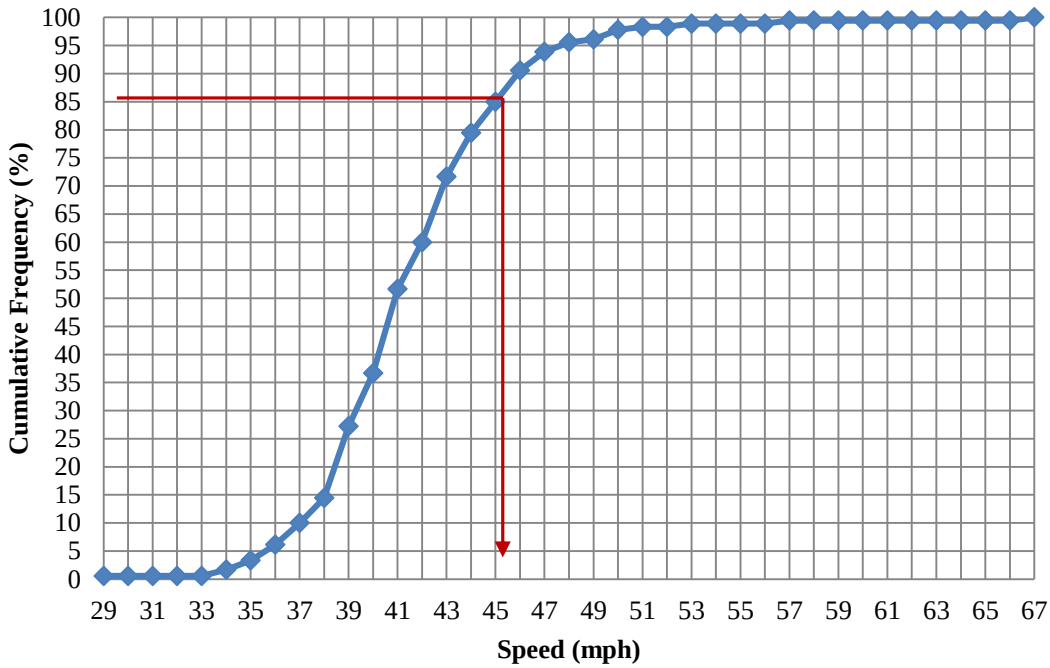

FIGURE 34 Cumulative frequency plot of spot speeds on eastbound approach of N 24th and Superior Street. From the graph, 85% speed = 45.0 mph

TABLE 27 Intersection information and frequency table of spot speeds on westbound approach of N 24th and Superior Street

N 24th and Superior Street

Intersection: N 24th and Superior Street
Approach: N 24th Street
Direction of Travel: WB
Speed limit: 40 mph
Observers: from previous study
Observations: 180

Speed Group	Number Observed f_i	Class Mid Value u_i	f_i/u_i	Frequency (%)	Cumulative Frequency (%)	Observed Speed (mph)
28	1	28.5	0.0351	0.56	1	29
29	0	29.5	0.0000	0.00	1	30
30	1	30.5	0.0328	0.56	1	31
31	2	31.5	0.0635	1.11	2	32
32	5	32.5	0.1538	2.78	5	33
33	4	33.5	0.1194	2.22	7	34
34	4	34.5	0.1159	2.22	9	35
35	12	35.5	0.3380	6.67	16	36
36	15	36.5	0.4110	8.33	24	37
37	18	37.5	0.4800	10.00	34	38
38	15	38.5	0.3896	8.33	43	39
39	26	39.5	0.6582	14.44	57	40
40	22	40.5	0.5432	12.22	69	41
41	14	41.5	0.3373	7.78	77	42
42	14	42.5	0.3294	7.78	85	43
43	8	43.5	0.1839	4.44	89	44
44	7	44.5	0.1573	3.89	93	45
45	4	45.5	0.0879	2.22	96	46
46	3	46.5	0.0645	1.67	97	47
47	1	47.5	0.0211	0.56	98	48
48	2	48.5	0.0412	1.11	99	49
49	0	49.5	0.0000	0.00	99	50
50	1	50.5	0.0198	0.56	99	51
51	0	51.5	0.0000	0.00	99	52
52	0	52.5	0.0000	0.00	99	53
53	0	53.5	0.0000	0.00	99	54
54	0	54.5	0.0000	0.00	99	55
55	1	55.5	0.0180	0.56	100	56
	180		4.6011	100		

Speed values from previous study

Mean speed = 180/4.6011 = 39.1 mph

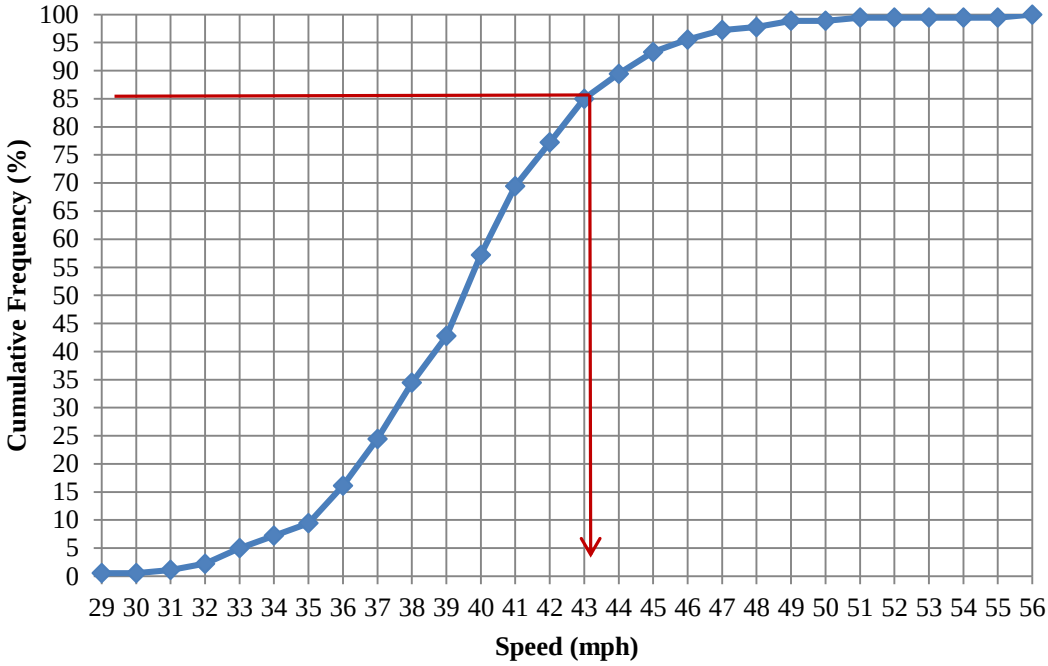

FIGURE 35 Cumulative frequency plot of spot speeds on westbound approach of N 24th and Superior Street. From the graph, 85% speed = 43.0 mph

Appendix A3.2 S 56th and Saltillo Road

TABLE 28 Intersection information and frequency table of spot speeds on eastbound approach of S 56th and Saltillo Road

S 56th and Saltillo Road

Intersection: S 56th and Saltillo Road
Approach: Saltillo Road
Direction of Travel: EB
Distance of speed trap from intersection: 492.2ft
Speed limit: 55 mph
Observers: Manogna, Kiran
Date: 1/9/2008
Time of study: 1:45pm – 2:45pm
Weather: 36˚ F
Observations: 125
Distance of radar gun from speed trap: 3.5ft from shoulder, 15ft from speed trap

Speed Group	Number Observed f_i	Class Mid Value u_i	f_i/u_i	Frequency (%)	Cumulative Frequency (%)	Observed Speed (mph)
30	1	30.5	0.0328	0.8	0.8	31
31	0	31.5	0.0000	0	0.8	32
32	2	32.5	0.0615	1.6	2.4	33
33	2	33.5	0.0597	1.6	4	34
34	1	34.5	0.0290	0.8	4.8	35
35	4	35.5	0.1127	3.2	8	36
36	3	36.5	0.0822	2.4	10.4	37
37	3	37.5	0.0800	2.4	12.8	38
38	0	38.5	0.0000	0	12.8	39
39	2	39.5	0.0506	1.6	14.4	40
40	10	40.5	0.2469	8	22.4	41
41	6	41.5	0.1446	4.8	27.2	42
42	9	42.5	0.2118	7.2	34.4	43
43	8	43.5	0.1839	6.4	40.8	44
44	4	44.5	0.0899	3.2	44	45
45	11	45.5	0.2418	8.8	52.8	46
46	4	46.5	0.0860	3.2	56	47
47	8	47.5	0.1684	6.4	62.4	48
48	10	48.5	0.2062	8	70.4	49
49	6	49.5	0.1212	4.8	75.2	50
50	8	50.5	0.1584	6.4	81.6	51
51	2	51.5	0.0388	1.6	83.2	52
52	8	52.5	0.1524	6.4	89.6	53
53	2	53.5	0.0374	1.6	91.2	54
54	2	54.5	0.0367	1.6	92.8	55
55	1	55.5	0.0180	0.8	93.6	56
56	3	56.5	0.0531	2.4	96	57
57	1	57.5	0.0174	0.8	96.8	58
58	2	58.5	0.0342	1.6	98.4	59
59	2	59.5	0.0336	1.6	100	60
	125		2.7892	100		

Mean speed = 125/2.7892 = 44.8 mph

FIGURE 36 Speed trap on eastbound approach of S 56th and Saltillo Road

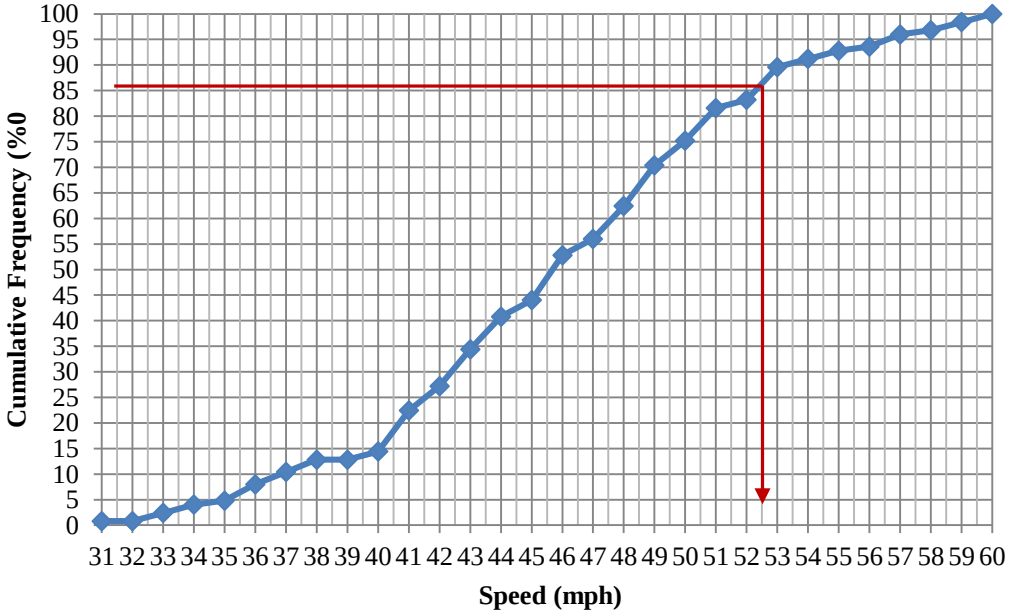

FIGURE 37 Cumulative frequency plot of spot speeds on east bound approach of S 56th and Saltillo Road. From the graph, 85% speed = 52.3 mph.

TABLE 29 Intersection information and frequency table of spot speeds on westbound approach of S 56th and Saltillo Road

S 56th and Saltillo Road

Intersection: S 56th and Saltillo Road
Approach: Saltillo Road
Direction of Travel: WB
Distance of speed trap from intersection: 423.5ft
Speed limit: 50 mph
Observers: Justice, Vyas
Date: 1/9/2008
Time of study: 1:08 pm – 2:10 pm
Weather: 36˚ F
Observations: 125
Distance of radar gun from speed trap: 13ft from shoulder, 22ft from speed trap

Speed Group	Number Observed f_i	Class Mid Value u_i	f_i/u_i	Frequency (%)	Cumulative Frequency (%)	Observed Speed (mph)
30	1	30.5	0.0328	0.8	0.8	31
31	0	31.5	0.0000	0	0.8	32
32	0	32.5	0.0000	0	0.8	33
33	0	33.5	0.0000	0	0.8	34
34	0	34.5	0.0000	0	0.8	35
35	0	35.5	0.0000	0	0.8	36
36	0	36.5	0.0000	0	0.8	37
37	0	37.5	0.0000	0	0.8	38
38	0	38.5	0.0000	0	0.8	39
39	1	39.5	0.0253	0.8	1.6	40
40	0	40.5	0.0000	0	1.6	41
41	1	41.5	0.0241	0.8	2.4	42
42	0	42.5	0.0000	0	2.4	43
43	2	43.5	0.0460	1.6	4	44
44	4	44.5	0.0899	3.2	7.2	45
45	6	45.5	0.1319	4.8	12	46
46	3	46.5	0.0645	2.4	14.4	47
47	9	47.5	0.1895	7.2	21.6	48
48	12	48.5	0.2474	9.6	31.2	49
49	5	49.5	0.1010	4	35.2	50
50	6	50.5	0.1188	4.8	40	51
51	11	51.5	0.2136	8.8	48.8	52
52	12	52.5	0.2286	9.6	58.4	53
53	11	53.5	0.2056	8.8	67.2	54
54	8	54.5	0.1468	6.4	73.6	55
55	9	55.5	0.1622	7.2	80.8	56
56	7	56.5	0.1239	5.6	86.4	57
57	6	57.5	0.1043	4.8	91.2	58

TABLE 29 Intersection information and frequency table of spot speeds on westbound approach of S 56th and Saltillo Road (continued)

Speed Group	Number Observed f_i	Class Mid Value u_i	f_i/u_i	Frequency (%)	Cumulative Frequency (%)	Observed Speed (mph)
59	3	59.5	0.0504	2.4	96.8	60
60	1	60.5	0.0165	0.8	97.6	61
61	1	61.5	0.0163	0.8	98.4	62
62	0	62.5	0.0000	0	98.4	63
63	2	63.5	0.0315	1.6	100	64
	125		2.4392	100		

Mean speed = 125/2.4392 = 51.2 mph

FIGURE 38 Speed trap on westbound approach of S 56th and Saltillo Road

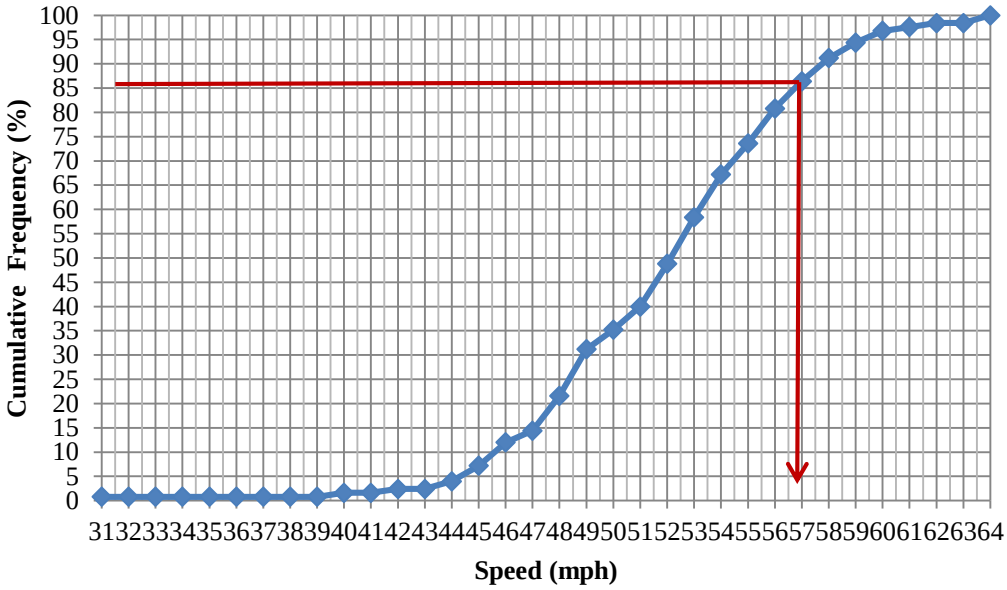

FIGURE 39 Cumulative frequency plot of spot speeds on westbound approach of S 56th and Saltillo Road. From the above graph, 85% speed = 56.8 mph.

TABLE 30 Intersection information and frequency table of spot speeds on southbound approach of S 56th and Saltillo Road

S 56th and Saltillo Road

Intersection: S 56th and Saltillo Road
Approach: S 56th Street
Direction of Travel: SB
Distance of speed trap from intersection: 984.4ft
Speed limit: 55 mph
Observers: Bhaven, Rama Krishna
Date: 1/9/2008
Time of study: 1:15 pm – 2:45 pm
Weather: 36˚ F
Observations: 125
Distance of radar gun from speed trap: 1ft from shoulder, 6ft from speed trap

Speed Group	Number Observed f_i	Class Mid Value u_i	f_i/u_i	Frequency (%)	Cumulative Frequency (%)	Observed Speed (mph)
38	1	38.5	0.0260	0.8	0.8	39
39	1	39.5	0.0253	0.8	1.6	40
40	1	40.5	0.0247	0.8	2.4	41
41	0	41.5	0.0000	0	2.4	42
42	4	42.5	0.0941	3.2	5.6	43
43	4	43.5	0.0920	3.2	8.8	44
44	7	44.5	0.1573	5.6	14.4	45
45	6	45.5	0.1319	4.8	19.2	46
46	6	46.5	0.1290	4.8	24	47
47	11	47.5	0.2316	8.8	32.8	48
48	6	48.5	0.1237	4.8	37.6	49
49	11	49.5	0.2222	8.8	46.4	50
50	12	50.5	0.2376	9.6	56	51
51	11	51.5	0.2136	8.8	64.8	52
52	11	52.5	0.2095	8.8	73.6	53
53	8	53.5	0.1495	6.4	80	54
54	4	54.5	0.0734	3.2	83.2	55
55	8	55.5	0.1441	6.4	89.6	56
56	8	56.5	0.1416	6.4	96	57
57	2	57.5	0.0348	1.6	97.6	58
58	1	58.5	0.0171	0.8	98.4	59
59	0	59.5	0.0000	0	98.4	60
60	1	60.5	0.0165	0.8	99.2	61
61	1	61.5	0.0163	0.8	100	62
	125		2.5118	100		

Mean speed = 125/2.5118 = 49.8 mph

FIGURE 40 Speed trap on southbound approach of S 56th and Saltillo Road

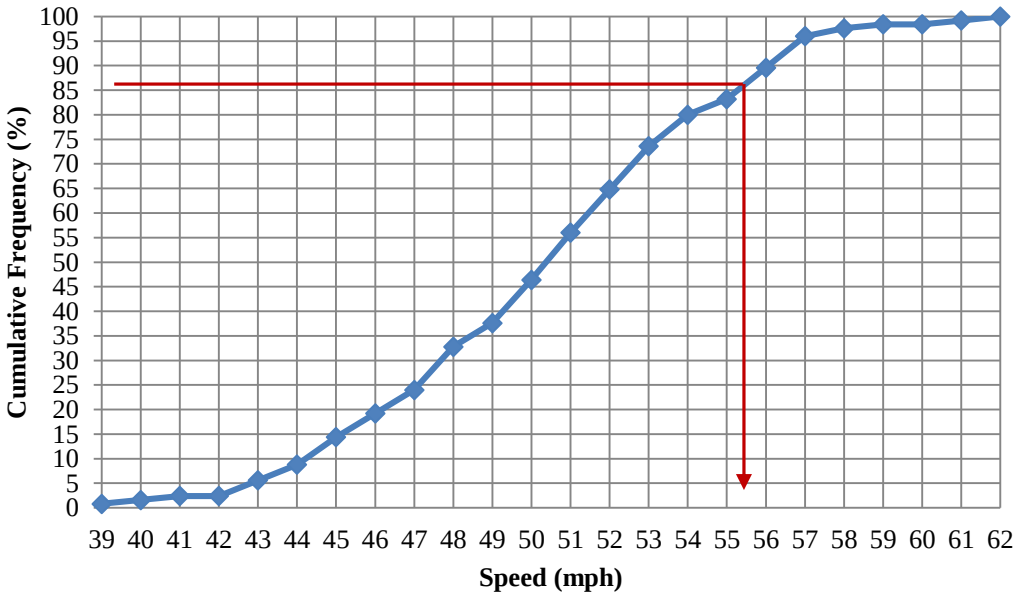

FIGURE 41 Cumulative frequency plot of spot speeds on southbound approach of S 56th and Saltillo Road. From the graph, 85% speed = 55.3 mph.

Appendix A3.3. S 90th and O Street

TABLE 31 Intersection information and frequency table of spot speeds on eastbound approach of S 90th and O Street

S 90th and O Street

Intersection: S 90th and O Street
Approach: O Street
Direction of Travel: EB
Distance of speed trap from intersection: 644.1ft
Speed limit: 65 mph
Observers: Manogna, Kiran
Date: 1/9/2008
Time of study: 4:00 pm – 5:00 pm
Weather: 36˚ F
Observations: 200
Distance of radar gun from speed trap: 4.9ft from shoulder, 16.5ft from speed trap

Speed Groups	Number Observed f_i	Class Mid Value u_i	f_i/u_i	Frequency (%)	Cumulative Frequency (%)	Observed Speed (mph)
31	1	31.5	0.0317	0.5	0.5	32
32	0	32.5	0.0000	0	0.5	33
33	1	33.5	0.0299	0.5	1	34
34	1	34.5	0.0290	0.5	1.5	35
35	0	35.5	0.0000	0	1.5	36
36	0	36.5	0.0000	0	1.5	37
37	0	37.5	0.0000	0	1.5	38
38	1	38.5	0.0260	0.5	2	39
39	2	39.5	0.0506	1	3	40
40	5	40.5	0.1235	2.5	5.5	41
41	5	41.5	0.1205	2.5	8	42
42	4	42.5	0.0941	2	10	43
43	10	43.5	0.2299	5	15	44
44	8	44.5	0.1798	4	19	45
45	6	45.5	0.1319	3	22	46
46	5	46.5	0.1075	2.5	24.5	47
47	13	47.5	0.2737	6.5	31	48
48	10	48.5	0.2062	5	36	49
49	8	49.5	0.1616	4	40	50
50	14	50.5	0.2772	7	47	51
51	14	51.5	0.2718	7	54	52
52	17	52.5	0.3238	8.5	62.5	53
53	18	53.5	0.3364	9	71.5	54
54	15	54.5	0.2752	7.5	79	55
55	10	55.5	0.1802	5	84	56
56	12	56.5	0.2124	6	90	57
57	9	57.5	0.1565	4.5	94.5	58
58	3	58.5	0.0513	1.5	96	59
59	2	59.5	0.0336	1	97	60
60	4	60.5	0.0661	2	99	61
61	1	61.5	0.0163	0.5	99.5	62
62	1	62.5	0.0160	0.5	100	63
	200		4.0127	100		

Mean speed = 200/4.0127 = 49.8 mph

FIGURE 42 Speed trap on eastbound approach of S 90th and O Street

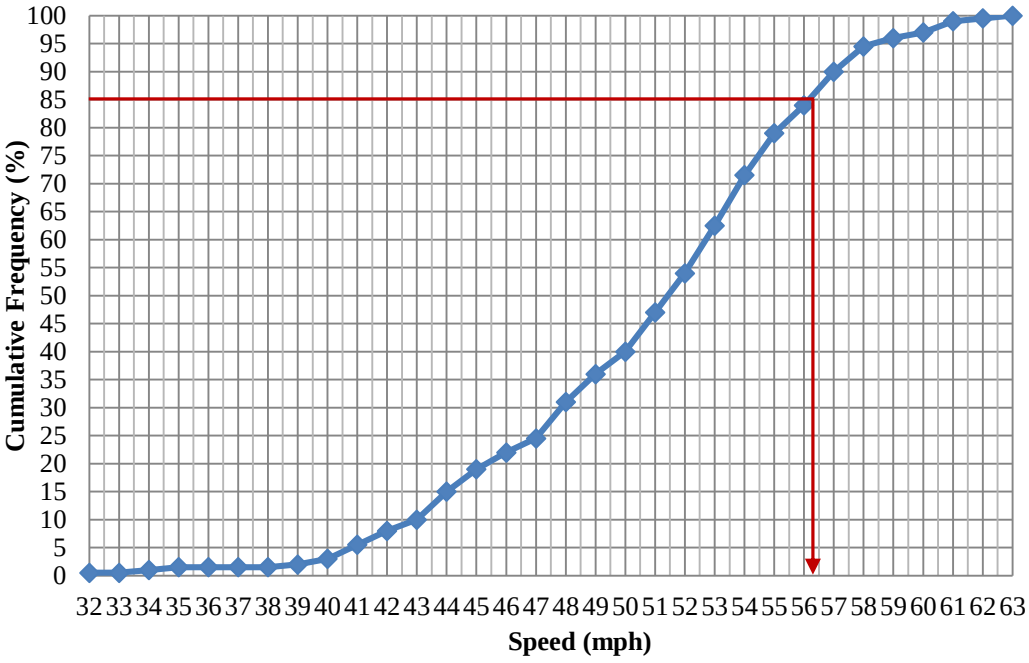

FIGURE 43 Cumulative frequency plot of spot speeds on eastbound approach of S 90th and O Street

From the above graph, 85% speed = 56.2 mph

TABLE 32 Intersection information and frequency table of spot speeds on westbound approach of S 90th and O Street

S 90th and O Street

Intersection: S 90th and O Street
Approach: O Street
Direction of Travel: WB
Distance of speed trap from intersection: 565.7ft
Speed limit: 60 mph
Observers: Justice, Vyas
Date: 1/9/2008
Time of study: 3:52 pm – 4:15 pm
Weather: 36˚ F
Observations: 200
Distance of radar gun from speed trap: 15ft from shoulder, 30ft from speed trap

Speed Groups	Number Observed f_i	Class Mid Value u_i	f_i/u_i	Frequency (%)	Cumulative Frequency (%)	Observed Speed (mph)
34	2	34.5	0.0580	1	1	35
35	3	35.5	0.0845	1.5	2.5	36
36	3	36.5	0.0822	1.5	4	37
37	4	37.5	0.1067	2	6	38
38	8	38.5	0.2078	4	10	39
39	8	39.5	0.2025	4	14	40
40	9	40.5	0.2222	4.5	18.5	41
41	10	41.5	0.2410	5	23.5	42
42	11	42.5	0.2588	5.5	29	43
43	11	43.5	0.2529	5.5	34.5	44
44	13	44.5	0.2921	6.5	41	45
45	13	45.5	0.2857	6.5	47.5	46
46	13	46.5	0.2796	6.5	54	47
47	16	47.5	0.3368	8	62	48
48	21	48.5	0.4330	10.5	72.5	49
49	9	49.5	0.1818	4.5	77	50
50	11	50.5	0.2178	5.5	82.5	51
51	17	51.5	0.3301	8.5	91	52
52	5	52.5	0.0952	2.5	93.5	53
53	3	53.5	0.0561	1.5	95	54
54	0	54.5	0.0000	0	95	55
55	2	55.5	0.0360	1	96	56
56	3	56.5	0.0531	1.5	97.5	57
57	2	57.5	0.0348	1	98.5	58
58	3	58.5	0.0513	1.5	100	59
	200		4.4000	100		

Mean speed = 200/4.4 = 45.5 mph

FIGURE 44 Speed trap on westbound approach of S 90th and O Street

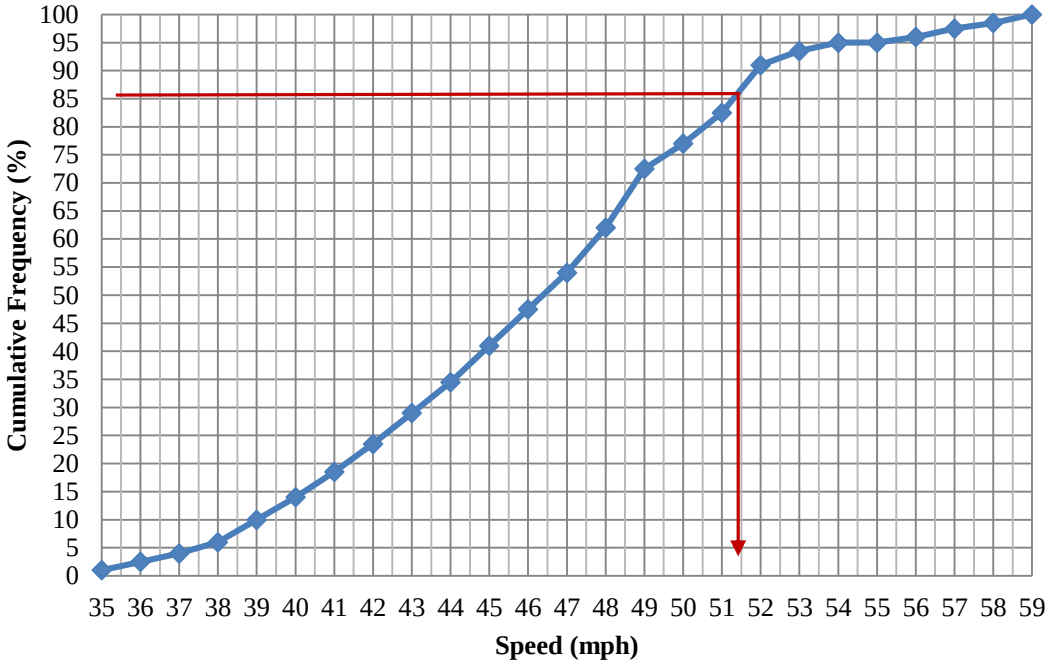

FIGURE 45 Cumulative frequency plot of spot speeds on westbound approach of S 90th and O Street. From the graph, 85% speed = 51.3 mph.

TABLE 33 Intersection information and frequency table of spot speeds on southbound approach of S 90th and O Street

S 90th and O Street

Intersection: S 90th and O Street
Approach: S 90 Street
Direction of Travel: SB
Distance of speed trap from intersection: 223.6ft
Speed limit: 20 mph
Observers: Bhaven, Krishna
Date: 1/9/2008
Time of study: 3:50 pm – 5:00 pm
Weather: 36˚ F
Observations: 200
Distance of radar gun from speed trap: 1ft from shoulder, 82ft from speed trap

Speed Groups	Number Observed f_i	Class Mid Value u_i	f_i/u_i	Frequency (%)	Cumulative Frequency (%)	Observed Speed (mph)
14	2	14.5	0.1379	1	1	15
15	0	15.5	0.0000	0	1	16
16	1	16.5	0.0606	0.5	1.5	17
17	8	17.5	0.4571	4	5.5	18
18	17	18.5	0.9189	8.5	14	19
19	11	19.5	0.5641	5.5	19.5	20
20	10	20.5	0.4878	5	24.5	21
21	17	21.5	0.7907	8.5	33	22
22	10	22.5	0.4444	5	38	23
23	30	23.5	1.2766	15	53	24
24	15	24.5	0.6122	7.5	60.5	25
25	18	25.5	0.7059	9	69.5	26
26	12	26.5	0.4528	6	75.5	27
27	22	27.5	0.8000	11	86.5	28
28	9	28.5	0.3158	4.5	91	29
29	7	29.5	0.2373	3.5	94.5	30
30	5	30.5	0.1639	2.5	97	31
31	2	31.5	0.0635	1	98	32
32	0	32.5	0.0000	0	98	33
33	3	33.5	0.0896	1.5	99.5	34
34	1	34.5	0.0290	0.5	100	35
	200		8.6082	100		

Mean speed = 200/8.6082 = 23.2 mph

FIGURE 46 Speed trap on southbound approach of S 90th and O Street

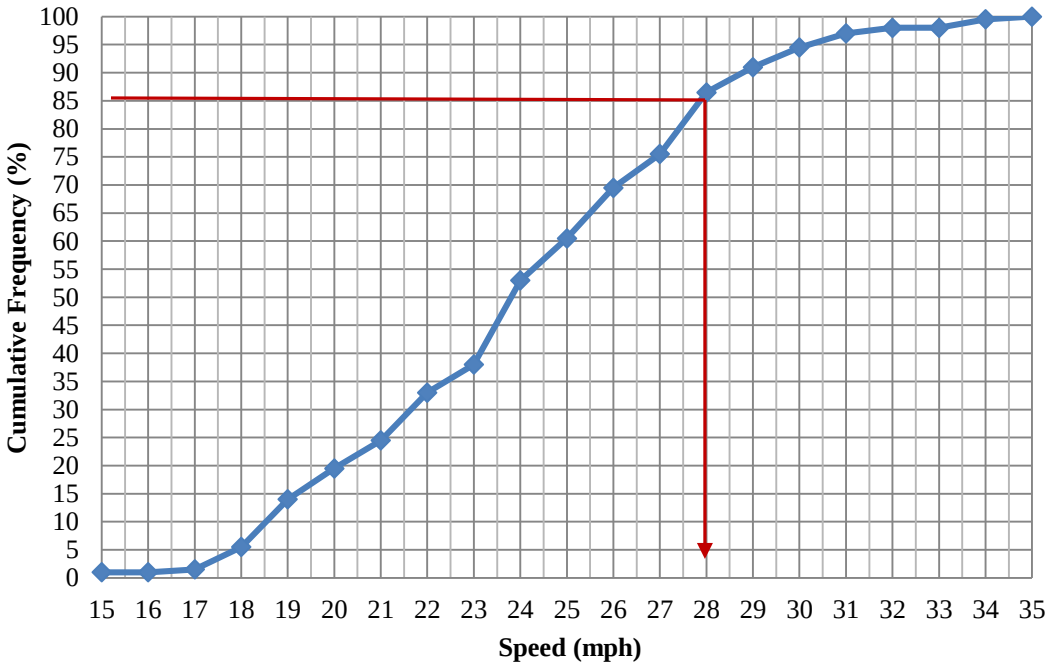

FIGURE 47 Cumulative frequency plot of spot speeds on southbound approach of S 90th and O Street. From the graph, 85% speed = 27.9 mph

Appendix A4 Vehicle Class Composition

TABLE 34 Vehicle composition

Site	Approach	C	S	M	L	LT	LTW	H	B	ST	BI	Total
N 24th and S	WB Thru 1	203	179	5	0	0	0	5	1	5	0	398
	WB Thru 2	189	165	6	0	0	0	6	1	5	0	372
	WB Lt	30	24	1	0	0	0	0	0	1	0	56
	Total	422	368	12	0	0	0	11	2	11	0	826
	NB Lt	16	15	0	0	0	0	0	0	0	0	31
	NB Rt	35	32	0	0	0	0	0	0	2	0	69
	Total	51	47	0	0	0	0	0	0	2	0	100
	EB Thru	250	217	11	0	0	0	7	1	3	0	489
	EB Thru and Rt	182	116	8	0	0	0	3	3	1	1	313
	Total	432	333	19	0	0	0	10	4	4	1	802
S 56th and S	EB Thru	129	47	23	12	89	8	3	0	2	0	313
	EB Lt	50	22	13	7	35	4	0	0	0	0	131
	Total	179	69	36	19	124	12	3	0	2	0	444
	SB Lt	94	23	21	6	42	1	3	1	0	0	191
	SB Rt	76	49	9	3	44	3	2	0	1	3	187
	Total	170	72	30	9	86	4	5	1	1	3	378
	WB Thru	131	33	25	2	75	9	6	0	8	4	289
	WB Rt	49	20	8	7	39	2	5	0	0	0	130
	Total	180	53	33	9	114	11	11	0	8	4	419
N 90th and O	EB Thru	162	59	37	10	59	3	18	2	34	0	384
	EB Lt	175	39	14	2	21	0	1	5	1	0	258
	Total	337	98	51	12	80	3	19	7	35	0	642
	SB Lt	13	2	0	0	2	0	0	0	1	0	18
	SB Rt	256	26	19	5	36	0	2	0	1	0	345
	Total	269	28	19	5	38	0	2	0	2	0	363
	WB Thru	150	48	36	14	73	4	9	3	39	1	376
	WB Rt	8	3	1	0	2	0	1	0	1	0	16
	Total	158	51	37	14	75	4	10	3	40	1	392

C = Car, S = SUV, M = Minivan, L = Large van, LT = Light truck, LTW = Light truck with trailer, H = Heavy truck, B = Bus, ST = Semi-trailer, BI = Bike

Total does not include bikes

Appendix A5 N 24th and Superior Street Field Average Queue Delay Calculations

TABLE 35 N 24th and Superior Street queue delay

Vehicle No.	Left Turn Queue Delay (m:s)	Right Turn Queue Delay (m:s)
1	0:10.61	0:11.26
2	0:6.75	0:1.50
3	0:4.15	0:3.34
4	0:39.60	0:18.44
5	0:38.83	0:9.92
6	0:7.54	0:9.75
7	0:45.67	0:10.24
8	0:38.90	0:1.55
9	0:0.10	0:53.82
10	0:2.34	0:46.60
11	0:23.73	0:55.19
12	0:2.76	0:42.14
13	0:44.44	0:8.80
14	0:6.95	0:29.43
15	0:1.95	0:29.73
16	0:3.90	0:28.32
17	0:1.29	0:7.63
18	0:5.95	0:6.28
19	0:8.38	0:5.27
20	1:23.42	0:16.11
21	0:0.10	0:6.30
22	0:18.66	0:2.35
23	0:12.41	0:0.10
24	1:18.38	0:18.73
25	1:21.07	0:25.10
26	0:1.69	0:1.60
27	0:0.10	0:3.13
28	0:3.91	0:0.10
29	0:47.29	0:4.95
30	0:0.10	0:33.06
31	0:19.75	0:1.64
32		0:1.26
33		0:2.69
34		0:19.14
35		0:0.10

TABLE 35 N 24th and Superior Street queue delay (continued)

Vehicle No	Left Turn Queue Delay (m:s)	Right Turn Queue Delay (m:s)
36		0:0.10
37		0:14.38
38		0:0.92
39		0:9.67
40		0:0.10
41		0:0.10
42		0:0.08
43		0:0.10
44		0:1.51
45		0:0.10
46		0:16.37
47		0:0.10
48		0:0.10
49		0:9.44
50		0:8.14
51		0:0.10
52		0:10.90
53		0:18.33
54		0:0.10
55		0:4.91
56		0:0.10
57		0:8.07
58		0:9.18
59		0:1.73
60		0:0.10
61		0:0.10
62		0:0.10
63		0:0.10
64		0:3.40
65		0:0.10
66		0:0.10
67		0:0.10
68		0:2.56
69		0:0.10
Total	10:40.72	10:36.96
Average	0:20.67	0:9.23

Bikes are not included in the analysis

$$\text{Total Average Queue Delay} = \left\lceil \frac{10{:}40.72 + 10{:}36.96}{31+69} \right\rceil$$

$$= 0{:}12.78 \text{ seconds}$$

APPENDIX B CALIBRATION DATA

Appendix B1 S 56th and Saltillo Road

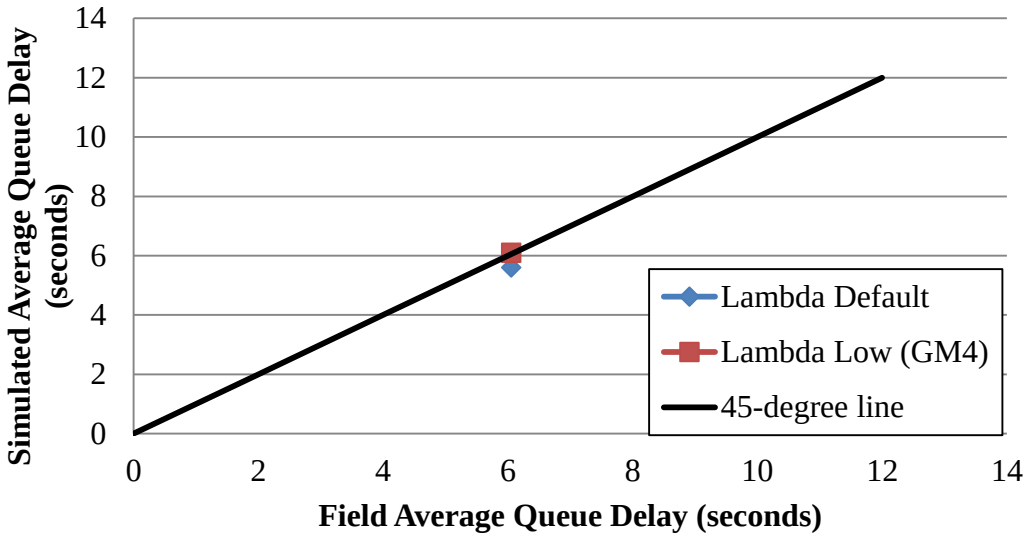

FIGURE 48 Lambda calibration direction for S 56th and Saltillo Road

TABLE 36 Calibration results of S 56th and Saltillo Road

Minor Street	Car Following Parameters	Field Average Queue Delay (s)	Sim Average Queue Delay (s)	Absolute Difference (s)	% Difference
LT Turn	Lambda = 2.8 (d)	9.86	6	3.56	36.11%
RT Turn	Mu = 0.8 (d)	2.16	5.2	3.04	140.74%
Total	Alpha = 4000 (d)	6.05	5.6	0.45	7.45%
LT Turn	Lambda = 1 (GM4)	9.86	6.3	3.56	36.11%
RT Turn	Mu = 0.8 (d)	2.16	5.9	3.74	173.15%
Total	Alpha = 4000 (d)	6.05	6.1	0.05	**0.82%**

Appendix B2 S 90th and O Street

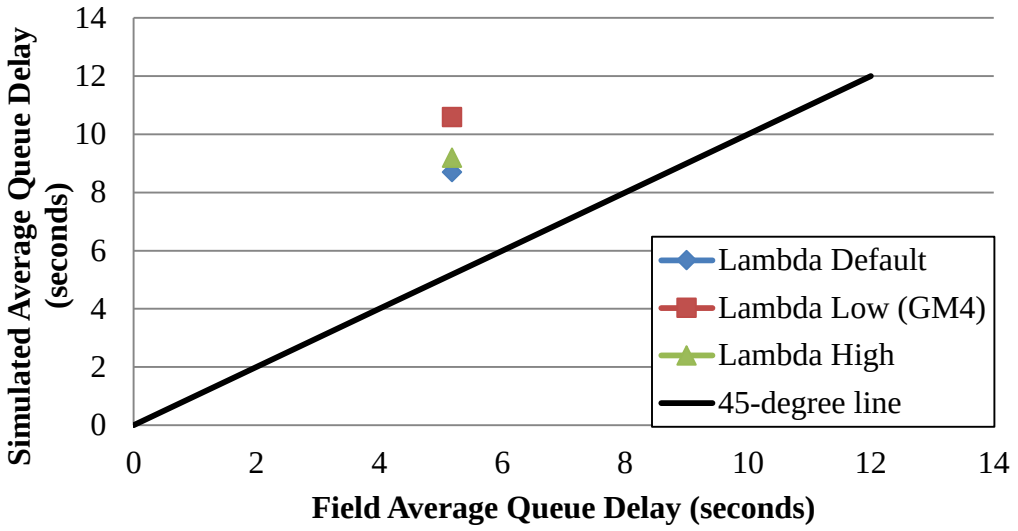

FIGURE 49 Lambda calibration direction for S 90th and O Street

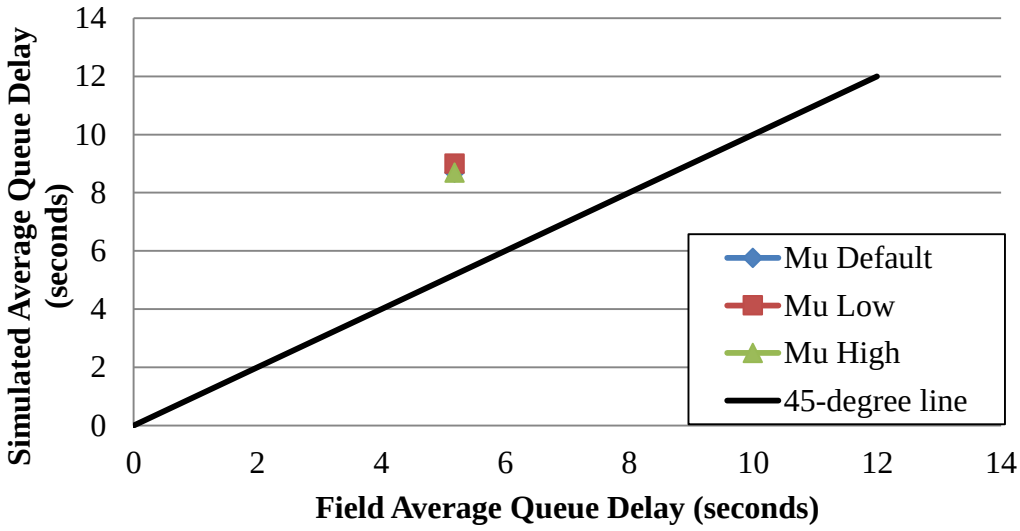

FIGURE 50 Mu calibration direction for S 90th and O Street

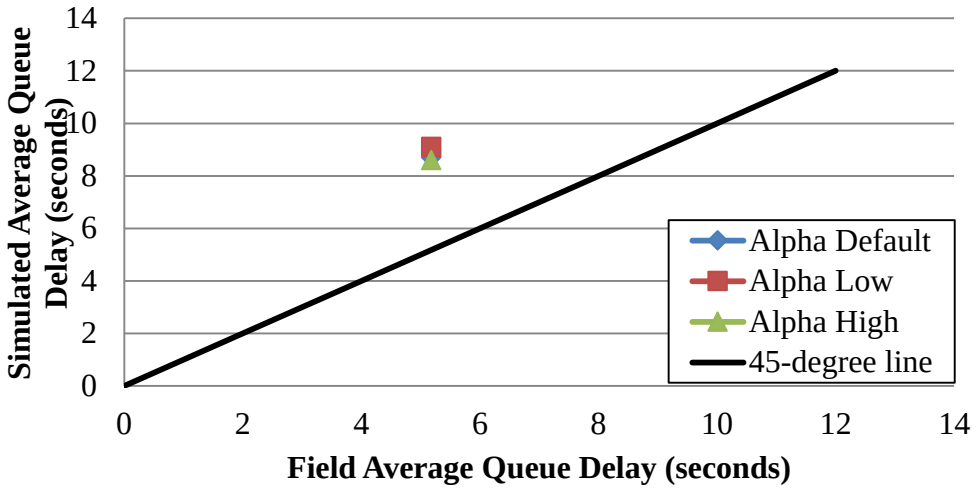

FIGURE 51 Alpha calibration direction for S 90th and O Street

TABLE 37 Calibration results of S 90th and O Street

Minor Street	Car Following Parameters	Field Avg Queue Delay (s)	Sim Avg Queue Delay (s)	Absolute Difference (s)	% Difference
LT Turn	Lambda = 2.8 (d)	15.57	4.8	10.77	69.17%
RT Turn	Mu = 0.8 (d)	4.64	8.9	4.26	91.81%
Total	Alpha = 4000 (d)	5.18	8.7	3.52	67.94%
LT Turn	Lambda = 1 (GM4)	15.57	5.1	10.47	67.24%
RT Turn	Mu = 0.8 (d)	4.64	10.9	6.26	134.91%
Total	Alpha = 4000 (d)	5.18	10.6	5.42	104.61%
LT Turn	Lambda = 4 (h)	15.57	4.6	10.97	70.46%
RT Turn	Mu = 0.8(d)	4.64	9.4	4.76	102.59%
Total	Alpha = 4000 (d)	5.18	9.2	4.02	77.59%
LT Turn	Lambda = 2.8 (d)	15.57	4.6	10.97	70.46%
RT Turn	Mu = 0.6 (l)	4.64	9.3	4.66	100.43%
Total	Alpha = 4000 (d)	5.18	9	3.82	73.73%
LT Turn	Lambda = 2.8 (d)	15.57	4.5	11.07	71.10%
RT Turn	Mu = 1 (h)	4.64	8.9	4.26	91.81%
Total	Alpha = 4000 (d)	5.18	8.7	3.52	67.94%
LT Turn	Lambda = 2.8 (d)	15.57	4.6	10.97	70.46%
RT Turn	Mu = 0.8(d)	4.64	9.4	4.76	102.59%
Total	Alpha = 1 (l)	5.18	9.1	3.92	75.66%
LT Turn	Lambda = 2.8 (d)	15.57	4.5	11.07	71.10%
RT Turn	Mu = 0.8(d)	4.64	8.8	4.16	89.66%
Total	Alpha = 9999 (h)	5.18	8.6	3.42	66.01%
LT Turn	Lambda = 2.8 (d)	15.57	4.7	10.87	69.81%
RT Turn	Mu = 0.8(d)	4.64	9	4.36	93.97%
Total	Alpha = 6000	5.18	8.8	3.62	69.87%
LT Turn	Lambda = 2.8	15.57	4.1	11.47	73.67%
RT Turn	Mu = 0.8 (d)	4.64	5.1	0.46	9.91%
Total	Alpha = 4000	5.18	5.1	0.08	**1.55%**

d = default, GM4 = General Motors fourth model, h = high, l = low

APPENDIX C SIMULATION RESULTS OF N 24TH AND SUPERIOR STREET

TABLE 38 Average queue delay for -30° skew angle

Run	Left Turn (s)	Right Turn (s)	Minor Street Total (s)
1	10.8	9.7	10
2	12.2	5.5	7.4
3	9.3	6.9	7.6
4	8.3	6.5	7
5	8.5	7.1	7.5
6	8.9	6.8	7.5
7	9.7	6.4	7.3
8	11.8	6.7	8.2
9	8.2	5.8	6.5
10	13.4	6.6	8.7
11	10.7	6.3	7.7
12	9	6.1	7
13	9.9	6.5	7.4
14	10.1	5.8	7.2
15	8.1	7	7.3
16	10.9	6.5	7.8
17	9.4	5	6.3
18	11.5	7.3	8.5
19	7.7	6.5	6.8
20	9.7	5.5	6.7
21	8.6	6.1	6.8
22	11.6	10.1	10.5
23	12.5	6.6	8.2
24	9.6	6.5	7.3
25	10.1	6.2	7.4
26	9.3	5.4	6.6
27	7	11.2	9.8
28	11.9	7.3	8.5
29	10.6	5.5	7.1
30	9	7	7.6
AVG	**9.94**	**6.75**	**7.67**

TABLE 39 Average queue delay for -15° skew angle

Run	Left Turn (s)	Right Turn (s)	Minor Street Total (s)
1	12.7	8	9.4
2	12.2	7.3	8.7
3	12.6	7.5	8.9
4	13.1	8.3	9.8
5	12.9	7.9	9.5
6	16.7	7.9	10.8
7	12.2	9.1	10.1
8	16.6	7.3	10.2
9	13.5	8.1	9.7
10	9.3	8.4	8.6
11	11.3	7.5	8.5
12	16.3	7.8	10.2
13	12.4	6.1	8.2
14	13.4	8.4	10
15	12.8	8.9	10
16	12.4	8.2	9.4
17	12	8.4	9.5
18	15.2	13.7	14.1
19	13.6	8.3	9.9
20	10.1	8.2	8.7
21	19.3	10	13
22	14.2	8.3	10
23	12.8	6.8	8.7
24	9.2	8.9	9
25	29.4	10.2	15.2
26	14.9	7.6	9.8
27	13.3	6.1	7.7
28	13.9	7.3	9.5
29	12.2	7.4	8.8
30	16.4	7.6	10.4
AVG	**13.90**	**8.18**	**9.88**

TABLE 40 Average queue delay for -10° skew angle

Run	Left Turn (s)	Right Turn (s)	Minor Street Total (s)
1	11.2	6.7	8.1
2	8.8	6.7	7.3
3	14	7.5	9.5
4	10.7	6.7	8
5	15.5	7.5	9.3
6	9.7	8	8.5
7	12.1	8.3	9.3
8	11.7	8.3	9.3
9	15	6.5	8.9
10	9.9	8.3	8.7
11	11.2	7.8	8.7
12	15.3	6.6	9.2
13	10.6	5.9	7.2
14	14.1	6.3	8.6
15	13.5	6.8	8.6
16	10.2	7.1	8.1
17	10.4	7.3	8.3
18	22.1	7.1	11.6
19	12.2	9	9.9
20	12.9	6.1	8.3
21	12.4	5.7	7.7
22	12.1	7.7	9
23	15.3	7.9	10.1
24	12.2	7.4	8.7
25	8.4	6.1	6.8
26	7.4	5.9	6.4
27	12	5.8	7.8
28	12.3	6.3	8.1
29	10.3	6.8	7.9
30	9.8	6.4	7.4
AVG	**12.11**	**7.02**	**8.51**

TABLE 41 Average queue delay for -5° skew angle

Run	Left Turn (s)	Right Turn (s)	Minor Street Total (s)
1	20.1	7.2	10.4
2	14.5	6.1	9.1
3	12.4	7.5	8.8
4	12.4	7.5	9
5	10.6	6.2	7.5
6	10.8	7	8
7	14.6	9.3	10.9
8	12.1	6	7.6
9	9.7	6.8	7.6
10	14.4	7.3	9
11	12.3	6.8	8.4
12	13.3	6.3	8.4
13	11.6	6.2	7.7
14	13.3	6.5	8.3
15	9.9	6.6	7.6
16	11.9	5.9	7.8
17	11.3	6.1	7.6
18	11.2	7.7	8.6
19	15.6	6.7	9.8
20	14.3	7.2	9.4
21	11.7	6.6	8.4
22	14.6	5.5	8
23	12.2	6.6	8.4
24	11.7	6.7	8.2
25	17.3	6.8	9.9
26	10.8	5.4	7
27	11.3	7.2	8.3
28	12.7	6	8.1
29	15.4	7.3	9.9
30	11.4	8.1	9
AVG	**12.85**	**6.77**	**8.56**

TABLE 42 Average queue delay for 5° skew angle

Run	Left Turn (s)	Right Turn (s)	Minor Street Total (s)
1	13.1	7.5	9.3
2	17.1	7.1	10.3
3	11	5.8	7.5
4	16.3	6	9.1
5	13.7	6.2	8.3
6	11.9	6.6	8.3
7	13.6	7.1	9.2
8	14.2	7.3	9.2
9	11.3	6	7.5
10	18.5	6.2	10.1
11	14.6	7	9.1
12	11.9	6.9	8.4
13	9.5	7.3	7.9
14	14.4	7.5	9.7
15	17.6	10.6	12.7
16	14.4	7.3	9.3
17	14.1	8.1	9.5
18	12.2	6.5	8.4
19	12.9	6.9	8.7
20	12.8	6.5	8.4
21	16.1	7	9.6
22	14.3	5.8	8.6
23	13.1	6.3	8.4
24	11.8	6.2	7.8
25	15.4	6	9
26	13.1	7.5	9.3
27	10.9	7.3	8.4
28	9.8	7	7.8
29	11.6	11.2	11.4
30	13.3	7.7	9.2
AVG	**13.48**	**7.08**	**9.01**

TABLE 43 Average queue delay for 10° skew angle runs

Run	Left Turn (s)	Right Turn (s)	Minor Street Total (s)
1	12.7	7.8	9.6
2	17.5	7.4	10.4
3	11	6.8	8.2
4	13.1	6.1	8.2
5	13.3	8.6	10
6	13.2	7.1	8.9
7	16.7	7.9	10.3
8	14.9	7.2	9.3
9	14.5	6.9	9.5
10	16.2	6.6	9.5
11	14.5	7.7	9.6
12	14.6	6.7	9.2
13	11.4	6.9	8.4
14	15.5	5.9	8.9
15	10.8	9.3	9.7
16	13	6.1	7.9
17	12	8.8	9.7
18	14.4	7.2	9.5
19	10.8	8.9	9.5
20	14	8.1	9.7
21	12.2	6.5	8.1
22	12	11.4	11.6
23	12.3	8.3	9.6
24	12.6	9.4	10.3
25	15.6	9.2	11.1
26	15.8	9	10.8
27	15.8	7.7	10.1
28	13.6	8.4	9.8
29	13.5	7.9	9.5
30	10.2	6.3	7.3
AVG	**13.59**	**7.74**	**9.47**

TABLE 44 Average queue delay for 15° skew angle runs

Run	Left Turn (s)	Right Turn (s)	Minor Street Total (s)
1	14.8	8	10.1
2	14.6	9.1	10.7
3	14.5	8.3	10.4
4	13.6	7.3	9.1
5	15.8	8.2	10.2
6	18.3	7	10.7
7	16.8	8.5	11.2
8	15	6.1	8.9
9	14.9	6.6	9.1
10	10.7	7.9	8.8
11	17.3	8	10.7
12	12.2	9.4	10.2
13	13.8	7.6	9.4
14	14.4	7	9.1
15	13.1	6.3	8.4
16	16	7.5	10.2
17	17.5	6.9	10.2
18	12.6	6	8.2
19	20.3	7.9	11.8
20	9.6	6.8	7.6
21	7.9	7.6	7.7
22	10.6	6.4	7.5
23	13.8	7.4	9.3
24	11.1	8.5	9.2
25	17.1	10.1	12.3
26	17.3	6.4	10
27	11.5	8.6	9.5
28	16.3	8.8	10.8
29	13.5	7.8	9.6
30	15.3	6.9	9.3
AVG	**14.34**	**7.63**	**9.67**

TABLE 45 Average queue delay for 30° skew angle runs

Run	Left Turn (s)	Right Turn (s)	Minor Street Total (s)
1	24.8	8.7	13.7
2	18.9	9.4	12
3	15.9	6.8	9.7
4	29.2	10.3	16.5
5	19.9	10.5	12.9
6	16.5	6.8	9.1
7	22.4	6.2	11.4
8	20.9	8.3	11.6
9	17.9	8	10.9
10	22.5	8.6	12.5
11	14.8	8.3	10
12	17.1	10.2	12.6
13	21.1	8.1	11.5
14	21.1	8.1	12.4
15	19.7	8.6	11.8
16	19.4	8.4	11.4
17	18.2	6.9	10.2
18	14.2	7.5	9.6
19	15.7	7.4	9.8
20	15	8.2	10.4
21	14.7	8.2	10
22	19.4	9.2	12.4
23	15.9	8.5	10.6
24	19	8.5	11.7
25	22.4	7.7	11.5
26	29.3	7.9	14.5
27	24.9	9.3	13.9
28	20	9.2	12.6
29	13.1	6.3	8.2
30	14.8	7.4	9.8
AVG	**19.29**	**8.25**	**11.51**

TABLE 46 Average queue delay for -1° skew angle runs

Run	Left Turn (s)	Right Turn (s)	Minor Street Total (s)
1	11.5	8.1	9.0
2	15.7	6.8	9.2
3	11.6	6.8	8.3
4	10.8	6.1	7.7
5	10.5	7.1	8.0
6	20.6	8.4	11.6
7	12.0	7.2	8.8
8	10.9	7.1	8.4
9	19.0	6.9	10.4
10	12.3	7.9	9.2
11	14.5	6.9	9.3
12	12.0	6.3	8.0
13	12.5	8.7	9.8
14	10.5	5.6	7.0
15	11.4	6.5	8.0
16	14.4	7.3	9.4
17	15.6	6.2	8.7
18	11.9	6.0	7.9
19	13.9	6.7	8.9
20	10.0	7.1	7.9
21	11.4	7.6	8.8
22	14.2	7.4	9.5
23	13.9	6.5	8.9
24	8.2	6.8	7.3
25	14.4	6.3	8.8
26	12.8	6.5	8.5
27	12.9	6.7	8.3
28	10.2	6.5	7.6
29	10.5	5.9	7.3
30	10.4	8.0	8.7
AVG	**12.7**	**6.9**	**8.6**

TABLE 47 Average queue delay for -2° skew angle runs

Run	Left Turn (s)	Right Turn (s)	Minor Street Total (s)
1	14.0	8.2	10.0
2	11.4	6.8	8.2
3	13.8	6.6	8.9
4	12.8	8.2	9.5
5	11.3	8.2	9.1
6	9.7	7.7	8.2
7	16.5	6.2	9.2
8	7.8	6.9	7.2
9	10.6	11.1	11.0
10	11.0	8.1	8.8
11	11.6	7.5	8.8
12	11.9	6.4	7.9
13	18.3	8.7	11.3
14	13.7	6.9	8.6
15	8.2	7.0	7.3
16	10.4	6.7	7.8
17	14.6	6.0	8.5
18	10.7	6.1	7.3
19	11.2	7.4	8.5
20	17.6	6.5	9.9
21	10.9	7.3	8.3
22	11.5	7.8	8.8
23	9.4	6.2	7.2
24	13.6	6.5	8.4
25	8.9	6.9	7.5
26	10.4	7.2	8.0
27	13.1	6.6	8.6
28	13.5	8.9	10.2
29	16.3	6.2	8.9
30	17.2	6.2	9.7
AVG	**12.4**	**7.2**	**8.7**

TABLE 48 Average queue delay for -3° skew angle runs

Run	Left Turn (s)	Right Turn (s)	Minor Street Total (s)
1	9.3	6.3	7.2
2	9.3	7.7	8.1
3	10.8	8.2	9.0
4	9.9	7.3	8.0
5	24.2	6.2	11.8
6	12.2	6.9	8.1
7	13.6	6.2	8.5
8	12.5	7.2	8.7
9	13.2	7.3	8.9
10	13.3	6.9	8.8
11	17.1	7.5	10.3
12	12.7	7.8	9.3
13	12.3	6.8	8.4
14	13.0	7.2	8.8
15	14.2	8.7	10.4
16	11.4	8.1	9.1
17	14.6	8.7	10.4
18	12.5	6.8	8.4
19	11.3	6.9	8.2
20	9.0	7.5	8.0
21	15.6	7.3	9.6
22	13.8	7.5	9.4
23	8.7	6.7	7.2
24	13.2	6.8	8.7
25	12.9	6.9	8.5
26	12.1	7.7	9.0
27	11.6	6.6	8.1
28	11.2	8.0	9.0
29	14.6	6.8	8.8
30	16.0	6.2	9.3
AVG	**12.9**	**7.2**	**8.9**

TABLE 49 Average queue delay for -4° skew angle runs

Run	Left Turn (s)	Right Turn (s)	Minor Street Total (s)
1	16.0	10.1	11.7
2	12.5	10.8	11.3
3	9.9	6.0	7.3
4	12.8	7.1	8.6
5	14.0	7.9	9.7
6	11.6	12.0	11.8
7	13.6	6.9	8.9
8	13.9	7.7	9.4
9	13.4	6.7	8.7
10	11.0	7.6	8.7
11	10.9	7.6	8.7
12	11.6	7.2	8.5
13	12.5	8.8	10.0
14	8.3	6.2	6.9
15	9.3	6.7	7.6
16	15.4	9.0	10.9
17	13.0	6.8	8.6
18	14.6	8.5	10.2
19	16.1	7.8	10.2
20	17.1	8.9	11.5
21	13.9	7.5	9.7
22	10.8	6.5	7.6
23	10.6	5.8	7.2
24	14.7	8.0	9.7
25	12.0	8.2	9.4
26	10.9	9.5	9.8
27	12.2	5.9	8.1
28	9.7	7.3	8.1
29	14.2	7.3	9.3
30	12.6	6.8	8.5
AVG	**12.6**	**7.8**	**9.2**

TABLE 50 Average queue delay for 1° skew angle runs

Run	Left Turn (s)	Right Turn (s)	Minor Street Total (s)
1	17.4	7.4	10.6
2	13.1	5.9	7.9
3	16.2	6.8	9.8
4	10.2	5.8	7.1
5	10.2	7.1	8.0
6	15.4	7.4	10.0
7	12.7	6.8	8.4
8	11.3	6.8	8.1
9	14.5	8.0	10.0
10	9.6	8.5	8.8
11	19.0	8.2	11.3
12	13.1	6.8	8.6
13	9.7	7.0	7.8
14	11.2	7.4	8.5
15	14.4	8.2	10.0
16	12.8	7.5	8.9
17	17.4	7.4	10.6
18	14.6	6.6	8.9
19	8.9	6.4	7.1
20	15.9	7.4	9.7
21	11.9	6.3	8.0
22	11.8	7.5	8.6
23	14.4	6.9	9.5
24	13.5	7.2	9.2
25	11.3	8.6	9.4
26	10.6	6.6	7.7
27	14.8	8.1	10.3
28	14.0	8.3	9.9
29	13.3	6.3	8.5
30	11.3	5.7	7.7
AVG	**13.2**	**7.2**	**9.0**

TABLE 51 Average queue delay for 2° skew angle runs

Run	Left Turn (s)	Right Turn (s)	Minor Street Total (s)
1	19.2	7.2	10.4
2	12.6	8.0	9.2
3	10.2	6.8	7.8
4	16.5	8.7	11.0
5	19.2	9.0	11.9
6	13.8	6.4	8.4
7	11.8	5.8	7.4
8	18.6	6.6	10.3
9	12.8	6.8	8.7
10	11.4	6.2	7.6
11	14.0	7.1	9.2
12	15.7	6.7	9.3
13	12.7	7.9	9.4
14	17.4	5.4	8.8
15	15.6	6.1	8.7
16	13.9	7.5	9.2
17	13.3	6.4	8.2
18	11.8	7.3	8.5
19	14.2	8.3	9.9
20	9.7	6.2	7.4
21	10.8	10.9	10.9
22	11.0	7.1	8.4
23	15.5	8.4	10.5
24	8.8	7.4	7.8
25	12.6	9.4	10.3
26	19.1	6.6	10.2
27	13.8	6.7	8.7
28	12.8	6.9	8.7
29	12.5	6.2	8.1
30	10.0	6.2	7.3
AVG	**13.7**	**7.2**	**9.1**

TABLE 52 Average queue delay for 3° skew angle runs

Run	Left Turn (s)	Right Turn (s)	Minor Street Total (s)
1	11.9	5.8	7.5
2	11.9	7.0	8.4
3	13.6	7.3	9.1
4	13.8	6.9	9.0
5	15.1	6.2	8.9
6	14.3	6.9	9.2
7	12.1	7.2	8.6
8	13.3	6.7	8.8
9	10.3	7.6	8.3
10	15.9	6.4	9.4
11	11.5	7.6	8.7
12	13.7	8.7	10.2
13	14.9	6.8	9.1
14	17.6	8.5	11.0
15	8.1	6.3	6.8
16	12.8	6.4	8.2
17	12.6	9.1	10.2
18	12.1	6.4	8.1
19	14.1	7.1	9.0
20	12.4	6.3	8.0
21	11.5	6.3	7.7
22	10.3	6.5	7.7
23	12.8	6.3	8.4
24	16.4	7.6	10.0
25	11.6	7.8	8.9
26	18.3	6.7	10.4
27	9.2	7.5	8.0
28	18.1	9.6	12.2
29	13.8	6.9	9.2
30	9.9	6.8	7.7
AVG	**13.1**	**7.1**	**8.9**

TABLE 53 Average queue delay for 4° skew angle runs

Run	Left Turn (s)	Right Turn (s)	Minor Street Total (s)
1	11.5	6.2	7.7
2	12.2	6.5	8.3
3	10.4	6.5	7.7
4	9.4	7.7	8.2
5	9.1	5.7	6.7
6	16.5	8.0	10.4
7	15.7	8.1	10.1
8	11.5	8.7	9.7
9	13.6	14.2	14.0
10	11.4	7.7	8.9
11	10.6	7.3	8.3
12	12.3	7.2	8.8
13	12.1	6.2	7.8
14	10.9	7.4	8.5
15	15.6	6.4	9.0
16	15.6	6.7	9.5
17	22.4	6.7	11.4
18	12.5	8.0	9.2
19	9.6	8.3	8.7
20	10.7	6.1	7.5
21	12.2	7.0	8.5
22	14.4	5.6	8.2
23	10.3	8.0	8.6
24	16.4	6.8	9.7
25	11.8	8.9	9.7
26	12.3	6.5	8.4
27	9.5	6.7	7.5
28	15.9	8.4	10.8
29	11.6	8.9	9.7
30	11.2	8.7	9.4
AVG	**12.6**	**7.5**	**9.0**